EFFECTS OF EXTRACELLULAR MAGNESIUM ON SKELETAL MUSCLE

FUNCTION

A Thesis submitted for the degree of Doctor of Philosophy

in the University of London

Tebogo Rosemary Molefhe

Physiology Department

University College

University of London

June 1992

1

ABSTRACT

Calcium uptake by the sarcoplasmic reticulum is thought to be too slow to explain the rapid relaxation seen in frog skeletal muscle. It has been suggested that calcium binding by parvalbumin a myoplasmic calcium and magnesium binding protein, aids the calcium pump in achieving the rapid rate observed.

This work, which investigates the role of magnesium in determining the rate of calcium removal by parvalbumin following activation shows that increasing extracellular magnesium ion concentration results in a decline in maximum force production during the latter stages of a prolonged contraction. High extracellular magnesium ion concentration also increases relaxation rate and labile heat production, processes which reflect calcium binding to parvalbumin during the substitution reaction: Pa-Mg + Ca $\rightleftharpoons$ Pa-Ca + Mg. These observations suggest the removal of calcium from troponin and the myoplasm by parvalbumin when the concentration of calcium binding sites on parvalbumin is raised.

The changes described above are thought to be mediated by an increase in intracellular magnesium levels when the extracellular magnesium ion concentration was high. The role of intracellular magnesium ion concentration was tested by the construction of a model in which the magnesium concentration in the intracellular compartment was raised directly. The model shows that increasing intracellular magnesium ion levels increases relaxation rate and diminishes force production in a manner similar to that seen when a muscle is bathed in medium with a high extracellular magnesium concentration. The changes are accompanied by an increase in parvalbumin-calcium at the expense of parvalbumin-magnesium.

The findings of this study, therefore, suggest that seasonal changes in intracellular magnesium ion concentration could regulate changes in relaxation rate in frogs, which are poikilotherms, by increasing the concentration of parvalbumin-magnesium in the myoplasm and so the concentration of calcium buffer in the myoplasm.

ACKNOWLEDGEMENTS

I would to like to thank all those who have supported me during my period of studentship especially Suzanne Phillips, Oneilwe Mmolawa, and Wendy Lecoge whose friendship has been constant. I would also like to thank my supervisor Professor Roger C. Woledge whose excellent and patient guidance has opened my eyes to physiology. Lastly, I would like to thank my family especially my parents Nompunzi Patience and Topo James Molefhe for their concern and unfailing support. Ke a leboga.

CONTENTS

CHAPTER 2 METHODS

CHAPTER 3   **THE EFFECT OF INCREASING EXTRACELLULAR MAGNESIUM ION CONCENTRATION ON FORCE PRODUCTION AND RELAXATION RATE**

LIST OF FIGURES

11

12

13

LIST OF TABLES

CHAPTER 1

INTRODUCTION

1.1 INTRODUCTION

Muscles are the organs of locomotion in animals. The speed with which they function is important in determining the success with which a predator catches its prey. For the prey, its very survival can depend on the speed of escape. It is with these considerations that this project was undertaken.

Frogs undergo rapid repetitive contractions at low temperatures as part of their escape response. In order for these rapid contractions to take place, the antagonistic muscles producing the movement must relax rapidly. The question that arises is how are these animals, which are poikilotherms, able to relax quickly enough to carry out this repetitive or "burst" activity at low temperature. Is the action of the of the calcium pump of the sarcoplasmic reticulum, the "relaxing" organelle of the muscle, whose activity is temperature dependent (Ogawa et al., 1980), adequate to explain the rapid removal of the calcium which initiates contraction from the myoplasm and hence the rapid relaxation required even when the animals are in a cold environment?

It has been suggested that the rapid relaxation described above is possible at low temperature because of the presence of parvalbumin (Briggs, 1975, Gerday and Gillis, 1976, Pechere et al., 1977), a calcium and magnesium binding protein which is found

in high concentrations in fish and frog muscle (Hamoir, 1955, Gosselin-Rey and Gerday, 1977, Tanokura et al., 1986, Hou et al., 1991). This myoplasmic protein (Gillis et al., 1979) has two EF-hand calcium-magnesium binding sites similar to those found on troponin (Potter et al., 1977, Pechere et al., 1971). Parvalbumin is therefore thought to provide an extra path for lowering the free calcium levels in the myoplasm following activation. A path which would increase relaxation rate by acting in parallel with the calcium pump of the sarcoplasmic reticulum to remove calcium from the myoplasm following activation. At low temperatures when the calcium uptake rate by the sarcoplasmic reticulum might not be adequate (Ebashi and Endo, 1968) calcium buffering by parvalbumin would provide an "extra" calcium sink. At low temperature, therefore, relaxation rate in frogs would be to expected reflect the concentration and calcium binding kinetics of parvalbumin in the muscle.

More information about the role of magnesium in relaxation can be obtained from measurements of heat production during contraction. When muscle contracts chemical energy, $\Sigma \eta n_i$, is converted to (heat + work), a relation defined as $\Sigma \eta n_i$ = heat + work where η is the extent of the chemical reaction and n_i is the molar enthalpy change of the reaction. When no work is done during a contraction, the heat production of that contraction is expected to reflect all the chemical energy changes of the contraction (Woledge, 1971, Homsher and Kean, 1978). The balance between the energy from the chemical reactions and the heat energy produced during isometric contractions can, therefore, give some indication of the identity of the reactions taking place during contraction and the extent to which they occur. One reaction which is known to occur following activation is the binding of calcium to parvalbumin. In the

presence of magnesium this reaction is an exothermic substitution reaction (Moeschler et al., 1980, Smith and Woledge, 1982). The heat component to which this reaction is thought to contribute, the labile heat, appears early in a contraction and decays with an exponential time course. The size and time course of decay of the labile heat during a tetanus should give some indication of the parvalbumin-magnesium concentration available to bind calcium in the myoplasm at the start of the contraction.

Since relaxation rate (Baron et al., 1975, Gillis, 1985) and labile heat rate (Woledge, 1982) during muscle contraction are thought to reflect the concentration of parvalbumin in the muscle when different muscles and animals are compared, it should be possible to use changes in these two muscle properties as indicators of the changes in the concentration of parvalbumin available to buffer calcium during contraction.

In muscle fibres, parvalbumin is thought to exist in three forms, apo-parvalbumin which is cation free parvalbumin, parvalbumin-magnesium and parvalbumin-calcium as described by the reaction scheme below:

$$Pa\text{-}Mg \quad \rightleftharpoons \quad Mg + Pa + Ca \quad \rightleftharpoons \quad Pa\text{-}Ca$$

Of these three species, parvalbumin-magnesium is thought to be important in relaxation since it is the parvalbumin species which is available to bind calcium. At rest, the concentrations of the three species is thought to be most strongly influenced by the free magnesium ion concentration of the myoplasm (Godt and Maughan,

17

1989). Free magnesium ions, however, are not passively distributed across the sarcolemma (Flatman, 1984, 1991).Its intracellular concentration is thought to be maintained by a sodium/magnesium exchanger on the sarcolemma (Blatter, 1991). It would be expected then that the free magnesium ion concentration in the myoplasm will be influenced by the concentration of magnesium and sodium ions in the extracellular medium (Fenn and Haege, 1942, Alvarez-Leefmans et al., 1987, Gonzales-Serratos and Rasgado-Flores, 1990, Altura et al., 1992). By extension, the concentration of parvalbumin-magnesium in the myoplasm, relaxation rateand heat production should be influenced by the magnesium ion concentration in both the extracellular and intracellular compartments.

1.2 CONTRACTION AND RELAXATION

1.2.1 The muscle components which participate in the contraction-relaxation cycle

Skeletal muscle is composed of fibres which are made up of myofibrils. Each myofibril comprises a network of transverse tubules (t-tubules), the sarcoplasmic reticulum and the myofilaments, Figure 1. (See Squire, 1986, for a review on muscle structure). When stimulated, the sarcolemma becomes depolarised. The transverse tubules, which are formed from invaginations of the sarcolemma then conduct the surface depolarisation to the core of the muscle thus providing a mechanism for the complete activation of the fibre (Peachey, 1965, Gonzalez-Serratos, 1975). This depolarisation of the sarcolemma results in a release of calcium from the sarcoplasmic reticulum (Endo, 1977) into the myoplasm where it initiates contraction (Ebashi and

18

Figure 1   A diagram of a frog muscle fibre showing the components

which participate in the contraction-relaxation cylcle.
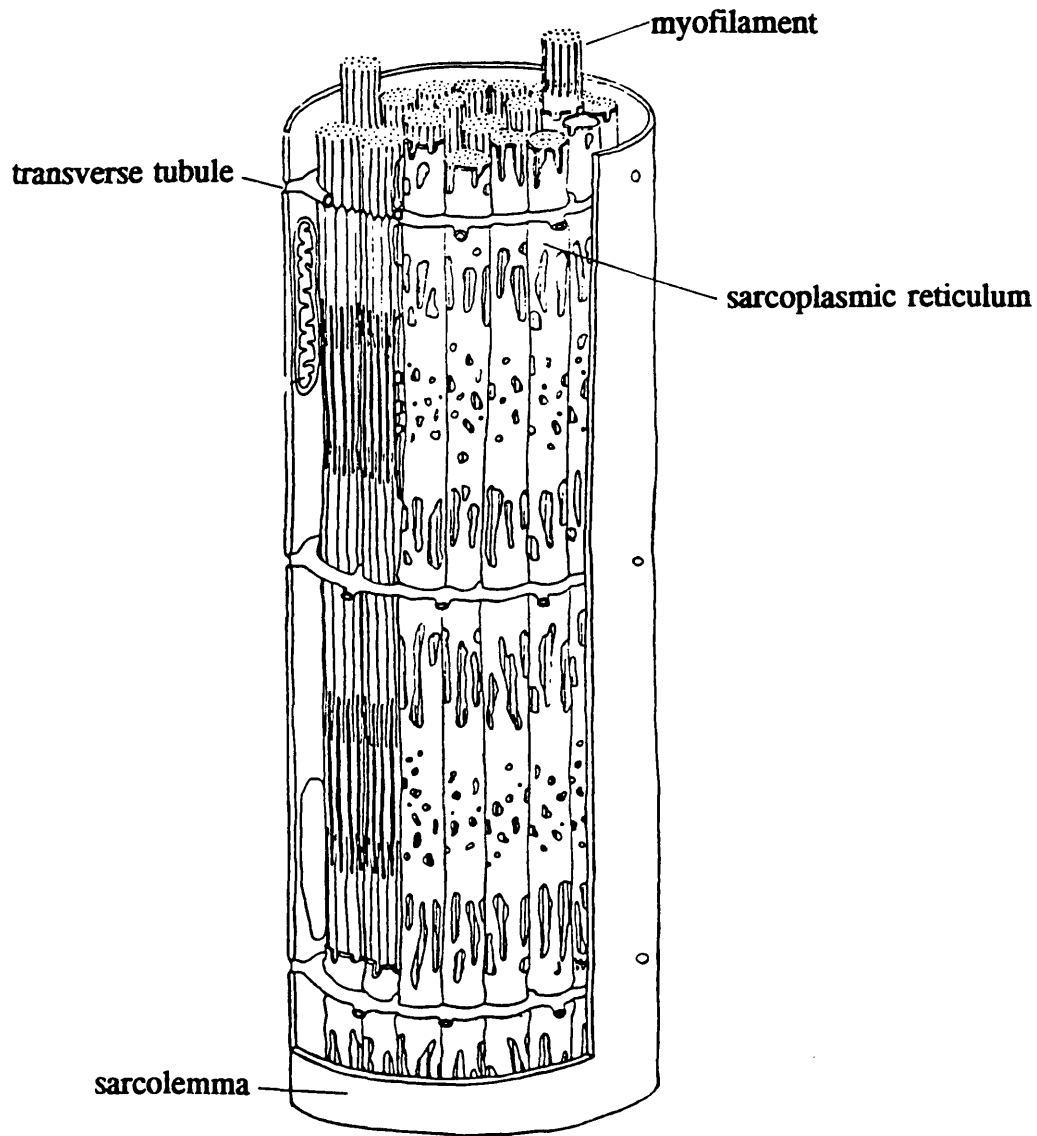
(taken from Woledge et al., 1985, p2)

Endo, 1968). Force development results when the thin filaments interact with the crossbridges of the thick filaments as explained by Huxley's independent force generator theory (Huxley, 1957, Huxley and Simmons, 1981, Huxley, 1991). The thin filament, mainly actin, houses troponin, the calcium sensitive protein which binds calcium during activation. The thick filament, myosin, has crossbridges and houses the ATPase enzyme responsible for hydrolysing ATP and providing energy for contraction.

1.2.2 Types of contractions

Following activation, muscle will either shorten, an isotonic contraction, or produce force at a constant length, an isometric contraction. The amount of force produced depends on 1) the degree of overlap between the myofilaments and the number of crossbridges available to interact with troponin as the thick and thin myofilaments interdigitate (Gordon et al., 1966) and 2) the duration of stimulation. In frog muscle, it has now been established that maximum isometric force is attained when a fibre is held at a sarcomere length, SL, between 2.0 μm and 2.13 μm inclusive (Huxley, 1980). This sarcomere spacing gives maximum overlap between myosin and actin, Figure 2.

1.2.3 The end of activation and relaxation

When stimulation ends the calcium responsible for initiating contraction must decrease to resting levels in order for the muscle to relax. This is achieved by its return to
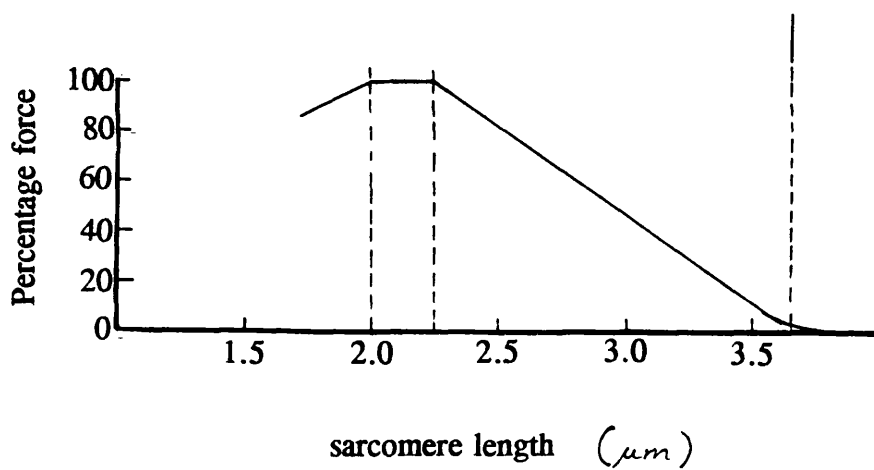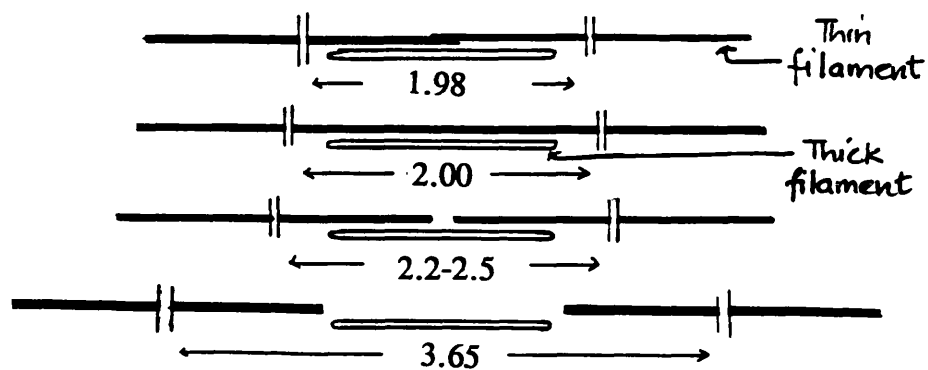
Figure 2 The relation between sarcomere length and isometric force. Maximum force

is shown to occur at sarcomere lengths between 2.05 μm and 2.25 μm.

(taken from Gordon at al., 1966)

the sarcoplasmic reticulum by the calcium pump of the sarcoplasmic reticulum (Hasselbach, 1964). The decrease in calcium concentration and the return of force to rest levels is described as relaxation. In this work, relaxation rate is defined to include all those processes that decrease the free calcium levels in the myoplasm. The rate of relaxation will therefore depend on the rate at which free calcium is removed by both the calcium pump of the sarcoplasmic reticulum and any myoplasmic calcium binding sites such as parvalbumin. This rate is influenced by a number of factors as described below.

1.2.3.1 Muscle fibre type

The speeds of contraction and relaxation vary in different muscles and depend on the fibre type(s) of the muscle. In the skeletal muscle of amphibians, five different muscle fibre types have been described (Lannergren and Smith, 1966, Smith and Ovale, 1973). The fibre types fall into two categories, tonic and twitch, which differ in mechanical properties as well as in innervation, histochemistry and biochemistry (Lannergren, 1979, Lannergren et al., 1982, Lannergren and Hoh, 1983).

Tonic fibres are innervated by multiple end plates and do not conduct action potentials. They show a graded response to stimulation as force summates from individual localised contractions. Twitch fibres, on the other hand, are innervated by one or two large motor end plates and give an all-or-none mechanical response to stimulation once their mechanical threshold is exceeded. Twitch fibres can be further divided into fast twitch and slow twitch. Fast twitch fibres generally have larger

diameters than slow twitch fibres. Once isolated, the weight:length ratio of the fibres,

~ 0.3, can be used to confirm fibre type to be fast twitch (Elzinga et al., 1989).

Parvalbumin concentration also appears to vary with muscle fibre type. Fast muscle

fibre types have been shown to contain higher concentrations of parvalbumin than

slow fibre types (Celio and Heizman, 1982, Heizman et al., 1984, Schmitt and Pette,

1991). It is therefore important to identify the muscle fibre type that is used in any

experiment. Parvalbumin is associated with muscles that undergo "burst" activity

during escape. These are the muscles which have been found to contain a high

content of fast twitch fibres.

1.2.3.2 The activity of the calcium pump of the sarcoplasmic reticulum

The sarcoplasmic reticulum regulates myoplasmic calcium levels through the action

of the calcium pump. The rate of calcium uptake from the myoplasm by the pump

is known to follow Michaelis-Menten kinetics (Inesi and Scarpa, 1972, Ogawa et al.,

1970, 1980). The velocity of calcium uptake by the pump can therefore be defined

as

$$d[Ca]/dt = V_{max} [Ca]/ (K_M + [Ca])$$

where V_{max} is the maximum pump velocity and K_M is the affinity of the pump for

calcium. The myoplasmic concentration of calcium will therefore determine the

turning on of the pump as well as the velocity at which the pump operates. The rate

at which the pump operates is highly temperature dependent: the Q_{10} of the pump has

been measured to be approximately 3 at temperatures below 25 C (Weber, 1976,

23

Ogawa, 1980). It would be expected therefore that the rate of calcium uptake by the sarcoplasmic reticulum in poikilotherms, *in vivo*, would be strongly influenced by the ambient temperature, hence the question of the adequacy of the calcium pump in producing rapid relaxation at low temperature. A rapid move from a warm terrestrial resting spot to cold water, as is often observed in frog, brings this question of ambient temperature and relaxation rate into even sharper focus. Seasonal variations in temperature would also result in the slowing of relaxation during the cold months (Agostini et al., 1990). So, again, is calcium uptake by the calcium pump of the sarcoplasmic reticulum alone adequate to explain relaxation rate at temperatures as low as 4 $^\circ$C.

1.2.4.2 Myoplasmic calcium binding sites

Calcium binding and release by the myoplasmic sites such as parvalbumin also influences the concentration of free calcium following stimulation. Parvalbumin will therefore affect both force generation by the myofilaments and the calcium pump activity in removing myoplasmic calcium. It is therefore important to assess the effectiveness of parvalbumin as a calcium buffer in frogs since its action can influence both initial relaxation and more importantly, relaxation during a series of contractions (Peckham and Woledge, 1986, Hou et al., 1991a)

In order for parvalbumin to be an effective calcium buffer at low temperature, the Q_{10} of the desired parvalbumin-magnesium/ calcium reaction should be fairly temperature independent. Hou et al. (1991b) give a Q_{10} of 1.2 at temperatures between 0° and

20°C for this reaction. This would make the variation in the concentration of parvalbumin buffer rather than the kinetics of the buffer reaction, the more important factor in determining its contribution to relaxation: a condition that would be of advantage at low temperature. Calcium dissociation from this site should also be slow enough to allow the sarcoplasmic reticulum to remove calcium from troponin before it is removed from parvalbumin. This delay would enable mechanical relaxation at a time when there is "extra" calcium in the myoplasm. Gillis and Gerday (1977) have reported the direction of calcium movement in the myoplasm following activation to be troponin→ parvalbumin → sarcoplasmic reticulum. This suggests the presence of parvalbumin-calcium does not limit calcium dissociation from troponin and the repriming of troponin for further contractions. The slow dissociation of calcium from parvalbumin, 1 s^{-1} (Hou et al., 1991) will however limit parvalbumin to being important only during activity which is of short duration. This has been reported as a slowing of relaxation with tetanus duration (Abbott, 1951, Curtin, 1976, Peckham and Woledge, 1985 Hou et al., 1990). The removal of calcium from parvalbumin by the sarcoplasmic reticulum then provides the last phase of relaxation (Cannell, 1982, 1986).

1.3 MAGNESIUM IN MUSCLE

1.3.1 Magnesium ion concentration in the myoplasm

Although the importance of magnesium in regulating calcium function in muscle is well established its role has been difficult to assess because of an inability to

determine the level of free magnesium with any confidence (Alvarez-Leefmans et al., 1987). The range of concentrations quoted for total myoplasmic magnesium falls between 11 mM and 16 mM (Godt and Maughan, 1989) inclusive. The measurement of free magnesium has, however, resulted in a wide range of concentrations, 0.3- 6 mM, being quoted by different workers using different techniques, Table 1. McGuigan and Blatter (1991) in a recent review on the interpretation of results from experimental measurements of free magnesium suggest the variation is due to the use of different magnesium binding constants in calculating the concentration of bound magnesium. When similar constants are used, the free magnesium concentration is estimated to be 0.2- 1 mM.

1.3.2 Can intracellular magnesium ion levels vary?

Gilbert (1960) using the radioisotope ^{28} Mg, showed that it is possible to exchange intracellular magnesium with magnesium in the extracellular bathing solution. The magnesium flux, which was studied using whole muscle, showed that the exchange followed a slow time course and was complete in 5 hours. Fenn and Haege (1942) showed that it was possible to raise intracellular magnesium ion concentrations by raising extracellular magnesium from 0 mMto 4 mM. This dependence of the intracellular magnesium ion level on extracellular magnesium ion concentration has been confirmed (Blatter and McGuigan, 1986, Alvarez-Leefmans, 1986). More recently, Blatter (1990), using the ion selective ligand ETH51114 has shown that bathing isolated fibres from the tibialis anterior muscle of frog in Ringer's solution with 10 mM or 20 mM magnesium ion concentrations can raise the intracellular free

Table 1 A summary of some of the determinations of free magnesium ion levels in fro muscle.

Method		Ref
^{31}P NMR spectrum of PCR. (Calculated value depends on K_D of PCr/Mg. 4^0C	3-4.4	Cohen & Burt 1977
Absorbance of light by Meta Iochromic dyes. (chosen to minimize Ca^{2+} and H^+ interference) Room temperature		Baylor Chandle & Marshall 1982
(i) Arsenazo I	3-6	
(ii) Arsenazo II	0.5-1.2	
(iii) Dichlorophosphanazo III	0.2-0.3	
Magnesium selective microelectrode	3.3	Hess, Metzger Weingart, 1982
^{31}P NMR of ATP (Calculated value depends on K_D of ATP/Mg). 25^0C.	0.6	Gupta & Moore 1980
Calculated from concentration of Mg and known K_D's of magnesium chelators.	3.4	Nanninga 1961
Calculated from K_D's of magnesium chelators & total Mg concentration.	0.8	Maughan, 1983
Calculated from flux measurements of ^{28}Mg radioisotope.	0.9	Gilbert 1960
Magnesium selective microelectrode Rana temp tibialis ant. ETH5114.	0.9	Blatter 1991

27

magnesium level from 0.93 mM to 1.86 mM, an increase of 105%.

1.3.4 The control of parvalbumin calcium buffer levels by magnesium

At rest, when the free magnesium concentration is high compared to calcium concentration, 0.06 μM (Blinks et al., 1978, Cannell, 1982), the equilibrium of the reaction scheme shown previously (p3) is expected to favour parvalbumin-magnesium. However, parvalbumin affinity for calcium, K_{α} is 10^4 times higher than parvalbumin affinity for magnesium (Benzonan et al., 1972, Potter et al., 1978, Ogawa and Tanokura, 1986). The reaction scheme therefore gives equilibrium concentrations of approximately 60% parvalbumin-magnesium and 40% parvalbumin-calcium (Hou et al., 1991). Godt and Maughan (1989) arrive at similar concentrations based on calculations of magnesium binding in the myoplasm. The apo-parvalbumin concentration is estimated to be < 1%.

1.4 SOME EVIDENCE FOR THE PRESENCE OF MYOPLASMIC CALCIUM BINDING SITES

Endo (1977) estimated calcium release from the sarcoplasmic reticulum to be about 700 μM. Of this calcium, 280 μM binds to troponin. There is therefore a shortfall of at least 420 μM calcium binding sites when the free calcium level is maintained at 7 μM during a tetanus (Cannell (1984). Somlyo et al. (1981, 1985) traced the location of calcium before and during a tetanus. They showed that during a tetanus most of the calcium in the sarcoplasmic reticulum, at rest, is translocated to the

myoplasm. They suggested that the only myoplasmic site with the capacity to bind 420 μM calcium is parvalbumin.

A number of workers using intracellular calcium ion indicators have shown that following stimulation, free calcium rises rapidly then dips to a new level that is maintained for the duration of the contraction (Blinks et al., 1978, Cannell, 1984, Baylor et al., 1978). The dip suggests the binding of calcium to a myoplasmic site during this period.

The presence of a transient which does not follow the same time course as the calcium transient following activation has been demonstrated (Irving et al., 1989). It is suggested that the size, 0.47 - 1 mM, and the time course of this transient points to the possibility that it arises from magnesium dissociation from parvalbumin.

1.5 MAGNESIUM AND HEAT PRODUCTION DURING CONTRACTION

Aubert(1956) showed that in toad whole muscle there are two components to the heat liberated during a contraction; a component that appears early in a contraction and decays with an exponential time course, the labile heat rate, and a component that is liberated at a steady rate throughout the course of the contraction, the stable heat rate. Curtin et al. (1981) showed that these two heat components exist and can be measured in isolated frog muscle fibres, the preparation used in this study.

Studies on energy balance during a contraction show that, in frog muscle, some of the heat produced during an isometric contraction cannot be explained by the actomyosin-ATPase reaction associated with crossbridge cycling and the ATPase reaction of the calcium pump of the sarcoplasmic reticulum alone (Curtin and Woledge, 1979). This heat which is extra to the ATPase activity of the fibre, described as "unexplained" heat at the time it was first studied systematically, was shown to follow the same time course as the labile heat rate described by Aubert (1956). The "unexplained" heat and the labile heat are now thought to reflect the same processes (Curtin and Woledge, 1979, Gillis et al., 1984, Peckham and Woledge, 1985).

1.5.1 Labile heat

Labile heat is produced early in a contraction and decays with an exponential time course. The amount of labile heat liberated during contraction depends on the concentration of parvalbumin in the muscle when different muscles are compared (Woledge, 1982, Heizman et al., 1984, Peckham and Woledge, 1986). If labile heat production and relaxation rate reflect the same process, these two muscle properties would be expected to show similar changes during contraction. Both should decrease with tetanus duration and both their rates should decrease in the second of two closely spaced tetani. These changes in heat production and relaxation rate have been observed during contraction (Abbott, 1950, Aubert, 1956, Curtin, 1976, Peckham and Woledge, 1986, Westerblad and Lannergren, 1990, 1991). The decrease in heat rate in these conditions, therefore, is also thought to reflect a decrease in labile heat production as the parvalbumin-magnesium calcium buffer is depleted.

The stable heat is thought to reflect heat production during calcium cycling (Curtin and Woledge, 1978, Rall. 1982) between the crossbridges (Yamada et al., 1976) and the sarcoplasmic reticulum (Smith, 1972, Homsher et al., 1972). The amount of stable heat produced will therefore depend on the maximum force produced (Elzinga et al., 1985) and the rate of calcium uptake by the pump of the sarcoplasmic reticulum during contraction. In isometric contractions when the overlap between the myofilaments is held constant, the calcium concentration is high enough to fully activate the calcium pump. The fractional contribution of the two processes, 40:60 calcium pump to crossbridge cycling respectively (Smith, 1972). , to the stable heat rate would be expected to remain the same in fibres contracting at the same sarcomere length (Aubert and Gilbert, 1980, Elzinga et al., 1984, Kometani and Yamada, 1984, Peckham et al., 1984).

In order to test the effect of raising magnesium on the stable heat rate, the effects of high magnesium on the force-velocity characteristics of the fibre, which gives an indication of crossbridge turnover (Edman, 1979) and power output by the fibres, which gives a measure of actomyosin ATPase activity during the contraction (Homsher and Davies, 1979), were determined. Some deductions could thus be made about the effect of increasing free magnesium on the crossbridges.

In the sarcomere length range between 1.67 μm and 2.13 μm inclusive, the maximum velocity for crossbridge turnover V_{max} is independent of the force produced (Edman,

31

1979) and hence the intracellular calcium concentration. A measure of V_{max} therefore gives information about the effect of the solution one crossbridge turnover. The force-velocity relation of a fibre is described by a hyperbola. The relation between the velocity of shortening and force development can be described by Hill's equation (1938):

$$V' = (1-P') / (1 +P'G),$$

where $V = V/V_{max}$, $P' = P/P_0$ and $G = P_0/a$: V = velocity, P = force, V_0 = maximum velocity of shortening and P_0 = maximum force production. The curvature of the hyperbola, a/P_0, gives an indication of the ratio of crossbridges producing positive and negative force. It also gives an indication of velocity of shortening which will result in maximum power output.
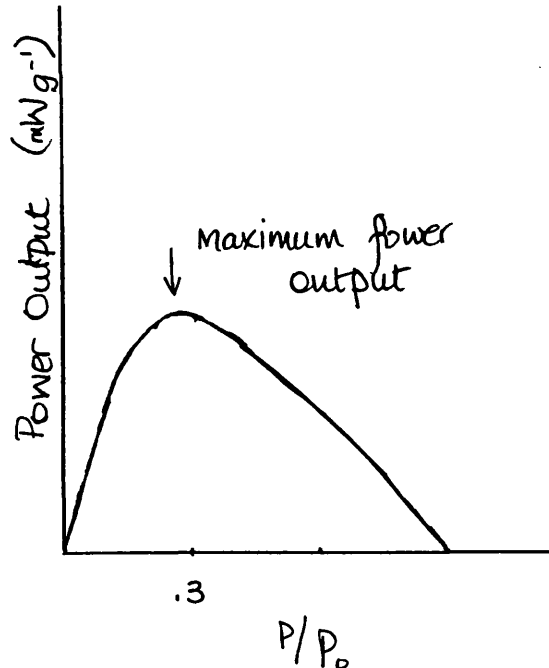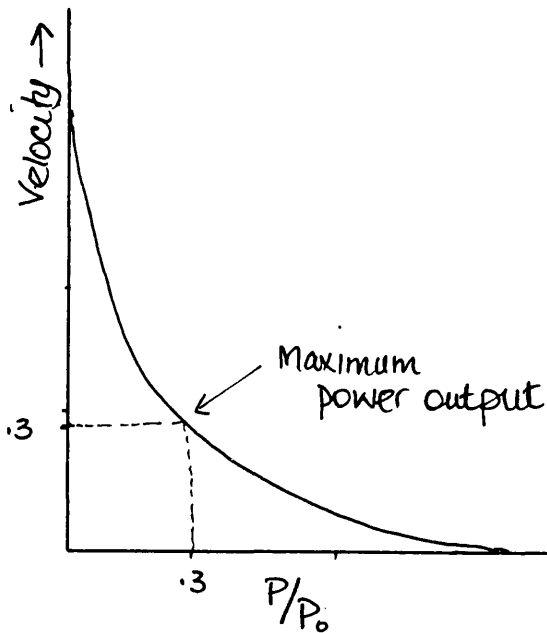
A comparison of the curvatures of the P-V curves will therefore give some information about changes in the ratio of the crossbridges producing positive force to those producing negative force at a particular velocity of shortening and hence indicate changes in crossbridge turnover.

The power output of the fibre, calculated as (force x velocity), gives a measure of the rate at which work is done by the muscle. The maximum power output and the velocity at which it occurs is determined by the curvature of the force-velocity curve, a/P_o. Information on the power output of the fibres can thus give an indication of any changes in the rate of calcium cycling by the crossbridges. This measure can also be used to separate the effect of magnesium on the crossbridges from its effect on the calcium pump of the sarcoplasmic reticulum if the effect exerted is on only one of these two ATPase components.

1.6 Is the binding of calcium to parvalbumin important during activation or relaxation?

Apo-parvalbumin has a calcium affinity similar to that of troponin (Benzonana et al., 1972). Parvalbumin is also found at a much higher concentration, 760 μM (Hou et al., 1991), than troponin at 70 μM (Endo, 1977) in the myoplasm. Parvalbumin could therefore effectively compete with troponin for calcium following activation. However, at rest, the apo-parvalbumin concentration is low, < 1% of the total parvalbumin in the myoplasm, compared to parvalbumin-magnesium and parvalbumin-calcium concentrations which are approximately 1.2 mM and 0.8 mM respectively

33

(Godt, 1989). The potential competition between parvalbumin and troponin for calcium is therefore greatly reduced. The important parvalbumin reaction then becomes the buffering of calcium by parvalbumin-magnesium. Since calcium and magnesium are known to bind at the same site on parvalbumin (Ogawa and Tanokura, 1986a, Potter et al., 1978), the slow dissociation of magnesium from parvalbumin (Potter et al, 1987, Hou et al., 1991) and the concentration of free magnesium (Moeschler et al., 1980) can combine to slow the kinetics of the parvalbumin-magnesium/ calcium substitution reaction sufficiently to provide a delay between calcium binding to troponin and calcium binding to parvalbumin. The important calcium buffering reaction of parvalbumin then becomes a relaxation reaction.

1.7 Aims of this Thesis

This thesis investigates the effect of magnesium on some properties of muscle with a view to defining further the role of magnesium in setting the concentration of parvalbumin-magnesium in muscle and hence the role of parvalbumin-magnesium in relaxation. This has been done by testing the effect of raising the extracellular magnesium ion concentration on relaxation rate, heat production and the power output of the muscle. The effect of extracellular magnesium ion concentration on parvalbumin is thought to be mediated by an increase in the concentration of intracellular free magnesium. A model, in which the intracellular magnesium ion concentration is raised to the level expected from the high magnesium treatment described by Blatter(1990) is also constructed. This provides a theoretical model which can be used to predict the effects of raising intracellular magnesium levels

34

directly on relaxation rate during a contraction. A comparison of the predictions from the model with the experimental results will hopefully shed some light on the possible mechanisms available for adjusting parvalbumin-magnesium levels and hence the relaxation rate during different seasons.

CHAPTER 2

METHODS

2.1 MUSCLE PREPARATION

Single fibres and small bundles of 2-3 fibres dissected from the tibialis anterior muscle

of the frog *Rana temporaria* were used. The frogs, which were stored at 4 °C prior

to experimentation, were killed by double pithing before excising the *tibialis anterior*

longus and the *tibialis anterior brevis* muscles for dissection. During dissection, large

fibres were selected so that only fast twitch fibres were used (Elzinga et al., 1989).

Aluminium or platinum T-clips (T-clips) were clipped over the tendons left attached

to the isolated fibres. These clips were later used to mount the fibre in the

experimental bath, Figure 3. The dissection was carried out in Ringer's solution with

a concentration of 1 mM magnesium at room temperature. The choice of muscle to

use in a particular experiment was random.
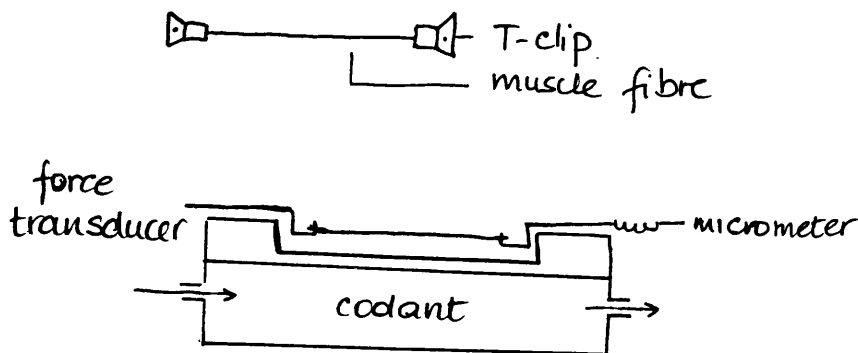
Figure 3.

2.2 EXPERIMENTAL SET UP

The experimental set up for stimulation and recording is shown in Figure 4. In it is included:

1) a programmable Digitimer, D4030, which was used to drive the stimulator, the oscilloscope or computer used to collect data and the motor attached to the length transducer. It was also used to determine the duration and frequency of stimulation,

2) a bath which contained Ringer's solution and into which the fibre was placed during the mechanical experiments. The bath had a thermocouple thermometer, T, for monitoring temperature as well as a suction line permanently mounted on its sides. This bath was replaced by a thermopile during the heat experiments,

3) a micrometer which was used to adjust muscle length. The micrometer was attached to a motor, Dual Mode Servo, Cambridge Technology, which was used to change fibre length during the experiments on the power output of the fibres,

4) a stimulator, Isolated stimulator type 2533, which provided direct electrical stimulation to the muscle via two platinum wire electrodes placed at the ends of the bath and transversely across the fibre,

5) a force transducer connected as the variable resistance arm of in a Wheatstone bridge circuit. An AE801 variable resistance transducer made by Sensonor of Horten, Norway was used to record force production in the mechanical experiments. During the heat experiments the force was measured and amplified using a Cambridge Technology Series 400 force transducer system.

6) an amplifier, RS, which was used to amplify the signal from the AE801 force transducer before it was recorded. An ANCOM-DC3A low noise chopper amplifier

37
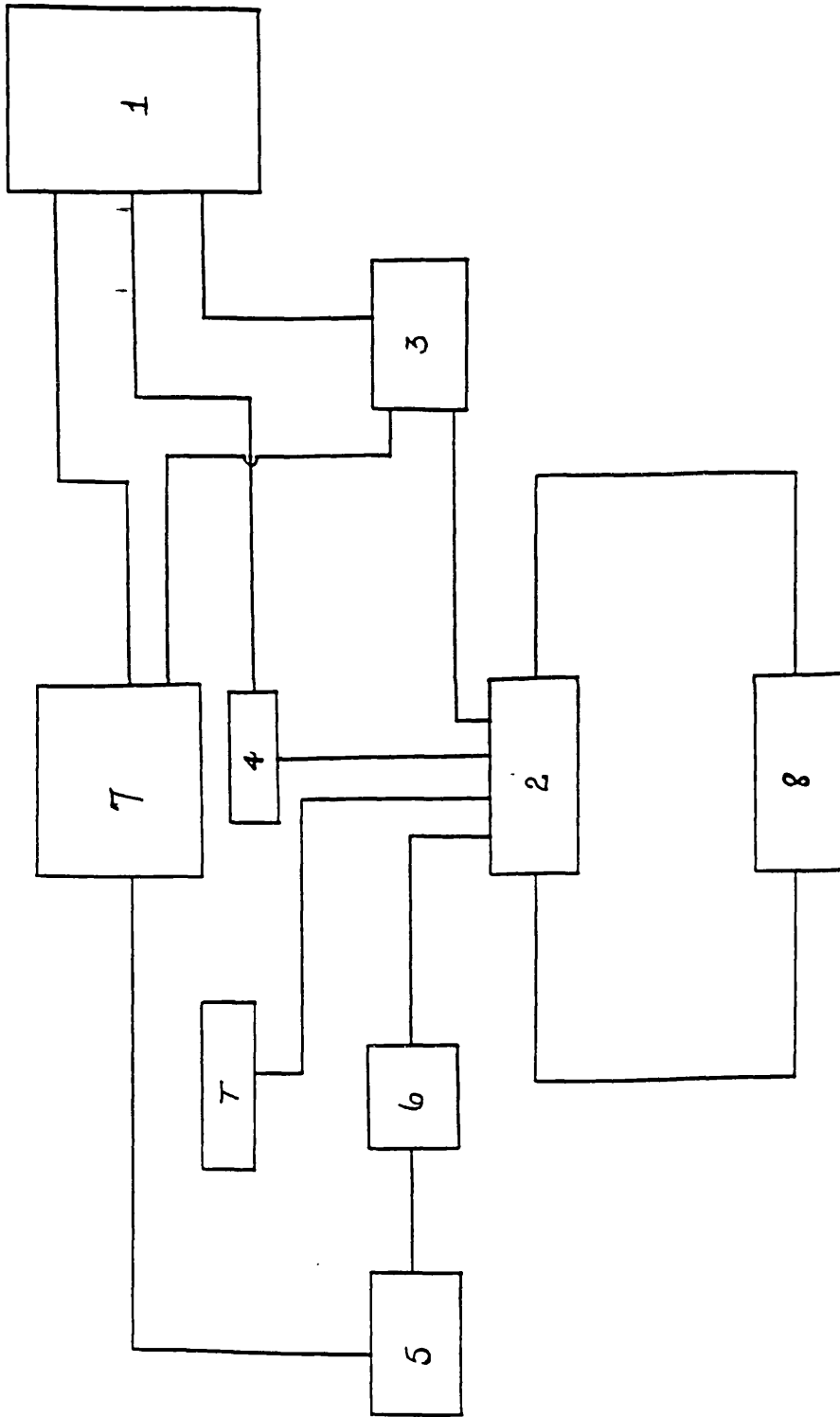
Figure 4   A diagram of the experimental set up used

was included in the setup to amplify the thermopile signal from which heat production was calculated.

7) an oscilloscope or computer which was used to collect the experimental records and store them on diskette,

8) a Churchill thermocirculator which was used to regulate temperature during the mechanical experiments. It was replaced by a coolant filled "jacket that could be closed during the periods when heat measurements were made. The jacket had a recess above the thermopile so the fibre was not crushed and the heat collected from the fibre flowed in only one direction.

2.3 MOUNTING OF FIBRE PREPARATION IN THE EXPERIMENTAL CHAMBER

2.3.1 Mounting of the fibre in the experimental chamber

A transfer trough filled with the control solution was used to transfer the isolated fibres to the experimental chambers which formed part of the experimental set up shown in Figure 4. The fibres were suspended between a force transducer and a hook attached to a micrometer using the T-clip attached to the fibres. This arm was used to adjust the length of the fibre when necessary. It otherwise served as an immovable attachment so that the contractions studied were fixed-end isometric contractions.

2.3.2 Mounting of the fibres on the thermopile

In the heat experiments, the muscle fibre preparation was attached to a Cambridge transducer and a micrometer as described above. The fibre preparation was placed on the surface of the thermopile in good thermal contact with the thermocouples of the pile. In order to keep the heat capacity of the system low compared to that of the muscle, nearly all the solution transferred to the thermopile with the fibre during mounting was drained using a piece of filter paper touched to the surface of the pile before the fibre was stimulated. A piece of filter paper saturated with a 50% Ringer's solution was placed in the recess above the fibre. This arrangement provided a vapour saturated environment for the fibre. The Ringer's solution in the recess was also used to balance the loss of moisture from the chamber during the experiment.

2.4 SOLUTIONS

The experiments described in the following chapters were designed to test the effect of raising extracellular magnesium ion concentration on muscle function. A series of modified Ringer's solutions with magnesium chloride concentrations of 1, 5, 10 and 20 mM was prepared using the solute concentrations presented in Table 2. The sodium chloride concentration in the high magnesium Ringer's solution was decreased in order to make the solutions approximately isosmolar (Blinks, 1965, Burchfield and Rall, 1986).

Table 2   Composition of solutions

NaCl	KCl	CaCl$_2$	MgCl$_2$	HEPES	Osmol*
115.0	2.5	1.8	1.0	5.0	243.4
110.0	2.5	1.8	5.0	5.0	245.4
100	2.5	1.8	10.0	5.0	240.4
85.0	2.5	1.8	20.0	5.0	240.4

the concentrations are given in mM

*HEPES is excluded from this calculation

2.4.1 Changes of solution during the mechanical experiments

During the mechanical experiments the solution in the bath was changed and the bath washed using the following procedure: a volume of the new solution equal to twice the volume of the bath was added to the bath and suctioned using a syringe and a suction line permanently fixed on the bath. A third addition of the solution was then allowed to remain in the bath. Care was taken to ensure the volume of the solution remaining in the bath was the same throughout the experiment so that the current density in the bath during stimulation was constant. A cover slip was sometimes used for this purpose. At other times the baseline of the force recording channel gave a good indication of the level of the solution. The changes in solution were carried out rapidly in order to avoid concentration and temperature gradients in the bath.

2.4.2 Changes of solution during the heat experiments

The thermopile was washed using the procedure described above before a third addition of solution was retained and left to bathe the fibres for 10 minutes. After ten minutes, this solution was also removed and the temperature of the thermopile allowed to equilibrate before stimulation continued.

In the first two experiments, the new solution was introduced to the bath via a convoluted tube placed in contact with the "jacket" housing the thermopile so the new solution was cooled to the equilibrium temperature of the system before it came in contact with the fibre on the thermopile. The solution was removed by suctioning via

42

the same tube. This arrangement decreased the time required for the temperature to equilibrate after each change of solution. In the third experiment, the "jacket" housing the thermopile was opened and the new solution added directly onto the pile. The solution used to wash the pile during the changes of solution was removed by touching filter paper to the thermopile. A period of between 5 and 10 minutes was then required for the temperature to equilibrate.

2.5 TEMPERATURE CONTROL

2.5.1 Temperature control in the mechanical experiments

The experiments were carried out at temperatures between 2 $^\circ$C and 7 $^\circ$C. The solution in the experimental bath was kept at a constant temperature by circulating a 50% (by volume) water/alcohol coolant (freezing point -30 $^\circ$C) under the experimental chamber using a Churchill Thermocirculator. The temperature of the solution in the bath was monitored using a nickel-constantan thermocouple mounted in the bath and held at the same level as the fibre preparation.

2.5.2 Temperature control in the heat experiments

These experiments were carried out at 5.5 $^\circ$C. The muscle fibre preparation was placed on a thermopile housed in the middle section of a "jacket" through which coolant was circulated. The coolant circulating in the different sections of the jacket was from the same source so the equilibrium temperatures of the different sections of

43

the jacket were similar to the equilibrium temperature monitored in the block with the thermopile. It was important to maintain the similarity in the equilibrium temperatures as the jacket acted as a sink towards which heat flowed from the active portion of the thermopile during contraction. This way the only direction for heat flow would be from the hot junctions of the thermopile to the cold junctions of the jacket. No other temperature gradients would be present in the system.

2.6 DETERMINATION OF OPTIMAL CONDITIONS FOR MAXIMUM FORCE PRODUCTION

2.6.1 Stimulus voltage

The stimulus voltage required for the production of maximum force was determined using twitches. An electrical stimulus, delivered to the muscle via platinum wire electrodes placed transversely across the fibres, was used in the mechanical experiments. In the heat experiments, end-to-end stimulation was delivered to the fibre via the T-clips used for mounting the fibre on the thermopile.

After the threshold stimulus was determined, the stimulus voltage was increased and the fibre stimulated every 60 s until an increase in voltage, with the pulse width constant, resulted in no increase in force. The pulse width was then adjusted until the best combination between pulse width and stimulus voltage for producing maximum twitch force, while keeping the stimulus energy low, was obtained. In the experiments on the force-velocity characteristics of the fibres, a constant current

generator, was used. Again, the current density used was the lowest possible for maximum force production.

2.6.2 Length

The maximum stimulus voltage was determined with the fibre held at slack length when no resting tension was recorded. Following the attainment of the stimulus voltage optimal for the production of maximum twitch force, fibre length was increased in 0.25 mm steps until a new maximum twitch force was reached. The muscle length was then kept constant at this value for the duration of the experiment.

In the experiments used to determined the force-velocity characteristics of the fibres, fibre length was set using sarcomere length information from the laser diffraction pattern of the fibre, Figure 5. Again the muscle was set at slack length and the sarcomere length, SL, determined. The fibre length was then adjusted from this length to a maximum sarcomere length of 2.6 μm, in order to determine the SL-tension characteristics of the fibre. The twitch force was determined after each 0.1 μm length adjustment. The sarcomere length of the fibres was set at 2.2 μm at the beginning of the experiments so the fibre shortened from a length corresponding to this sarcomere length.

The fibre length during the experiment was measured using a Leitz dissected microscope (x10 magnification) and an eyepiece micrometer.

Figure 5 A diagram of the arrangement of the apparatus used to determine sarcomere

length using laser diffraction
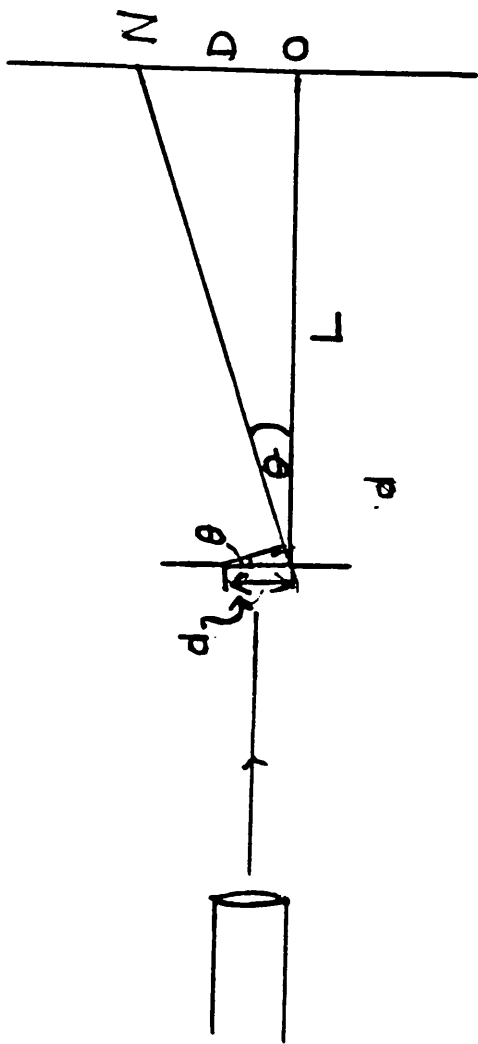
The size of the aperture, d, causing the diffraction pattern can be defined as:

$$d = n\lambda/\sin\Theta$$

where n is the order of the diffraction pattern, λ is the wavelength of the light fron from the laser beam and

Θ is the angle subtended between the angle of incidence of the light and the nth order diffraction pattern.

The angle Θ, is defined as $((\tan^{-1}(D/L))$, where D is the distance between 0 and nth oerder diffraction

2.6.3 Frequency of stimulation

A short tetanus, 300 ms duration, was used to determine maximum tetanic force. Thee fusion frequency was determined by increasing the stimulation frequency until the plateau of the tetanus was just fused. The stimulation frequencies used were between 10 and 20 Hz inclusive. The stimulation frequency was kept constant throughout each experiment in order to ensure the rate at which calcium was delivered from the sarcoplasmic reticulum to the myoplasm was little influenced by this variable.

The stimulus voltage was increased 50% at the end of the determination of the optimal stimulus parameters in the control solution to ensure optimal stimulation of the fibres when the solution was changed to the high magnesium solution (Howell et al., 1984) since increasing extracellular cation concentration increases the mechanical threshold of fibres.

2.7 DETERMINATION OF MUSCLE WEIGHT

At the end of the experiment the fibre preparation was cleaned by removing any dead fibres still be attached to the healthy fibres: the dead fibres were opaque whereas the live fibres were clear. The preparation was then dried and weighed using a Cahn Electrobalance 26 that measured weight to 0.1 μg.

2.8 MEASUREMENT OF FORCE

The force was measured using a force transducer connected in a Wheatstone bridge in which it formed the variable resistance of the bridge. During contraction the fibre, mounted on a hook attached at right angles to the transducer causes a distortion of the transducer which results in current flow in the Wheatstone bridge circuit. The signals obtained from this current flow were amplified before they were recorded on an oscilloscope. Nicolet 4094, 3091 and 402 oscilloscopes were used as well as a desktop PC that had been converted to function in oscilloscope mode using the software package MICROSCOPE.

The force transducers used were calibrated by hanging metal blocks of known weight on he hook used for mounting the fibres in the bath. The relation between the force exerted by various weights against the voltage recorded on the oscilloscope was found to be linear in the range of forces measured. The sensitivity of the AE801 transducers used was in the order of 1.768 mN/V.

2.9 MEASUREMENT OF HEAT

Heat production during contraction was calculated from records of temperature change obtained using a 12 mm Hill-Downing type thermopile consisting of constantan-chromel thermocouples, similar to that described by Curtin et al. (1981). The thermopile signals obtained then have to be converted to measures of temperature and heat. In order to make this conversion, the sensitivity of the each couple of the

48

thermopile, the Seebeck coefficient (α), must be known. Heat production can then be calculated from a knowledge of the heat capacity, C, of the system.

Peltier heating, which results from passing a small current, in this case less than 100 μA, through a thermopile can be used to determine both C and α for the system (Kretzschmar and Wilkie, 1972, 1975). Current passed through a thermopile will cause a small reversible transfer of heat between the region of the pile being heated, the hot junction, and the cold junctions of the pile. In the arrangement of the thermopile used here, the cold junctions are at the edges of the metal block on which the thermopile rests and the jacket housing the pile. The temperature gradient between the hot junctions, in the active region of the thermopile and the large heat sink of the cold junctions will result in current flow in the circuit which can then be recorded as a potential difference, the thermopile signal.

2.9.1 Determination of the heat capacity of thermopile

During peltier heating the rate at which heat is delivered to the system is defined as $C_\Delta T/dt$ where ΔT is the temperature change recorded during the heating. The temperature change recorded depends on the number of couples heated, n, the size of the peltier current passed, I, and α, the sensitivity of the couples of the pile. The rate of heat delivery can therefore be defined as $ITn\alpha$. The relation between the rate at which heat is delivered to the system and the rate at the heat change is measured by the pile can be summarized as $ITn\alpha = C_\Delta T/dt$. If peltier heating is carried out long enough for the temperature to reach equilibrium, the rate of cooling is equivalent

to the rate of heating. Therefore, the rate at which heat is delivered to the system can be determined from a record similar to that in Figure 6a: a cooling curve obtained following peltier calibration heating.

The rate of cooling following the end of peltier heating, $T_o \, e^{-t/r}$ depends on the equilibrium temperature of the system during heating, T_o. The initial rate of cooling can be determined graphically from a semilogarithmic plot of the cooling curve of a peltier calibration record. The heat capacity of the system can then be defined as $ITn\alpha/(\Delta T/dt)$. This determination of the heat capacity of the system assumes a knowledge of α. If α is unknown, it can be determined using the method described below.

2.9.2 Determination of the Seebeck coefficient

The Seebeck coefficient can be determined using peltier calibration heating and metal blocks of known heat capacity (Kretzschmar and Wilkie, 1972, 1975). The initial rate of voltage change, dV_o/dt, of the thermopile signal during peltier heating is proportional to the rate of heat change in the system and depends on the sensitivity of each couple, α, used during the measurements . It also depends on the number of junctions, n, from which the signal is collected ie $dV_o/dt = (dT_o/dt)n\alpha$. The rate of temperature change, dT_o/dt, is defined as $ITn\alpha/C$. Therefore, the initial rate of voltage change can be defined as $ITn^2\alpha^2$. The heat capacity of this system, C, shared between the thermopile and the metal blocks used in the determination.

So, $dV_o/dt = ITn^2\alpha^2 \cdot (1/C_M + C_T)$. A plot

a.

rate of heating   rate of cooling

beginning of heating   end of heating
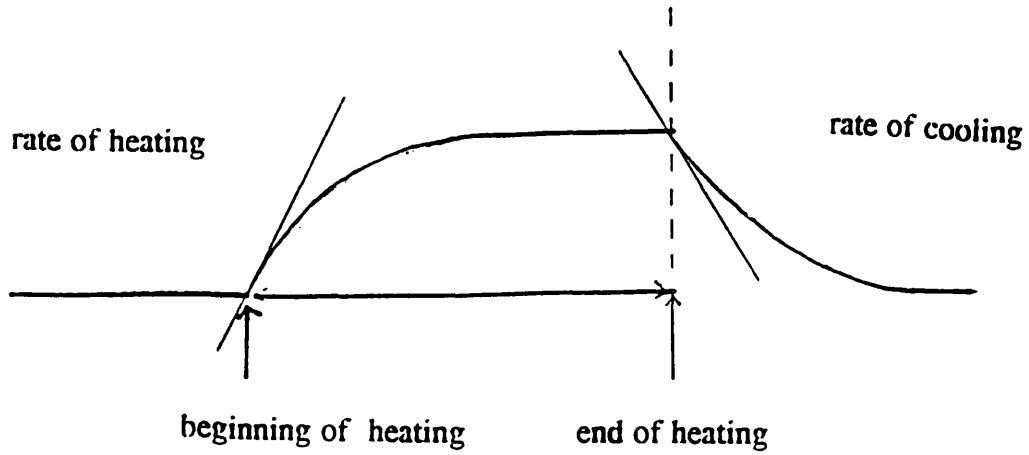
Figure 6a An example of a thermopile collected during a long period of peltier heatingpeltier heating.

b.

slope $1/ITn^2\alpha^2$

C_T

$C_M \longrightarrow$
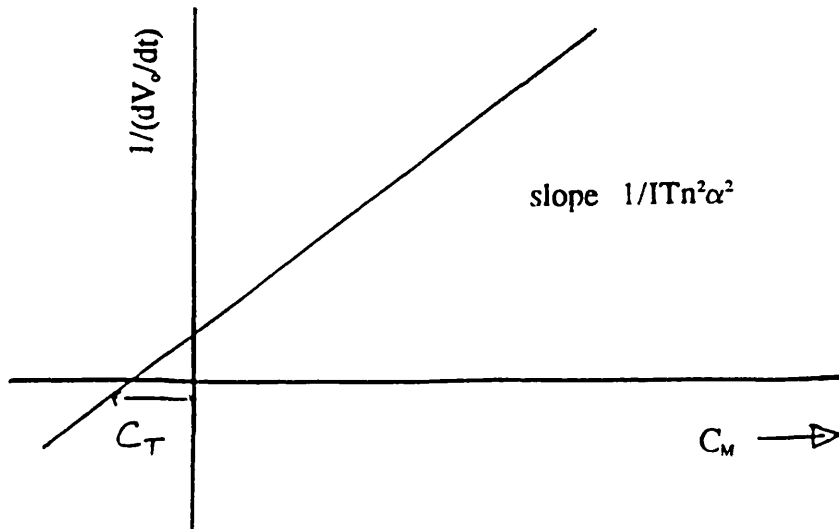
Figure 6b The relation between voltage change and the heat capacity of the heat recording system.of C_T is the heat capacity of the thermopile and C_M is the heat capacity of the metal blocks used in the calibration.

46

of $1/(dV_o/dt)$ against C_M as shown in Figure 6b, will give a line with a slope of $1/ITn^2\alpha^2$ and an intercept of C_T. I, T and n are constants, so, α can be determined from the slope of this line.

2.9.3 Calibration of the thermopile signals

The rate at which heat is delivered to the system during peltier heating is measured in Js^{-1} and gives a proportional voltage change of dV_o/dt measured as Vs^{-1}. The calibration of the can be defined as (rate of heat delivered/rate of voltage change) J/V.

2.10 NORMALISATION OF RECORDS

In order to compare the results obtained in different works the measurements of force, velocity, heat and power output made have to be normalised. In this work the measurements made are normalised following the methods described by Woledge et al. (1985, p18-19).

2.11 CRITERIA USED FOR SELECTING DATA

The experiments reported here compared the effect of increasing the magnesium concentration in Ringer's solution from 1 mM to 20 mM it was important that each fibre was tested in 1) the control solution, 2) the high magnesium solution and 3) the control solution again. The results included in this report were from fibres which a) completed this cycle, b) had undergone three repeatable contractions in each solution

52

and c) maintained at least 80% maximum force throughout the course of the experiment. These criteria led to a less than 50% success rate.

CHAPTER 3

THE EFFECT OF INCREASING EXTRACELLULAR MAGNESIUM ION
CONCENTRATION ON FORCE PRODUCTION AND RELAXATION RATE

3.1 INTRODUCTION

Relaxation rate gives a measure of the rate of calcium removal from the myoplasm
and troponin by the calcium pump of the sarcoplasmic reticulum and parvalbumin.
In order to assess the contribution of parvalbumin to relaxation this rate has to be
measured at a time when the changes in the levels of free calcium in the myoplasm
are independent of calcium dissociation from troponin. It has been suggested that
this might be possible in the first 5% fall in tension (Peckham and Woledge, 1985)
when relaxation rate is due to the changes in the myoplasmic calcium levels alone.

Ashley and Ridgway (1970), using barnacle muscle, showed that light emission by
aequorin, a bioluminescent calcium binding dye can be used to measure free calcium
levels in living muscle. Following this pioneering work, aequorin has been used in
different muscles to measure calcium transients and thus changes in free calcium
during contraction and relaxation (Blinks et al., 1978, Cannell, 1984). Measurements
using other intracellular calcium ion indicators have shown similar results to those
obtained using aequorin (Irving et al. 1989, Baylor et al., 1978). The measurement
of force production and the accompanying changes in calcium transients during a
tetanus can be used to determine the period, during contraction, when myoplasmic

calcium changes appear to be independent of calcium cycling between the crossbridges and the sarcoplasmic reticulum, and so determine a period when myoplasmic calcium binding sites most influences changes in free calcium.

Figure 7, shows that records of force production during a tetanus can be divided into five sections; 1) the rising phase, 2) the plateau phase, 3) the linear phase, 4) the exponential phase and 5) the post mechanical relaxation phase. Each one of these phases reflects different calcium handling processes in the muscle as described below.

3.1.1 The rising phase

Following stimulation, there is a rapid increase in light emission by aequorin. This increase in light emission is accompanied by a rapid rise in force. The increased light emission confirms calcium entry into the myoplasm during this period and the rise in force confirms calcium binding by troponin to form the TnCa complex which initiates contraction. This initial phase of contraction is therefore inappropriate for the study of calcium binding to parvalbumin as the changes in free calcium are too strongly influenced by the calcium-troponin reaction.

3.1.2 The plateau phase

During this period of contraction the force remains approximately constant. The aequorin light signal, however, is shown to decline and then rise to a value lower than that reached initially. The decrease in light signal following the attainment of
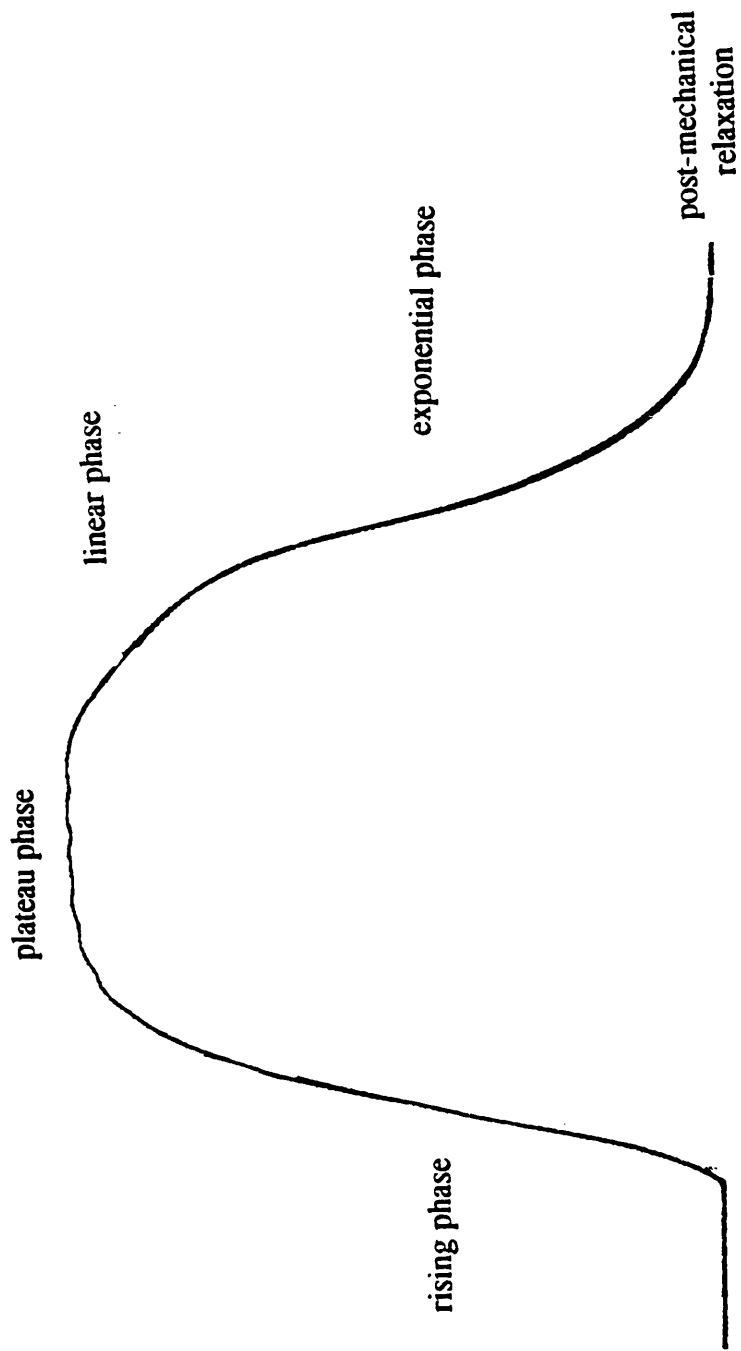
Figure 7   A diagram showing the five phases of contraction.

maximum force suggests the binding of calcium to a site other than troponin. The effect of this site on the levels of free calcium is, however, hidden by the maintenance of a fairly steady force during a tetanic contraction.

The routes available for calcium removal during this phase of the contraction when a steady state between calcium concentration and force production has been attained are calcium return to the sarcoplasmic reticulum via the calcium pump and calcium binding to parvalbumin. The steady state suggests the rate of calcium dissociation from troponin is independent of calcium concentration in this part of contraction ie there is no net change in the concentration of the species taking part in the reaction Tn + Ca ⇌ TnCa, the force producing reaction. The finite decrease in light emission suggests that this effect is not due to calcium uptake by the sarcoplasmic reticulum as this process would be fully turned on at the calcium concentrations recorded during this phase. The route that then remains is the parvalbumin route. Interrupted tetani are used to unmask this effect.

3.1.3 The linear phase

After an interval without any change in tension following the end of stimulation, the tension falls in an approximately linear manner. The end of this period is marked by a sharp decline in force, the shoulder, which leads into the exponential phase. The shoulder coincides with internal sarcomere length adjustments (Edman and Flitney, 1982) and overlaps in time with calcium dissociation from troponin. During the linear decline in tension preceding this break the troponin-calcium remains approximately

58

in equilibrium with the free calcium concentration of the myoplasm. The changes in free calcium levels are therefore not strongly influenced by the dissociation of calcium from troponin. Changes in relaxation rate during this period would therefore be expected to reflect changes in calcium buffering by myoplasmic calcium binding sites.

3.1 4 The exponential phase

During this period, which occurs immediately after the shoulder, calcium is dissociating from troponin and the force is also falling rapidly. This period appears to represent the reverse of the calcium activation curve when the rate of calcium dissociation is rapid and non-linear. The exponential decline in force therefore appears to represent a rather complex set of processes when the dissociation of some calcium leads to an even more rapid dissociation of the remaining calcium. The emphasis here is on the reaction of calcium with troponin. It would be difficult to isolate the component of relaxation due to the parvalbumin-calcium reaction during this phase of contraction.

3.1.5 Post-mechanical relaxation

Following the end of mechanical relaxation, aequorin luminescence continues to decline towards rest levels with a slow time constant (Cannell, 1984). This slow calcium tail is thought to reflect calcium dissociation from a myoplasmic site other than troponin, possibly the dissociation of calcium from parvalbumin. The rate of relaxation during this phase suggested to depend on the rate of calcium dissociation

from parvalbumin, which is slow (Cuneal, 1984), and the rate of calcium uptake by the calcium pump of the sarcoplasmic reticulum. The calcium pump rate appears to be of particular importance here in lowering calcium level in the myoplasm to that seen at rest. This final rate of relaxation is important because it influences the rate at which the parvalbumin buffer is reprimed and hence available to buffer calcium in subsequent contractions. For the reasons laid out above, relaxation rate was measured during the linear period of force decrement in both the short and interrupted tetani. In summary, the calcium movements described above can be represented by the diagram below:
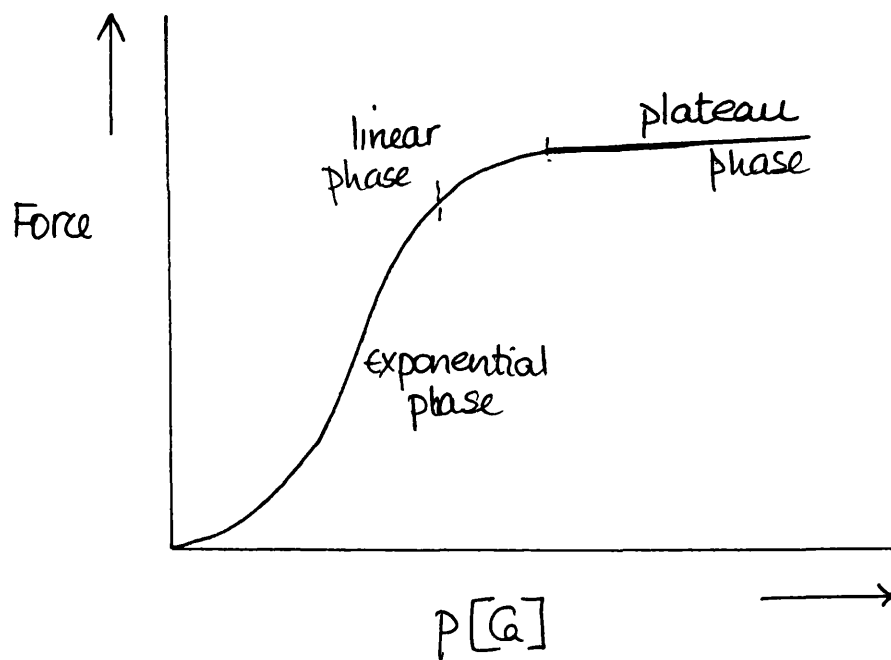
3.2 EXPERIMENTAL PROTOCOL

3.2.1 Stimulation

The optimal conditions for the production of maximum force were determined at the start of each experiment as previously described. The stimulation protocols then varied as follows: 1) in the study of the effect of increasing the dose of the extracellular magnesium ion concentration, tetani of 300 ms duration were recorded every a 10 minute, 2) during the experiments to determine the time course of the effect of magnesium, the fibres were stimulated every 2 minutes for 300 ms, 3) for the experiments on the interrupted tetani, the fibres were stimulated for a total of 5 s using a stimulation pattern in which a 200 ms stimulation period was followed by a 300 ms period of no stimulation. At least three interrupted tetani were measured in each solution with a 10 minute of recovery allowed between contractions.

3.2.2 Recording

A two channel recording was used to obtain the force record as well as the stimulus trace of that record. The short tetani during the dose-response experiments and the results of the time course experiments were recorded on a Nicolet 402 oscilloscope. The interrupted tetani were recorded on a computer functioning as an oscilloscope. The computer software package MICROSCOPE was used for these recordings. Force was measured using an AE801 force transducer in all these experiments.

3.4 CALCULATION OF RELAXATION RATE

A computer programme designed to measure a 2.5% fall in tension was written using the software package WFBASIC. Records obtained using MICROSCOPE were read into this programme before any analysis could be carried out. The programme was designed to determine the time of the last stimulus, T_{max}, from the stimulus trace, and the force at that time F_{max}, which is defined as the maximum force for that period of contraction, the time, $T_{97.5}$, at which the force reached 97.5% of F_{max}. The relaxation time, R, was calculated as $(T_{97.5} - T_{max})$. A second programme written in BASIC then calculated relaxation rate as (1/R). This gives ten measures of relaxation rate in the experiments using interrupted tetani. See Figure 8 for the constructions used.

In the experiments on the short tetani, relaxation rate was also measured for a 5% decrement in force. These records were made on a Nicolet 402 oscilloscope with a time resolution of 1 μs. The time for the 2.5% fall in tension was measured directly off the oscilloscope and the relaxation rate was then calculated as a reciprocal of this time. The same procedure was followed in determining the relaxation at 95% maximum force.

3.5 RESULTS

3.5.1 The effect of increasing magnesium on force production

Figure 9 shows examples of tetani obtained from muscles bathed in Ringer's solutions

62
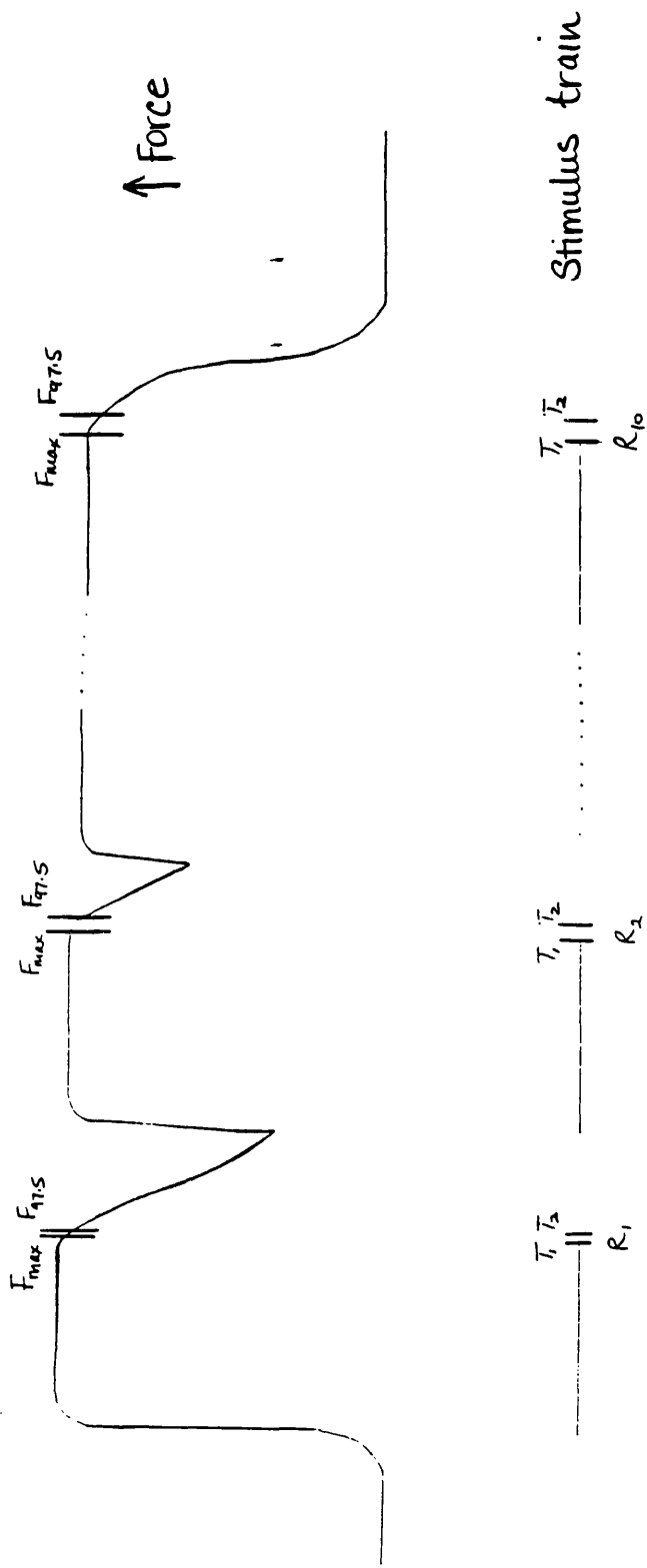
Figure 8 A diagram of an interrupted tetanus showing the method used to calculate relaxation time. The time of the last stimulus and the force at time was marked on the tetanus record, T_1. The velue of the force equal to 97.5% of this maximum force was then calculated and this point marked on the force record. Lastly the time at which this force was attained was determined, T_2. These calculations were then fed into a second computer programme which calculated relaxation time as (T_2-T_1). The relaxation rate for that phase of the contraction was then calculated as the reciprocal of this value, $(1/R)$.

with magnesium ion concentrations of 1, 5, 10 or 20 mM. The records show that raising extracellular magnesium ion concentration from 1 mM to 20 mM results in a decrease in the tetanic force produced. The records also show the magnesium effect to be dose dependent. Returning the fibre to the control solution restores the force. A plot of the percentage force developed (force is defined as 100% force in the control solution), as a function of the magnesium ion concentration in Ringer's, again shows the concentration dependent decline in force production when the extracelluar magnesium ion concentration is raised above 5 mM, Figure 10. The largest decrease in force, 11%, is seen when the fibre is in the 20 mM magnesium ion solution

3.5.2 The effect of increasing the concentration of extracellular magnesium on relaxation rate.

The records in Figure 9 also show that increasing the extracellular magnesium ion concentration decreases the time required for force to return to rest levels after the end of stimulation. When the shoulders of the records are enlarged and superimposed at the time of the last stimulus as shown in Figure 11, it becomes clear that relaxation is fastest when the fibres are soaked in the Ringer's solution with a magnesium ion concentration of 20 mM and slowest when in the control solution. Figure 12, shows plots of relaxation rate measured at 97.5% and 95% of maximum force. The relation between relaxation rate and extracellular magnesium ion concentration is shown to be positive and non-linear. The increase in relaxation rate appears to saturate at magnesium ion concentrations above 20 mM in both plots. The similarity in the

Figure 9   Typical records of force production by fibres in Ringer's solution with varying magnesium ion concentrations. Increasing the extracellular magnesium ion concentration from 1 mM (1) to 5 mM (2) to 10 mM (3) to 20 mM (4) results in a dose-dependent decrease in force. Returning the fibre to the control solution (5), reverses the high magnesium effect.

Figure 10   The relation between force production and extracellular magnesium ion concentration. Plotting the force as % maximum force +/- SEM (n=4) shows a linear relation between force decrement and extracellular magnesium ion levels above 5 mM.

50 mN mm^{-2}

·05s

Extracellular magnesium ion concentration (mM)
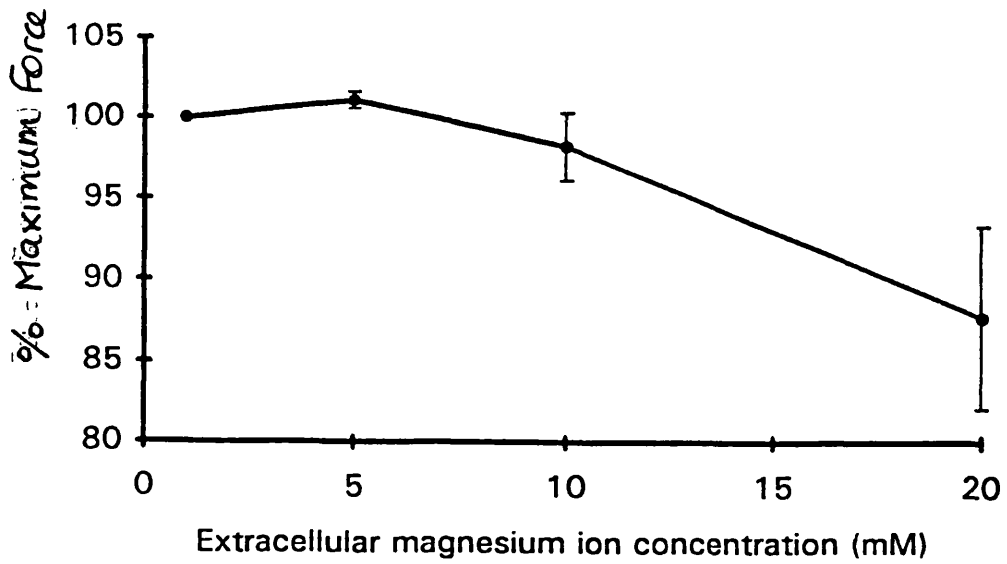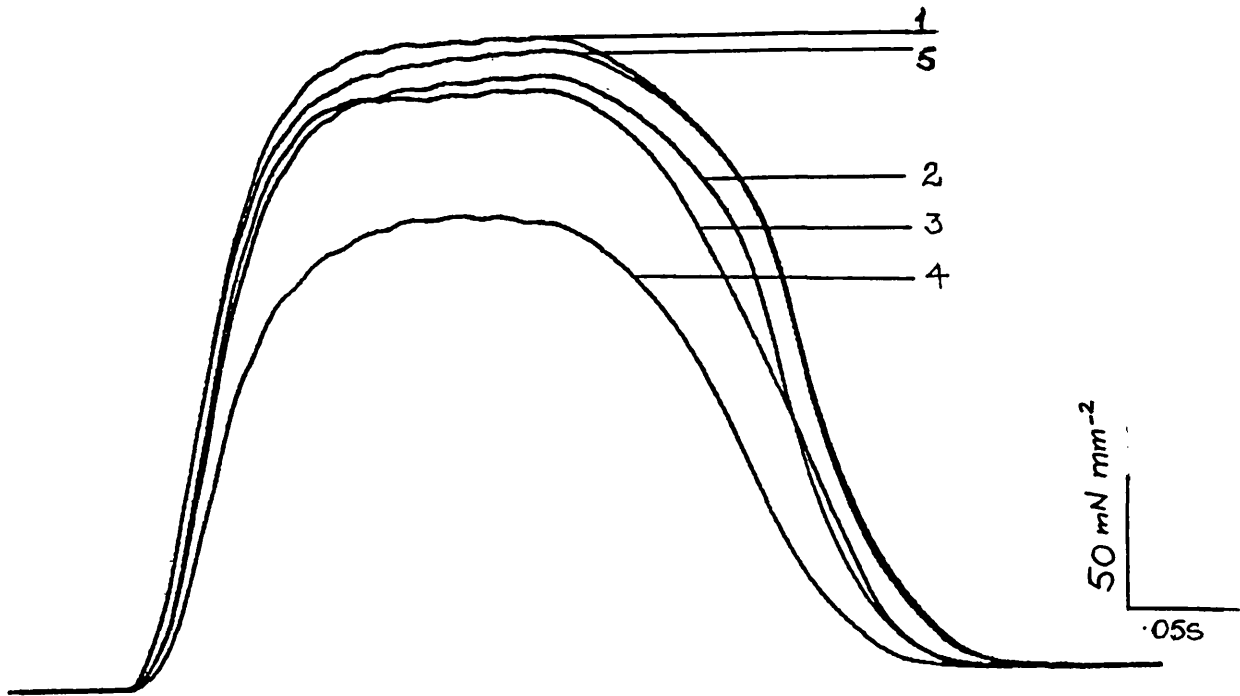
Figure 11   Records showing the end of the plateau and the beginning of the linear phases of contraction as defined in Figure 7.   This figure shows the records of tetanic force in Figure 9 enlarged and superimposed at the time of the last stimulus.   It shows that the rate at which the force decreases towards rest levels increases with increasing magnesium ion concentration.

Figure 12 This figure shows that increasing the concentration of free magnesium in Ringer's solution increase relaxation rate.   The relaxation rate +/- SEM, (n=4), measured at 97.5% and 95% of the force at the time of the last stimulus is dose-dependent.

LAST
STIMULUS

Force

time

1
5
2
3
4

25

20 ———————————————————— 97·5%

15 ———————————————————— 95·0%

Relaxation rate (/s)

10

5

0

0 2 4 6 8 10 12 14 16 18 20

Extracellular magnesium ion concentration (mM)
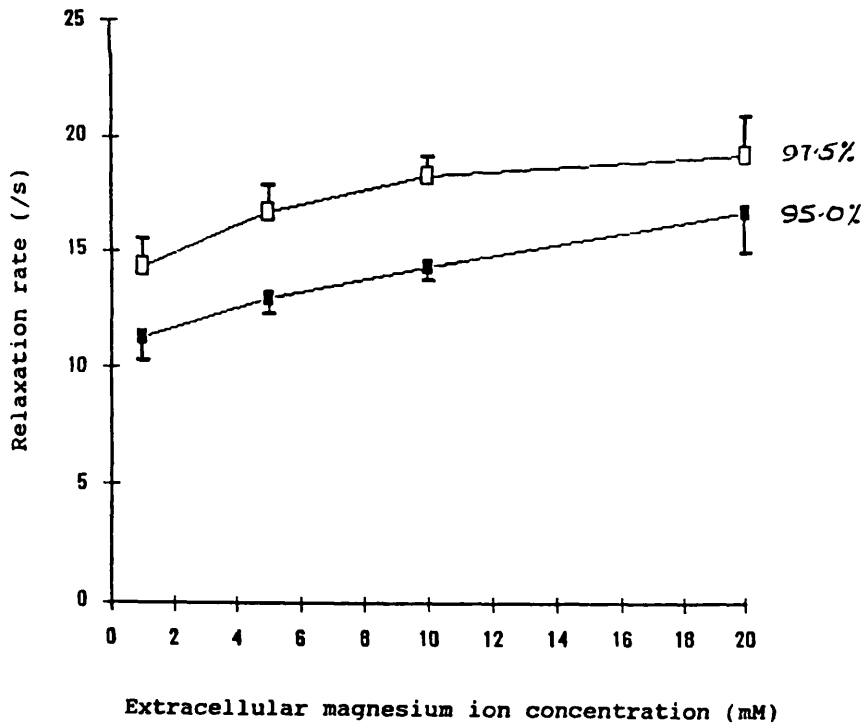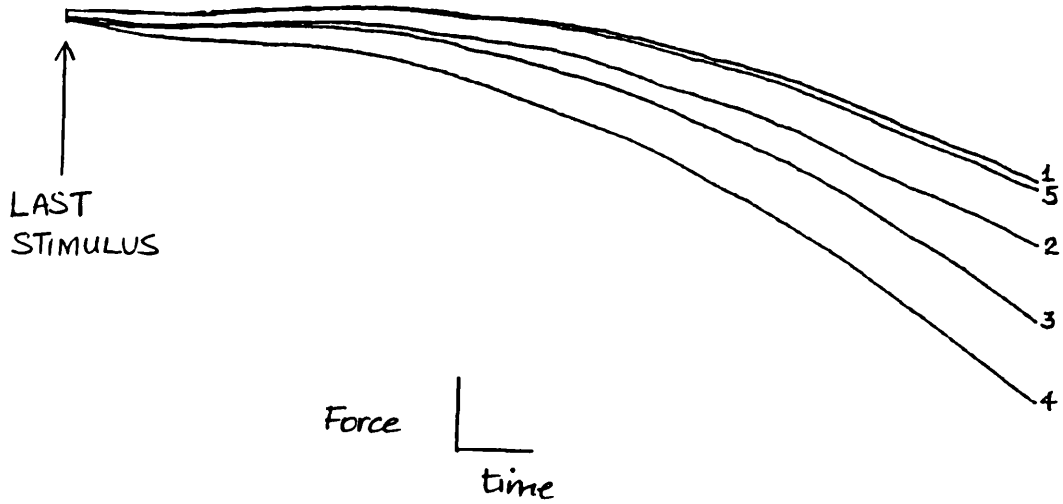
shapes of these plots suggests that the same processes are acting to reduce force at 97.5% tension as at 95%, the point at which Peckham (1985) measured relaxation rate.

3.5.2.1 The relation between force production and relaxation rate

In Figure 13 , the fractional changes in force and relaxation rate are compared as the extracellular magnesium ion concentration is raised. The force produced when the fibres are in the control solution and the relaxation rate measured in the control solution are defined as 100%. The difference in the shape of the plots shows that increasing the concentration of extracellular magnesium has qualitatively different effects on these muscle properties. High magnesium increases relaxation rate but decreases force. The relaxation rate also increases to a larger extent, in percentage terms, than the effect on force declines. This suggests the change in relaxation rate when extracellular magnesium ion concentration is raised cannot be attributed to the observed changes in force.

3.5.2.2 The effect of increasing extracellular magnesium ion concentration on individual fibres

A separation of the pooled data of relaxation rates presented in Figure 12 into the relaxation rates of the individual fibres, Figure 14, shows that the initial rates of relaxation vary amongst fibres from the same muscle and between muscles. In the three fibres from the same frog, the relaxation rates in the 1 mM magnesium ion

Figure 13 A comparison of the relation between the fractional increase in relaxation rate (●) and the fractional decrease in force (○) when the concentration of extracellular magnesium ions is raised from 1 mM to 20 mM. The data are means +/- SEM, n=4.

Extracellular magnesium ion concentration (mM)

Fractional change
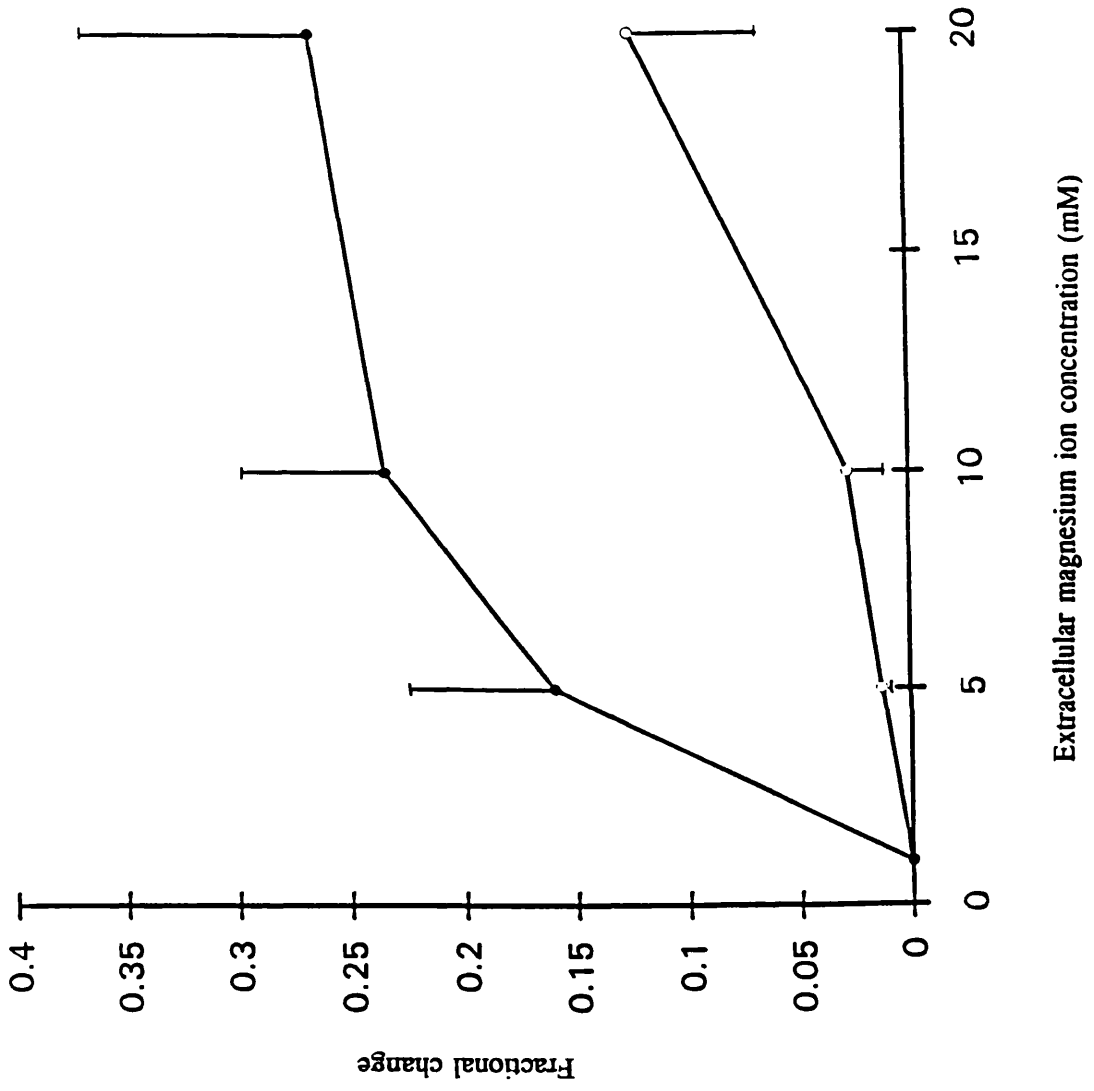
Figure 14 The relationship between relation rate and extracellular magnesium ion concentration in 4 different single fibres (three from the same frog) shows that the initial relaxation rates, measured in the 1 mM solution, vary in fibres from the same muscle. The relaxation rates then converge to a similar value in the fibres from the same frog. Each point represents the mean of several (3-6) observations from the same fibre.

Same muscle

Relaxation rate (/s)

Extracellular magnesium ion concentration (mM)
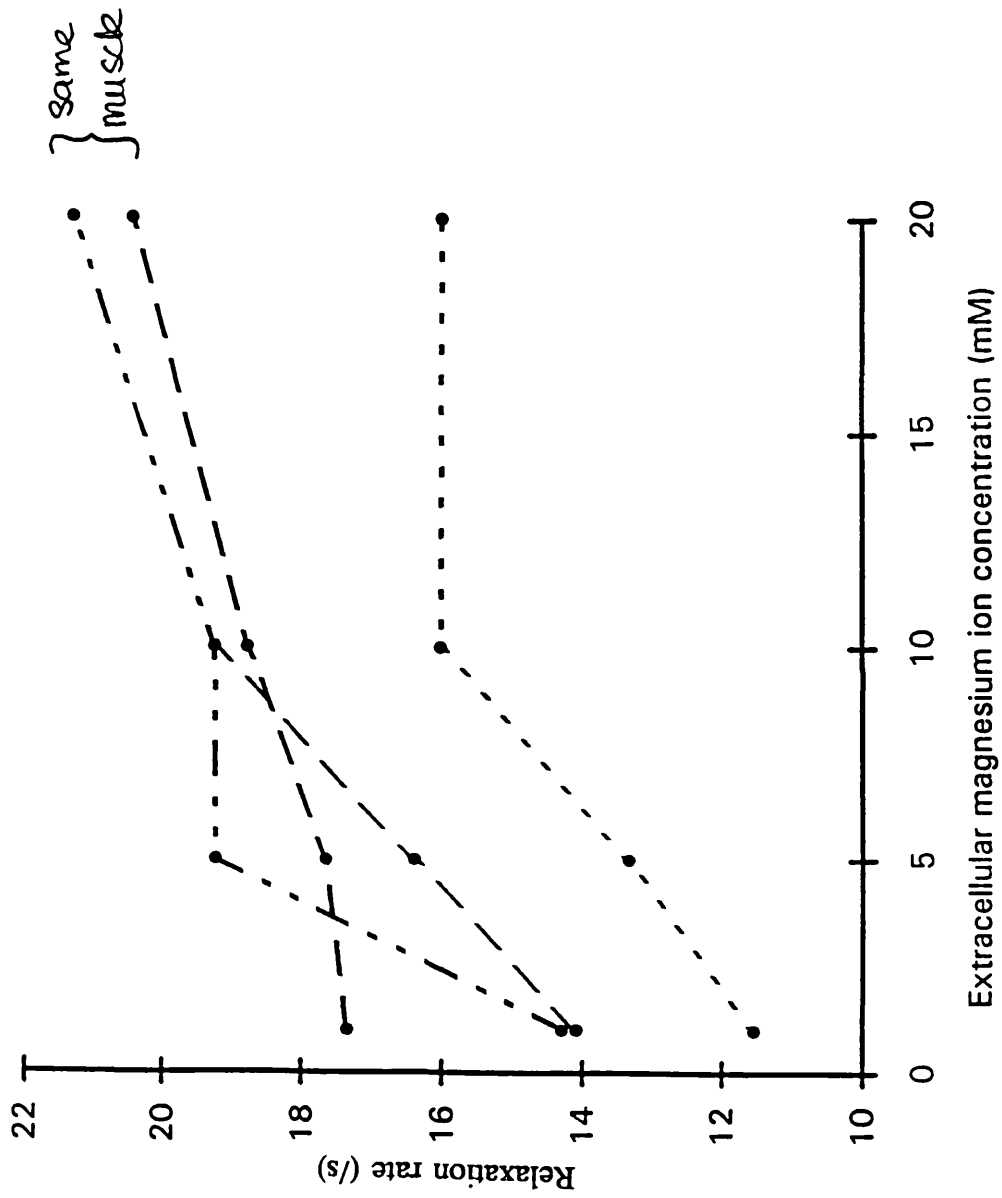
solution are different. However, increasing the concentration of magnesium in the extracellular fluid decreases the differences in the relaxation rates until the values converge at a magnesium concentration of 20 mM. A similar saturating effect is seen in the relaxation rate of the fourth fibre ie the relaxation rate increases from its value when in the control solution and reaches a constant value when the extracellular magnesium ion concentration reaches 20 mM. These results suggest a variation in intracellular magnesium ion concentrations in fibres with the same parvalbumin concentration.

An examination of the relation between relaxation rate in the control solution and the percentage increase in relaxation rate as extracellular magnesium ion concentration is raised, as presented in Figure 15, shows that the fibre with the lowest initial relaxation rate shows the greatest increase in relaxation rate. The fibre with the highest initial rate, on the other hand, shows a decrease in relaxation rate. This again suggests the possibility of different levels of the magnesium in fibres with the same total parvalbumin concentration.

3.5.3 The time course of the onset of the magnesium effect

Figure 16, shows the time course with which relaxation rate changes when extracellular magnesium ion concentration is raised. An increase in relaxation rate is seen in the first 2 minutes of exposing the fibres to the 20 mM magnesium ion solution. The relaxation rate then increases an average 42% in the next 10 minutes of the fibre bathing in the high magnesium solution. This increase is then maintained
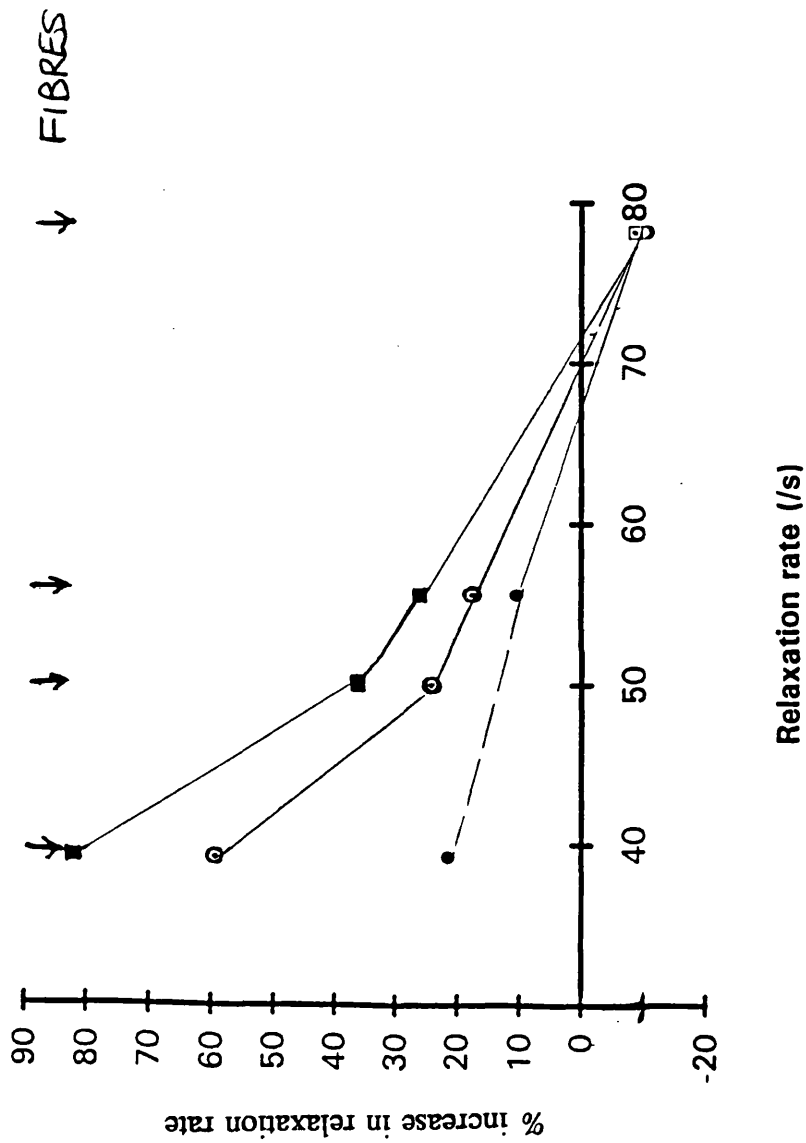
Figure 15 The increase in relaxation rate as extracellular magnesium ion concentration is raised from 1 mM to 5 mM ( ), 10 mM ( ) and 20 mM depends on the relaxation rate in the 1 mM magnesium ion solution. Each point represents an average of 3-6 observations on 4 fibres.
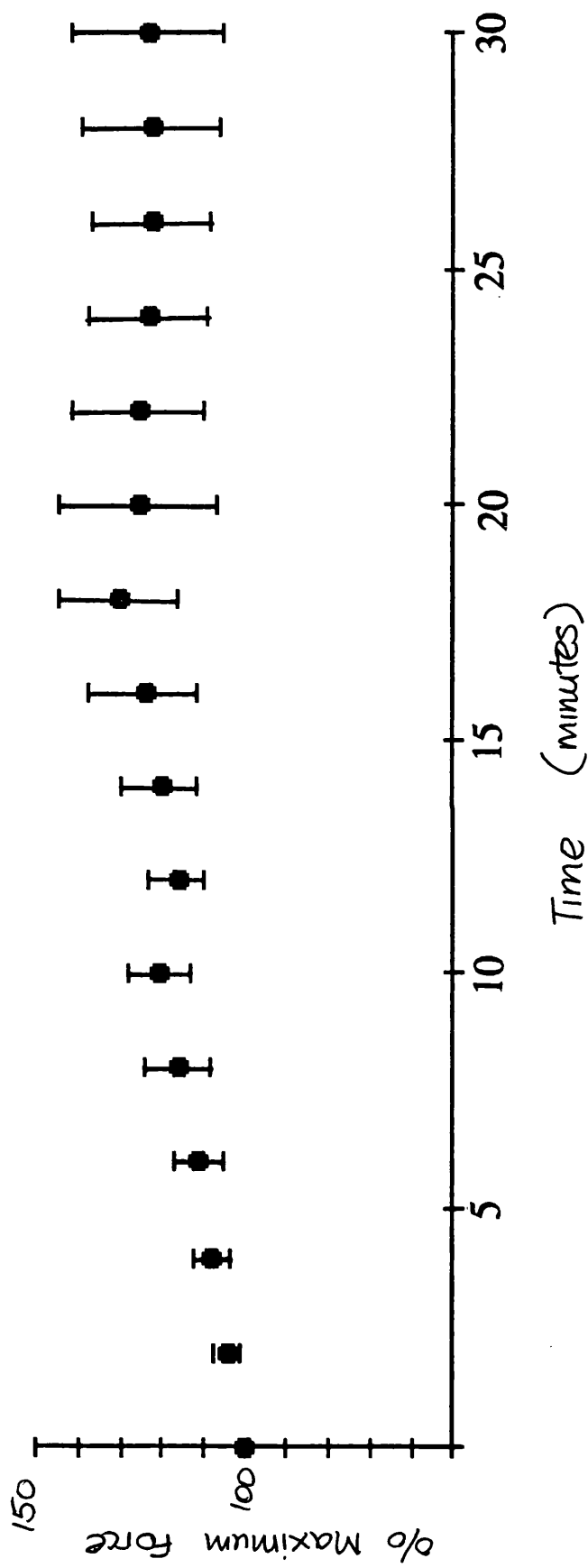
Figure 16 The relation between relaxation rate and incubation period in 20 mM

magnesium ion Ringer's. The data are presented as means +/- SEM (n=4).

for the duration of the incubation period. The large standard error measurements recorded at the end of the period of exposure to high magnesium for this data are thought to reflect a variation in the initial relaxation rates of the fibres used as previously suggested. These results suggest that changes in the free magnesium levels reach equilibrium in the first 10 minutes of exposure to the high magnesium solution. The maintenance of a steady relaxation rate after this period also suggests a saturation of the magnesium binding sites which influence relaxation during this time period.

3.5.4 The effect of increasing extracellular magnesium on relaxation rate during a prolonged contraction.

3.5.4.1 Force production

Figure 17 shows examples of interrupted tetani obtained from fibres contracting in Ringer's solution with magnesium ion concentrations of 1 mM and 20 mM. Force rises sharply to a maximum value which is then well maintained for the duration of the contraction when the fibre is in the control solution. When the fibre is exposed to the high magnesium ion solution, force rises rapidly to its maximum value in the first period of contraction. However, it then declines to a new value which is reached during the fourth period of contraction. This lower force is maintained for the duration of the contraction. On returning the fibre to the control solution, the force returns to its control level and again it is well as maintained. The decline in force during this early phase of contraction when the fibre is in the high magnesium ion solution suggests a "relaxing" effect of the myoplasmic sites on troponin ie the

Figure 17 Typical records of interrupted tetani show that increasing extracellular magnesium ion cancentration from (a) 1 mM to (b) 20 mM results in a decrease in the force during the plateau phase of the tetanus. The higher concentration of magnesium also increases relaxation rate as seen by the deeper troughs in the records during the periods when stimulation is interrupted. Returning the fibre to the fibre to the control solution, (c), restores both force and relaxation rate to the levels seen before exposure to high magnesium.

1 mM
after exposure

150 mN mm⁻²

2s

20 mM

1 mM
before exposure
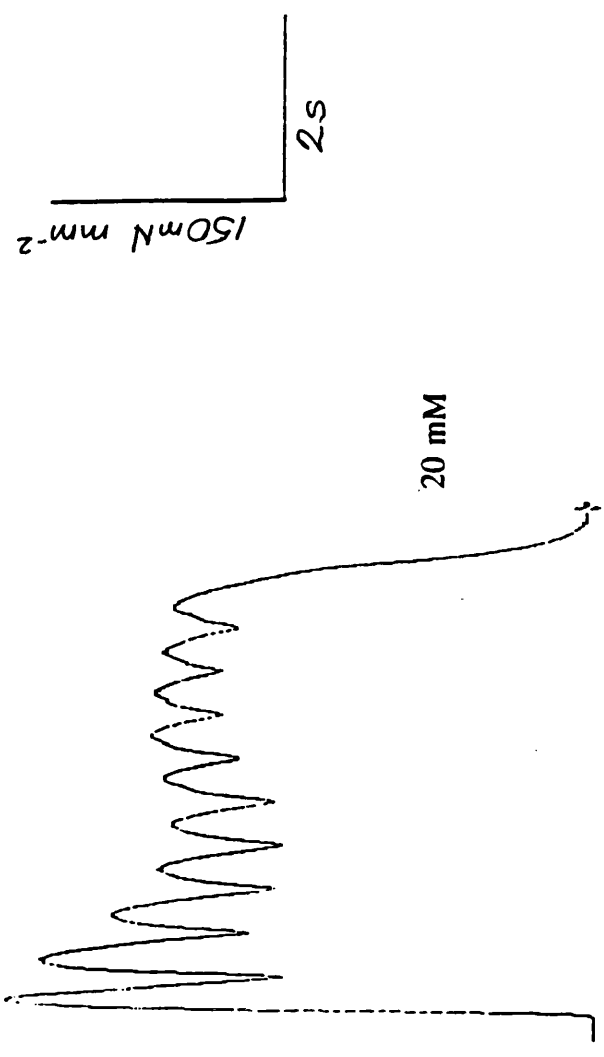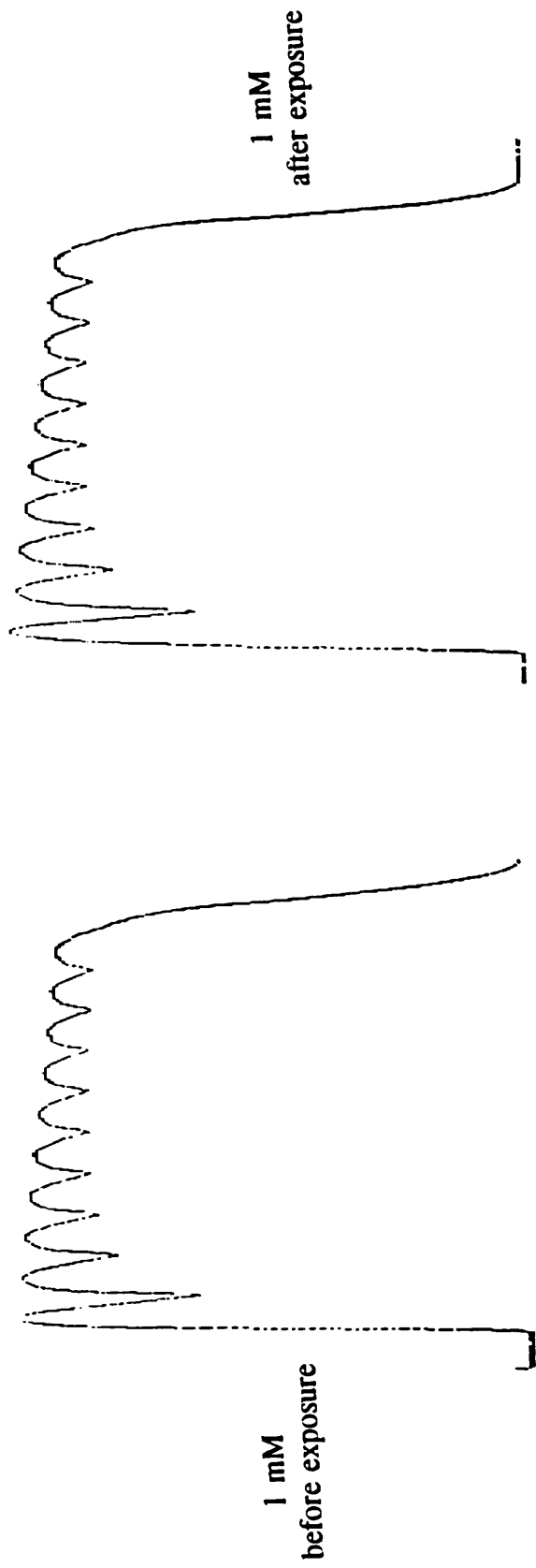
removal of calcium bound to troponin during the early part of the contraction to a myoplasmic site when its buffer capacity is raised.

3.5.4.2 Relaxation rate

The records of interrupted tetani in Figure 17, also show that force declines to different levels during the interruptions to stimulation in the two solutions. The value to which the force declines, seen as the trough during the period with no stimulation, gives a measure of the relaxation rate at that time of the contraction. The value to which the force declines during the interruption is lowest in the first period of contraction in both solutions. The decrease in force then diminishes until the interruptions to stimulation result in the same force decrement. In the contractions with the fibre in the control solution, this steady relaxation rate is attained within the first five periods of contraction. During the contraction in the high magnesium solution, the initial decrease in force is greater than that measured in the control solution and the final rate of relaxation is attained in the sixth period of contraction. This suggests the high magnesium solution increases the initial rate of relaxation rate and prolongs the period during which these sites are active.

In order to quantify these effects of high magnesium, plots of relaxation rate as a function of tetanus duration were constructed in, Figure 18. The plots show that relaxation is high at the beginning of contraction and then declines to a steady level which is maintained for the duration of the contraction. A comparison of the relaxation rates in the two solutions confirms the higher initial relaxation rate in the

Figure 18 The relation between relaxation rate and tetanus duration during interrupted tetani of 5 s duration. The fibres are bathed in 1 mM (o) and 20 mM magnesium ion (•) Ringer's solution. The data are plotted as relaxation rate +/- SEM, n=8.
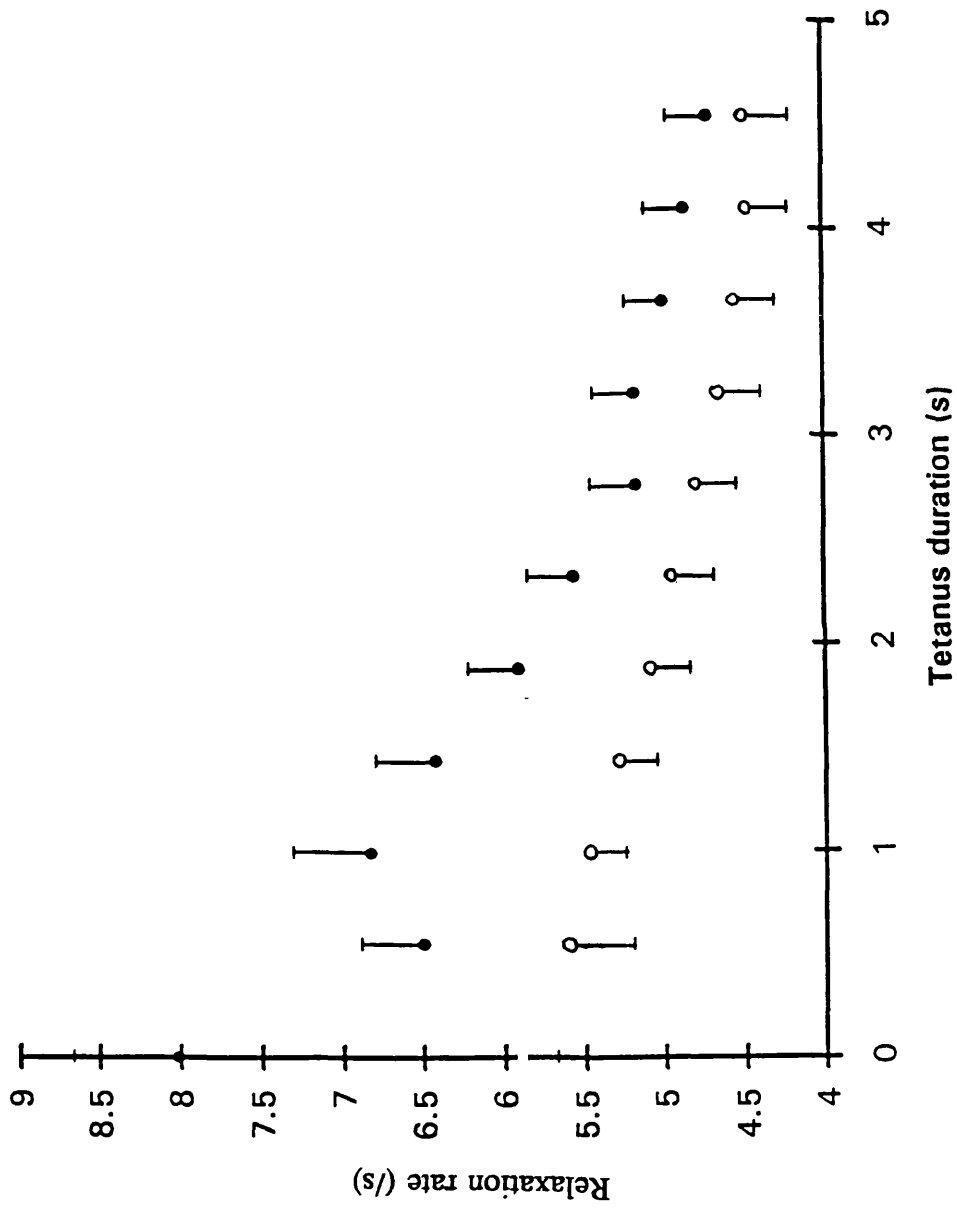
high magnesium ion solution initially. The final relaxation rate in the high magnesium solution then tends to the final rate measured in the control solution. Back extrapolation to time zero of the contractions which will give some measure of the initial parvalbumin-magnesium concentration in the myoplasm of the fibre in the rest period preceding the contractions shows that the initial relaxation rate in the high magnesium solution is significantly higher (p < 0.05) $8.02 +/- 0.89$ s^{-1} than in the control solution, $6.50 +/- 0.23$ s^{-1}, while the final relaxation rate increases only 7% from $4.55 +/- 72$. The effect is then reversed when the fibre is returned to the control solution.

Fitting a line to the experimental plots, Figure 19, shows that the relaxation rates in the two solutions can be described by a monoexponential of the form

$$R = R_I (1-e^{-t/\tau}) + R_F$$

where R is the relaxation rate at time t, R_I, is the "extra" relaxation rate, here attributed to the myoplasmic calcium buffers, and R_F, the final relaxation rate, which is attributed to the steady action of the calcium pump of the sarcoplasmic reticulum. From this relation, it can be seen that the changes in relaxation in the high magnesium solution can be explained by a higher initial concentration of calcium buffer and a slower time course for the saturation of these sites, the slower time constant.

When the contribution of the myoplasmic sites ie the parvalbumin sites to relaxation is isolated by the subtraction of the final relaxation rate from the initial relaxation rate (R_I-R_F), the contribution of parvalbumin to relaxation is seen to increase from 1.95 s^{-1} to 3.16 s^{-1}, an increase of 62%. A measure of the area between the plot and the

Figure 19 The data shown in Figure 18 have been fitted with a single exponential described by the equation $R = R_I (e^{if}) + R_F$. R_I is the initial relaxation rate and R_F is the final relaxation rate. Only one curve is seen because the 1 mM data (B) have been shifted to the right and up in order to superimpose it on the 20 mM data (A).
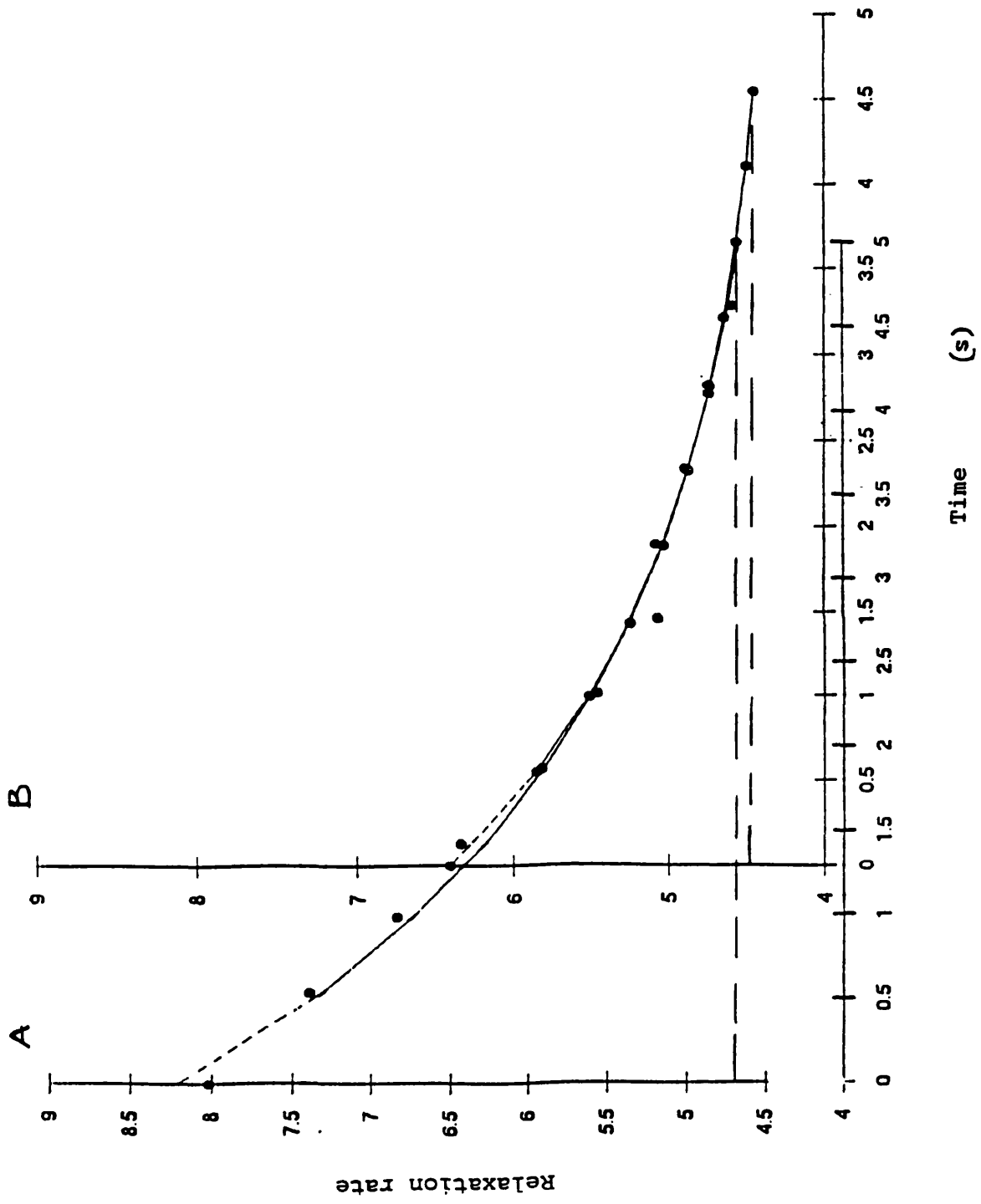
dotted line representing the final rate of relaxation on the superimposed records shows that the major difference in records is in the area in the early part of the contraction. This area which can be used to estimate the calcium concentration associated with parvalbumin during contraction, points to a greater handling of calcium by the myoplasmic calcium buffers in the high magnesium solution.

A summary of these findings is presented in Table 3.

3.6 DISCUSSION

Abbott (1950) reported a slowing of relaxation with tetanus duration, a phenomenon that is now described as the Abbott effect. Following the initial description of this effect, it has been demonstrated that the second of two closely spaced tetani has a slower relaxation rate than the first (Curtin, 1976). It has also been shown that resting muscle between contractions allows the relaxation rate to recover towards its initial value (Peckham and Woledge, 1985, Hou et al., 1991). These observations on the slowing and recovery of relaxation are attributed to a slowing of calcium uptake by the myoplasmic calcium buffer, parvalbumin, as the parvalbumin-magnesium concentration is reduced during a prolonged tetanus. Increasing the concentration of free magnesium at rest, as is suggested with this treatment, is expected to increase the initial concentration of parvalbumin-magnesium in the myoplasm and so result in an increase in the initial relaxation rate of the muscle following activation.

The concentration of the calcium buffer in the myoplasm is increased by raising the

Table 3 A summary of the effect of increasing extracellular magnesium ion concentration on relaxation rate.

	1 mM Mg^{2+}	20 mM Mg^{2+}	percent change
initial rate (s^{-1})	5.90 ± 0.2	8.02 ± 0.9	23
final rate (s^{-1})	4.55 ± 0.7	4.86 ± 0.2	7
Pa rate (s^{-1})	1.95	3.16	62
τ	0.93 ± 0.1	1.39 ± 0.2	50
area under curve	4.21 ± 0.3	6.73 ± 1.2	60

concentration of magnesium ions in the extracellular fluid and decreasing the extracellular sodium ion concentration at the same time. These changes in the extracellular fluid are expected to increase magnesium entry into the myoplasm as well as decrease magnesium extrusion by the sodium/magnesium pump of the sarcolemma (Blatter, 1991, Gonzalez-Serratos and Rasgado-Flores, 1990, Pusch et al., 1989). A return to the control solution is then expected to restore the sodium/magnesium pump to normal and so return the intracellular magnesium ion concentration to normal. Adjusting the concentrations of magnesium and sodium ions in the Ringer's solutions as described above is expected to double the concentration of free magnesium ions in the myoplasm when extracellular magnesium ion concentration is 20 mM (Blatter, 1990). The high magnesium solutions used in these determinations are expected to have no effect on either the membrane potential of the fibres nor their osmolarity (Blinks et al., 1978). The changes seen in the high magnesium solutions can therefore be attributed to the changes in ion levels alone.

A calculation of the acceptable limits of free magnesium concentration which would provide a sufficient concentration of parvalbumin to make it an effective buffer was carried out by Maughan and Godt (1989). This calculation, which was carried out using all the significant magnesium binding sites of the myoplasm, sets the range of free magnesium ion concentrations which would result in an effective parvalbumin-magnesium calcium buffer level between 0.8 mM (Maughan and Godt., 1988) and 2.5 mM (Somlyo and Somlyo, 1985) when total myoplasmic parvalbumin concentration is 1.0 mM. Outside these concentrations parvalbumin-magnesium is thought to be either too low or too high to influence relaxation. The values of parvalbumin-

magnesium outside these limits are either too low or too high to be effective or, the concentrations are not physiological concentrations already reported in frog muscle. The variation in intracellular magnesium ion levels expected with the treatment used in these experiments, 0.9 mM - 1.86 mM lies within acceptable range.

In muscle fibres with a parvalbumin concentration of 0.76 mM (Hou et al., 1991), a two-fold increase in free magnesium ion concentration should increase parvalbumin-magnesium concentration from 0.912 to 1.5 mM if the initial ratio of the concentrations of parvalbumin-magnesium to parvalbumin-calcium is 60:40. This would increase the concentration of parvalbumin sites which would become available to bind calcium by 228 μM.

The increase in the final rate of relaxation, the rate attributable to the calcium pump of the sarcoplasmic reticulum with this treatment, is 7%. If relaxation was determined by the rate of calcium uptake by the sarcoplasmic reticulum alone, a process that proceeds with a V_{max} of 700 mol $l^{-1}s^{-1}$ at 25°C and has a Q_{10} of 3 (Ogawa,1970,1980, Weber, 1976), the removal of 700 μM of calcium by the sarcoplasmic reticulum at 5°C would require approximately 10 s from 1 litre of muscle fibre water. A time period far in excess of that seen for relaxation.

The 60% increase in the contribution of the parvalbumin component of relaxation alone with this treatment suggests the increase relaxation rate seen in the high magnesium solutions arises from an increase in the concentration of parvalbumin-magnesium. The dose dependent increase also supports the contention that the

increase could be mediated by an increase in free magnesium when total parvalbumin content is stable.

Since the parvalbumin content of cells is known to be controlled by the innervation and activity of the muscle in which it is found, it can be expected that only a small variation in total parvalbumin content would show between muscles with fibres of the same fibre type. There is a suggestion of this effect in the results presented in Figure 13. The larger variation would however be expected from seasonal differences (Somlyo and Somlyo, 1981, Lopez et al., 1984) in the free magnesium ion levels of the myoplasm. The large increase in relaxation rate seen in these limits experiments would be expected to reflect this second source of variation.

At low temperatures, therefore, an increase in the concentration of parvalbumin-magnesium could be important in enhancing relaxation rate. This mechanism bypasses the need to depend on the ambient temperature for fast relaxation. Relaxation by parvalbumin can therefore compensate for a reduced calcium pump rate at low temperature.

CHAPTER 4

THE EFFECT OF INCREASING EXTRACELLULAR MAGNESIUM ION CONCENTRATION ON HEAT PRODUCTION

4.1 INTRODUCTION

The heat liberated during contraction has two heat rates: 1) labile heat rate and 2) stable heat rate (Aubert, 1956). The labile heat is attributed to calcium binding to parvalbumin and the stable heat to the ATPase activity associated with calcium cycling between the contractile proteins and the sarcoplasmic reticulum (Curtin and Woledge, 1979). If the increase in relaxation rate that is demonstrated in Chapter 3 is due to the binding of calcium to parvalbumin, as suggested, then an increase in the production of labile heat would also be expected with this treatment.

An increase in the heat produced when extracellular magnesium ion concentration is raised could, however, also reflect an increase in the stable heat rate of the muscle during this treatment. This heat derives from two processes as previously described: 1) the actomyosin ATPase and (Yamada et al., 1976), 2) the ATPase of the calcium pump of the sarcoplasmic reticulum (Homsher et al., 1972, Smith, 1972). An increase in the stable heat rate could thus be due to an increase in either one of these two components.

In order to test the effect of magnesium on the stable heat rate, the force velocity

characteristics and power output of the fibres were determined. The maximum velocity of shortening of the fibre gives information about crossbridge turnover (Edman, 1979) and the power output gives information about the rate of ATP utilisation by the crossbridges during the production of force (Kushmerick and Davies, 1969). From these experiments, some deductions can thus be made about the effect of raising magnesium ion concentration in the extracellular fluid on the crossbridges of the fibres and hence the effect of magnesium on the contribution of these processes to heat production.

The results reported in this chapter are presented in two sections: 1) the effect of raising extracellular magnesium ion concentration on heat production and 2) the effect of the high magnesium solution on the force-velocity characteristics and power output of the fibres..

4.2 EXPERIMENTAL PROTOCOL DURING THE HEAT EXPERIMENTS

4.2.1 The arrangement of the fibre on the thermopile

The fibres were isolated and mounted on the thermopile as previously described. Almost all the Ringer's solution transferred to the thermopile with the fibre was drained before the optimal conditions for maximum force production were determined. Measurements of heat production were made from a 3 mm length in the mid-section of fibre. This arrangement ensured that the heat was measured from a length of the muscle where there was little sarcomere length variation since force development and

ATP utilization is SL dependent (Curtin and Woledge, 1981). It also ensures the measurements are made away from the tendon ends where energy is stored during contraction and then released as heat when the stretch on the muscle is released is released during relaxation.

The thermopile used to make this measurement was 12 mm long and the lengths of the fibres used were all less than 6 mm. The measurement of heat in the midsection of the fibres also provided "protecting" regions at both ends of the fibre. These protecting regions are made up of a portion of the fibre lying over an inactive section of the thermopile. A slight shortening of fibre which would bring a portion of the fibre from the protecting region in contact with the active region of the thermopile would therefore result in no further temperature gradients being set up between the fibre and the thermopile.

4.2.2 Stimulation

The fibres were given a 3.0 s or 3.5 s continuous train of stimuli every 10 minutes. The stimulation period was chosen to exceed 2.7 s, the time at which the relaxation rate was seen to be have reached a steady rate (see Figure 19). The 3 s stimulation was thus expected to give a contraction long enough to also allow a period, at the end of the contraction, when all the labile heat was evolved and the stable heat rate could be determined.

Interrupted tetani were not used because fibre shortening during relaxation results in

an increase in heat production, (Curtin et al., 1984). This extra heat, due to the elastic components of the muscle as well as the heat from the internal work done on the stretching of sections of the fibre with short SL during internal length adjustments, would have to be subtracted from the heat produced in order to make an accurate estimate of the heat associated with calcium buffering by Pa-Mg since this reaction is not interrupted during the interruptions to stimulation.

4.2.3 Recording

A two channel recording of force production and thermopile signal was made during these contractions. The signal from the thermopile was amplified using an ANCOM DC3A chopper amplifier chopping at a frequency of 1 kHz before it was recorded on an oscilloscope. This amplifier is capable of amplifying the temperature signal 10^6 times. Force production during these experiments was measured using a Cambridge transducer, with a sensitivity of 5.143 mN/V. In two of the experiments force development and temperature change were recorded on a Nicolet 402 oscilloscope. In the third experiment a Nicolet 4094 oscilloscope was used.

4.2.4 Calibration of records

Heat production is calculated from thermopile signals of temperature change during a contraction as described in the methods. The Seebeck coefficient (α) of the couples used to convert the thermopile signal to measures of temperature was 83.2 μV/K. Several peltier calibration records were taken throughout the course of the experiment

in order to correct for changes in the heat capacity of the system as the solution bathing the fibre was changed. The heat capacity of the system, C, could thus be accurately-determined for each set of contractions. There was in fact no change in the peltier records obtained in the different sections of the each experiment. The similarity in these calibration records also confirmed the solution bathing the muscle was drained to the same extent following each change of solution. The calibration of the records was thus calculated as $(ITn\alpha)/(dV_O/dt)$ JV-1 where $ITn\alpha$ is the heat delivered during peltier heating and dV_O/dt is the initial rate of cooling, measured from the peltier calibration records.

4.2.5 Correction for heat loss

The heat produced by the muscle fibre on the thermopile is shared between the heat recorded by the couples of the pile and the heat lost in heating the system. Heat loss to the system results in an underestimation of the heat produced by the muscle during the contraction. The peltier records used for the calibration of the thermopile signal are also used to determine the rate of cooling from the system and hence the rate of heat loss. This cooling rate depends on the initial temperature of the system, here defined as the temperature reached after prolonged heating, and the rate constant for the cooling, $1/\tau$, where τ is the time constant of the cooling curve of the peltier calibration curve. The heat produced by the muscle is therefore equal to the heat lost to the system plus the heat recorded by the system

$H_T = C (\Delta T + 1/\tau \int \Delta T/dt)$, where $C\Delta T$ is the heat change recorded and $C/\tau \Delta T/dt$ is the heat lost through cooling.

4.2.6 Correction for stimulus heat

The current passed during stimulation of the fibres gives rise to joule heating of the system which is recorded as stimulus heat, the spikes seen on the heat records. This heat has to be subtracted from the heat loss corrected records. In the first of the experiments reported here the stimulus heat, produced, determined by passing a current of the same size as that used for stimulating the fibre without causing the fibre to contract, was found to be less than 10% of the total heat produced by the fibre during contraction. Therefore no correction for stimulus heat was made.

4.2.7 Analysis of records

Figure 20 shows records of force production, temperature change and heat production (corrected for heat loss). The labile heat and stable heat rate can be estimated from the heat loss corrected record by fitting a straight line to the linear potion at the end of the record of heat production: the labile heat is then given by the positive intercept at the time at which stimulation begins. A better resolution of the heat rate into its two components is achieved by measuring the heat from the heat loss corrected records at 500 ms intervals and plotting heat rate against tetanus duration. The EXCEL built-in function Solver was used to fit a monoexponential of the form

$H = H_a (e^{t/r}) + h_b$ to the curve iteratively and a correlation coefficient was calculated for each fit.
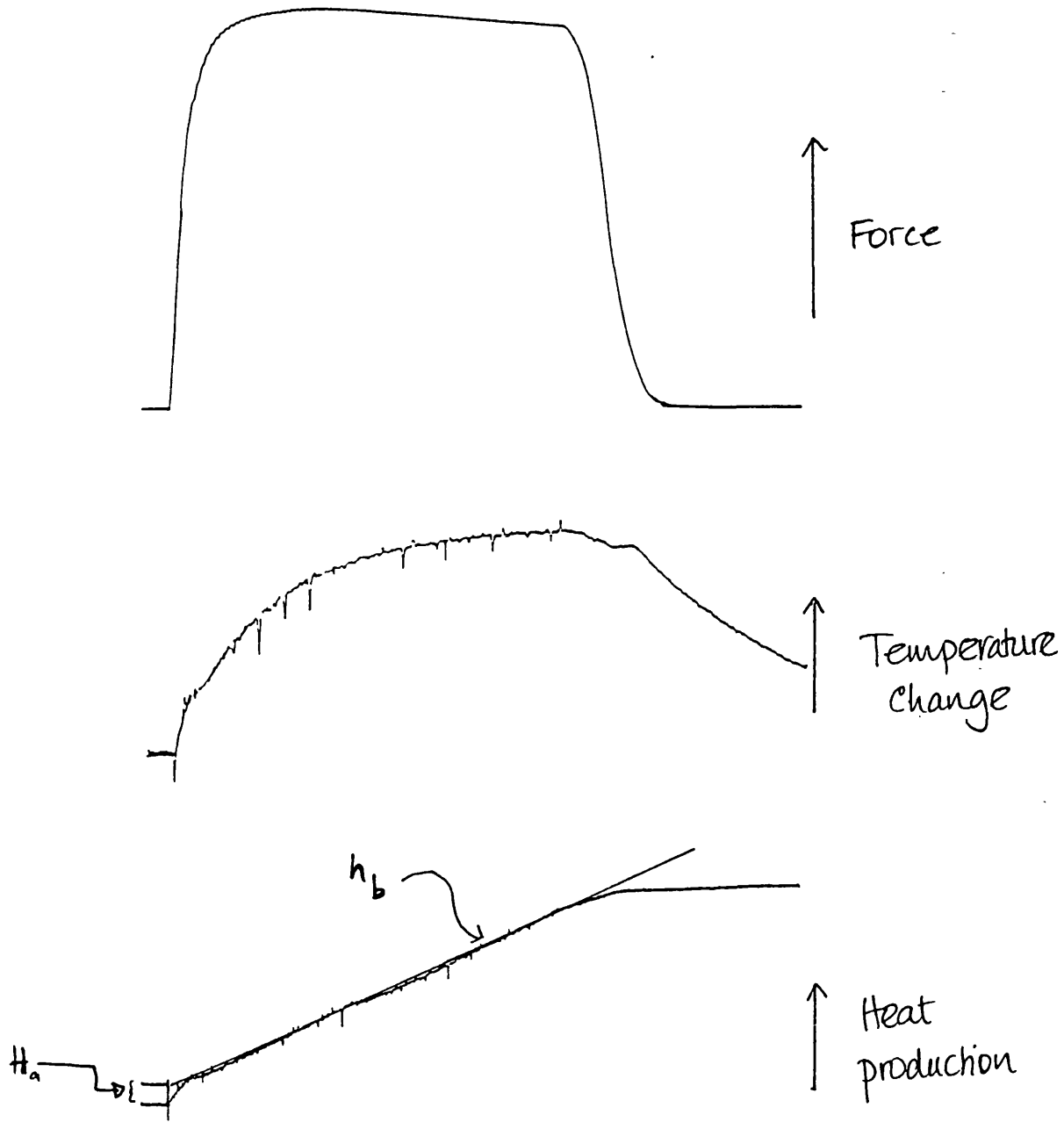
Figure 20 Examples of records of force production , temperature change and heat

production in a 3 s tetanic contraction. The stable heat rate, h_b is shown by the

dotted line and H_A is the labile heat. (See methods for further details).

4.3 EXPERIMENTAL PROTOCOL USED DURING THE DETERMINATION OF THE FORCE-VELOCITY CHARACTERISTICS OF THE FIBRES

4.3.1 Shortening pattern

Figure 21 shows the SL-tension relation of the fibres used in these experiments which was determined using laser diffraction information (See Figure 5 for details). The fibre length was then held at a length that gave a sarcomere length spacing of 2.2 μm at the beginning of each experiment. The fibres were allowed to shorten to a length where the SL was 2.4 μm. The Digitimer used to drive the stimulator and the recording system in the experiments on relaxation rate was programmed to activate the length transducer to release the muscle fibre at a particular time during a contraction. The time required for the fibre to shorten through this distance was varied in order to get a series of contractions with the fibre shortening at different velocities.

4.3.2 Stimulation and recording

A two channel recording of force production and length change was made during these experiments. A 500 ms stimulation period was used. This period of stimulation was set to initiate contraction and to continue throughout the release and for a period after shortening was complete in order for the muscle to redevelop force. Occasionally an instantaneous "step" release immediately preceded the constant velocity release. The step was sufficient in size to drop the tension close to the
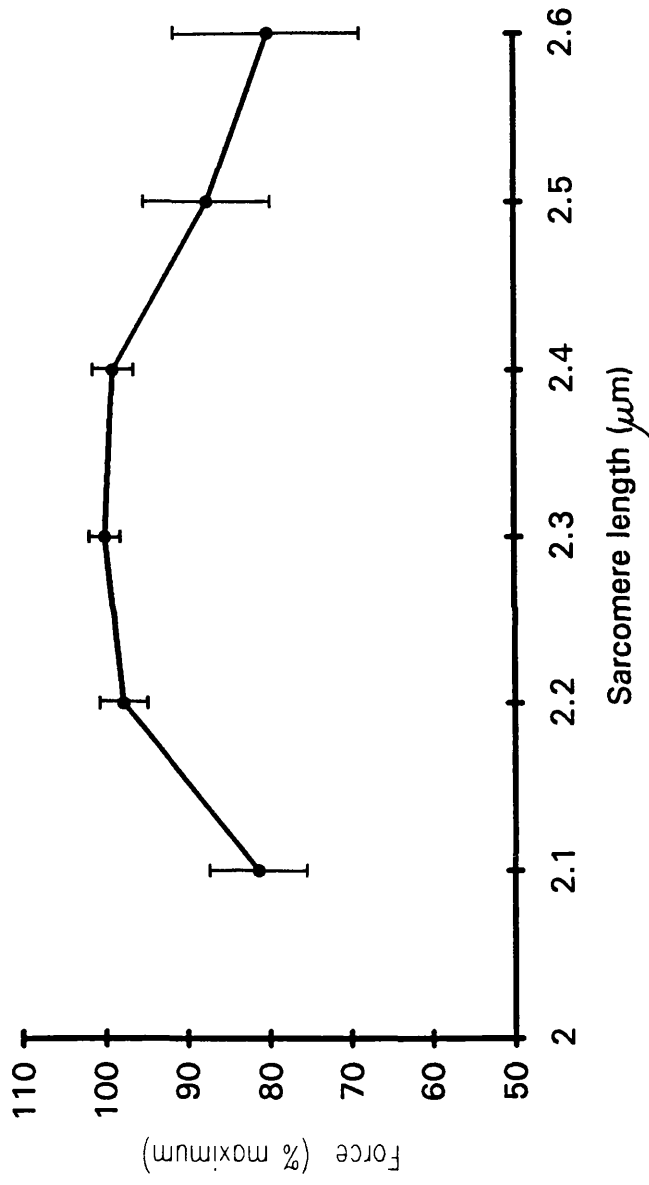
Figure 2/ Data showing the relation between sarcomere length and force development in the fibres used in the force-velocity experiments. The data shown as % maximum force +/- SEM, n=3, was obtained using the apparatus in Figure 5.

plateau force recorded during the release. The length changes and records of force production were recorded on a Nicolet 402 oscilloscope. The force was measured with a AE801 transducer, sensitivity 1.75 mN/V. The length transducer gave a calibration of 0.43 mm/V.

4.3.3 Analysis of records

The force-velocity relation of the fibres was calculated from the velocity of shortening, normalised for fibre length, and the ratio of force development calculated as P/P_o. The measures of force were made as shown below:
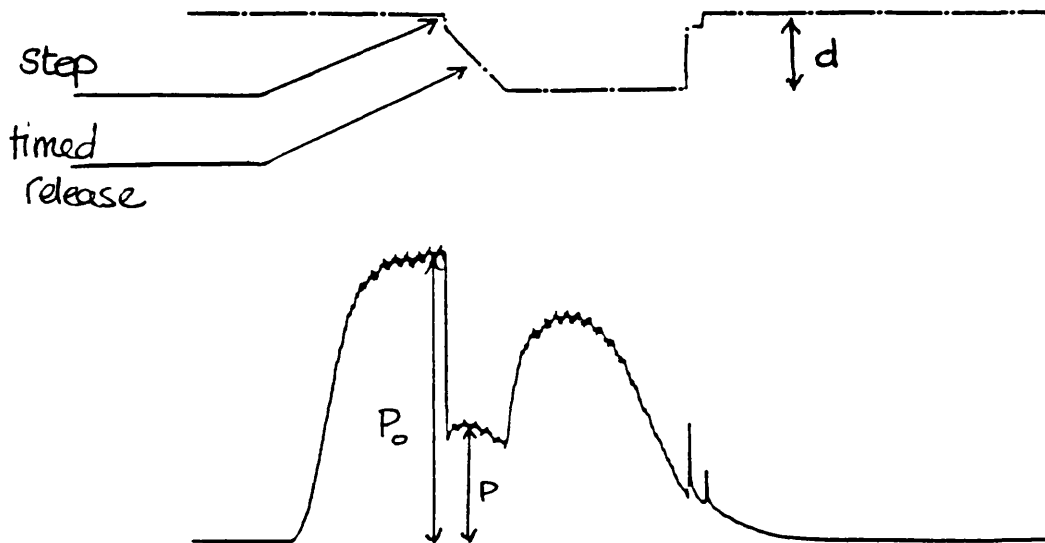
The force-velocity characteristics were plotted with the velocity of shortening normalised for fibre length. The power output (PV) of the fibres was then calculated from the force velocity data. A plot of the form, V' + (1-P')/ (1+P'G), Hill's

equation (1938), was then fitted to the curve of power output.

The power output in the high magnesium ion solution was normalised for maximum force in the control solution. The normalisation factor calculated as $P_{o-Mg}/P_{o-control}$ was then used to multiply the power measurements obtained during the contractions in the high magnesium solution.

4.4 RESULTS

4.4.1 Heat experiments

4.4.1.1 Force production

Records of force production from a fibre in the control or high magnesium solutions are shown in Figure 22. The force records, Figure 22b, show that the maximum force produced by the fibre, while in the control solution, is well maintained during the contraction. When the extracellular magnesium ion concentration is raised to 20 mM, the fibre produces a lower maximum force, approximately 89% of that produce in the control solution. The maximum force produced then declines to a lower steady level during the course of the contraction. On returning the fibre to the control solution, the force is restored to the control level and the plateau of maximum force is again well maintained.

Figure 22   Typical records of (a) temperature change, (b) force production and (c) heat production.   The fibre was bathed in Ringer's solution with a magnesium ion concentration of (1) 1 mM, (2) 20 mM, and (3) 1 mM.

1

2

3

c.

$150 \, mN \, mm^{-2}$

$1s$

$105 \, \mu J / mg / s$

b.

a.

103
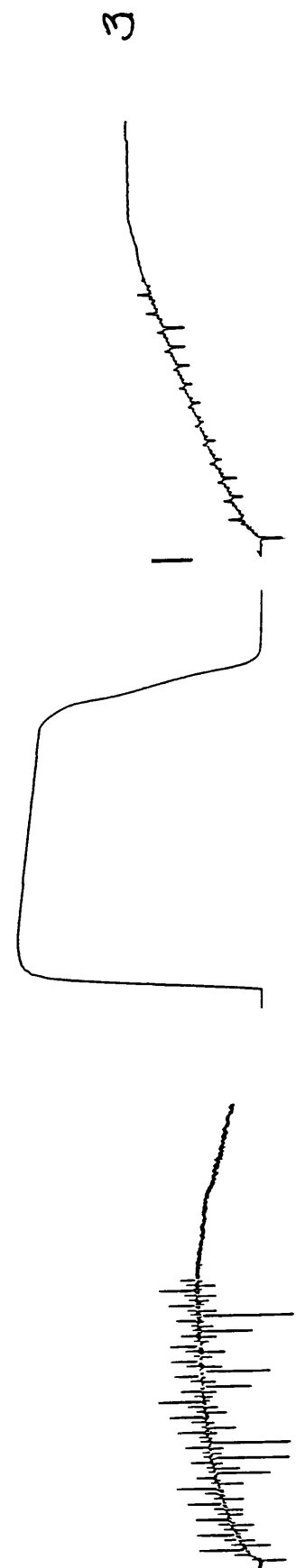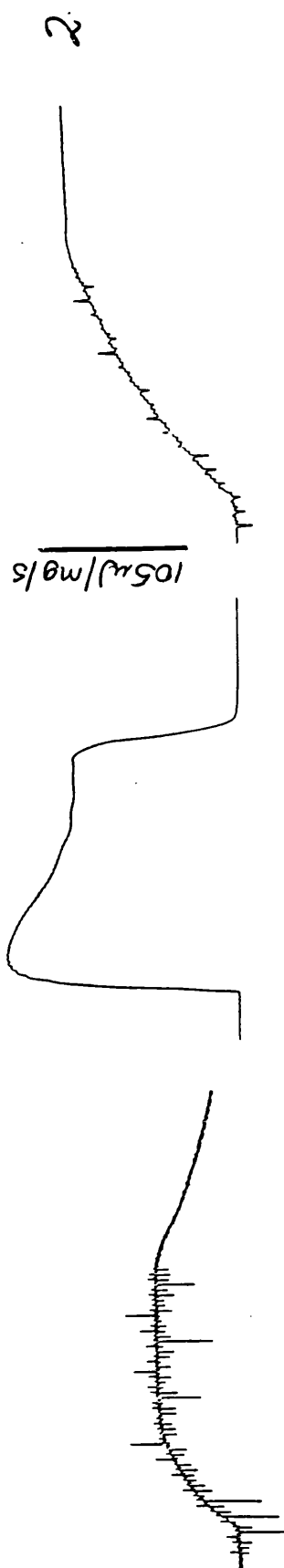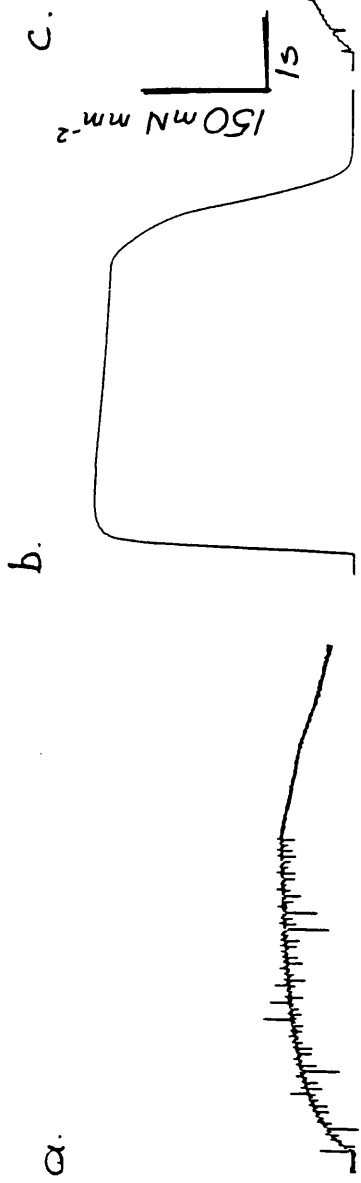
4.4.1.2 Temperature measurements

Figure 22 also shows records of temperature change, Figure 22d, from the same fibre.The rate of temperature change is highest during the early part of the contraction. The temperature then reaches a plateau at which the temperature remains constant while stimulation continues. Following the end of stimulation, there is a decrease in temperature. The rate at which the temperature declines at the end of the three contractions appears to proceed at a similar rate as shown by the parallel decline in the thermopile signal after the end of stimulation.

The temperature change recorded after the fibre was exposed to the Ringer's solution with 20 mM magnesium is higher than that recorded in the control solution. The increase in difference in the temperatures appears early in the contraction and is maintained when force declines. The maintenance of a steady temperature at a time when force is decreasing was unexpected.

4.4.1.3 Heat loss corrected records

The records of heat production, corrected for heat loss, show an increase in the amount of heat liberated during a contraction in Ringer's solution with a raised magnesium ion concentration, Figure 22 c. It is clear that the greater heat liberation occurs early in the contraction. An apparent increase in the stable heat rates is also evident as demonstrated by the greater slope of the heat record in the latter part of the contraction. This increase seems unlikely to arise from crossbridge cycling at a time

104

when force is decreasing.

In order to test for the source of the extra heat towards the end of contraction, the heat records were normalised for force production by constructing a plot of the heat produced against the force-time integral of that contraction. If the heat produced is due to a process associated with force production, the plot is expected to be a straight line tending to the origin. The slopes of the graphs would then be expected to be parallel in the control and high magnesium solutions if the heat recorded is from the same source. The positive intercept, seen in these plots suggests the presence of an exothermic reaction not associated with crossbridge kinetics, Figure 23. The slopes of the graphs, which are not parallel, also suggest there is more heat produced per unit of force in the high magnesium solution than in the control solution.

4.4.1.4 Rate of heat production

The heat loss corrected records, Figure 22b show an increase in the heat produced when extracellular magnesium ion concentration is raised. Differentiating these records shows, Figure 24, that the rate of heat production is highest at the beginning of contraction. It then declines to a steady level with tetanus duration. The final rate of heat production appears to be raised by the high magnesium solution. This observation suggests that the difference in slopes in the heat loss corrected records is real. Figure 25 , represents plots of heat rate in the three heat experiments from which these results are obtained. Although the plots show some variation in shape between the fibres, the rate of heat production is accurately described by the
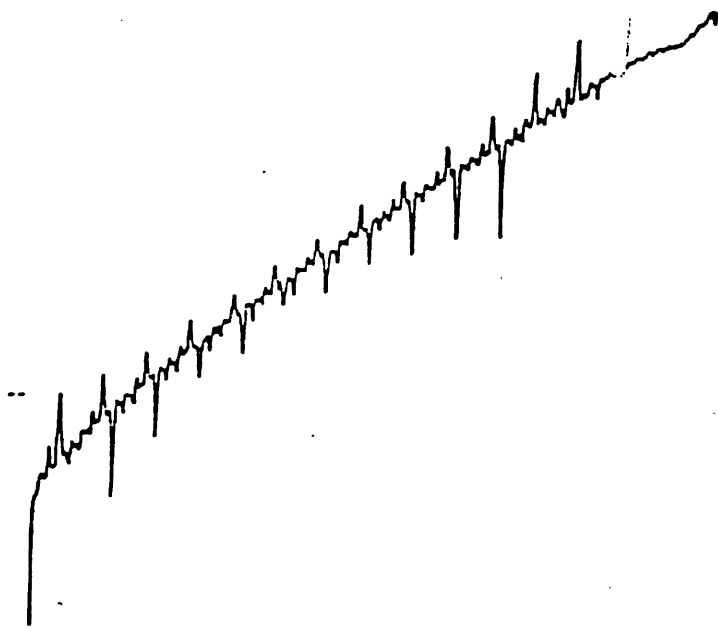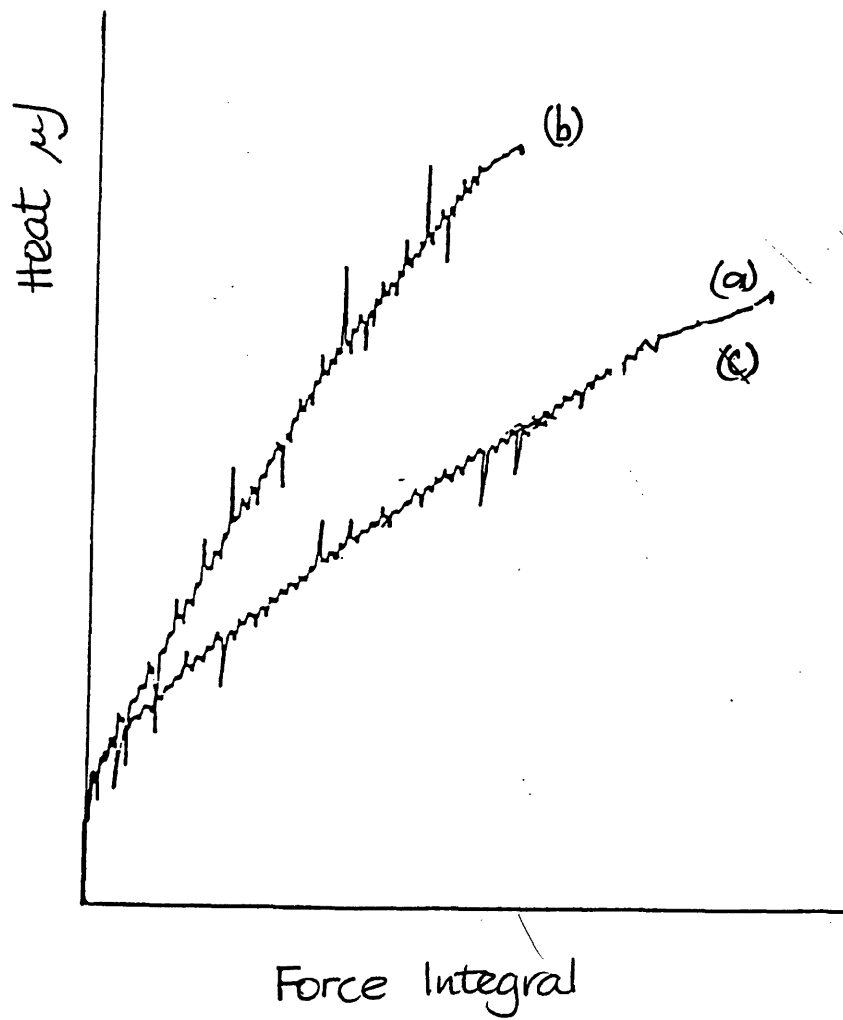
Figure 23 Examples of records of heat production normalised for force. When the

fibre was in (a) the 1 mM, (b) 20 mM, and (c) returned to the 1 mM magnesium ion

Ringer's solution.

Figure 24 Examples of the differentiated heat records. There is a greater rate of heat production at the beginning of all the heat record. Increasing the extracellular magnesium ion concentration from (1) 1 mM to (2) 20 mM increases the heat rate above that recored in the control solution. On returning to the 1 mM magnesium ion solution (3) the heat rate returns to that measured in the first control (1).

Heat rate

Time

1   2   3

109
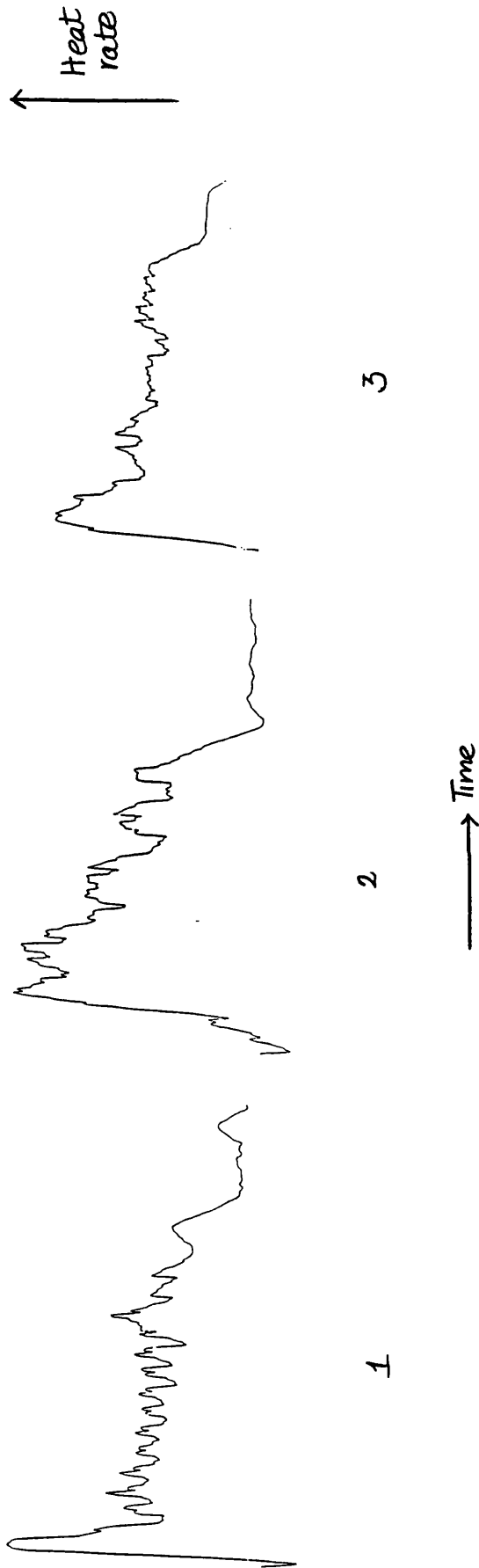
Figure 25   Plots of heat rate from three different fibres.   The heat rate in fibres, (a), (b) and (c) whole in bathing in the (1) 1 mM, (2) 20 mM and (3) 1 mM magnesium ion solution can be describe by a similar exponential.   The experimental data is fitted with an exponential of the equation $H = H_A (e^{vt}) + H_b$.
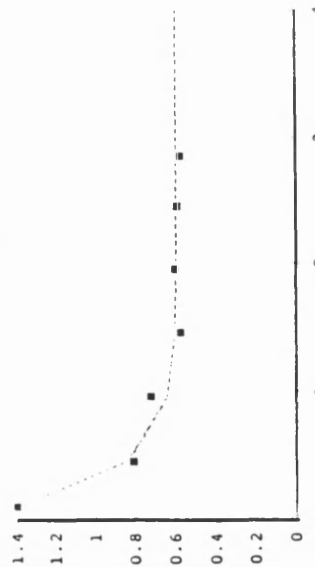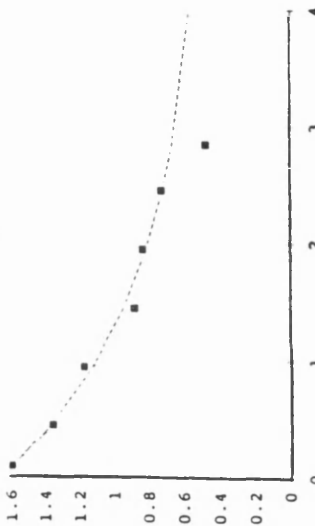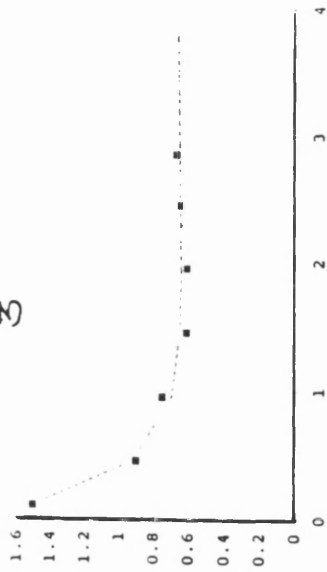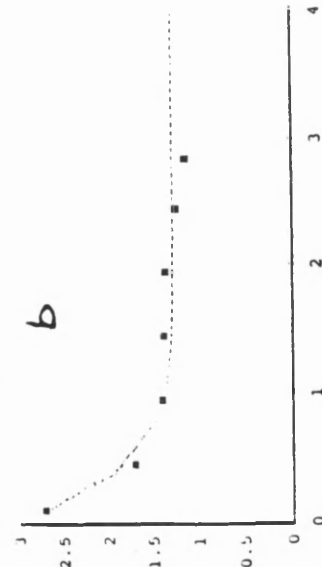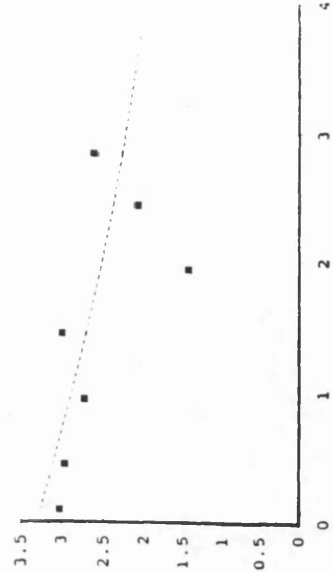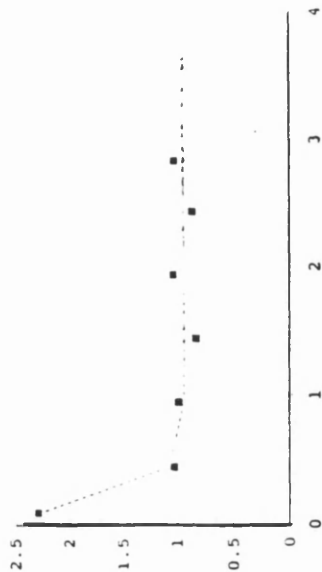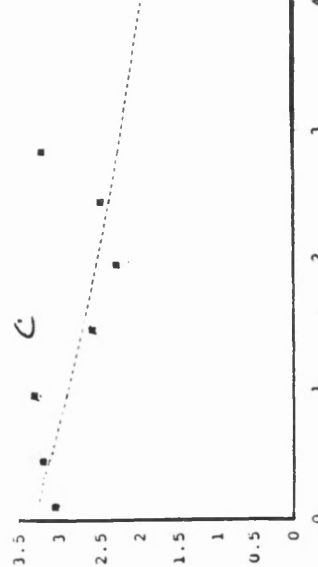
monoexponential $h = h_a (1-e^{t/\tau}) + h_b$. This exponential describes two phases to the heat production, $h_a(1-e^{t/\tau})$, the labile heat rate and h_b the stable heat rate. An examination of the area under the plots in Figure 25, shows that this area can be resolved in to two sections, the area below the dotted line which represents the stable heat rate and the area above the dotted line represents the labile heat rate. If the labile heat rate is due to calcium binding to parvalbumin during contraction, this area can be used to estimate the calcium that is bound to parvalbumin during contraction. In the high magnesium solution, this area is shown to be larger than in the control solution, an increase which suggests a greater calcium handling by parvalbumin when the magnesium ion concentration of the extracellular fluid is raised.

Figure 24, examples of the differentiated heat records, also illustrates the difficulties that would arise in an attempt to analyze heat records from interrupted tetani. Each time the muscle relaxed there would be extra heat liberated. This extra heat would have to be subtracted from the heat record in order to determine the size of the labile heat accurately. There is however no easy way to determine the exact contribution of this heat from the total heat produced.

4..4.1.5. Stable heat

There appears to be an increase in the stable heat rate of these fibres when in the high magnesium solution. This increase appears at a time when the force is decreasing. It therefore seems unlikely that it arises from the processes contributing to the stable heat rate. A summary of these results is presented in Table 4.

Table 4 The effect of increasing $[Mg^{2+}]$ from 1 mM to 20 mM on heat production.

	1 mM $[Mg^{2+}]$	20 mM $[Mg^{2+}]$	1 mM $[Mg^{2+}]$	% change
H_T (μJ)	29.3 ± 4	35.6 ± 4	28.3 ± 2	+18.80
LH ($\mu J/mg$)	169.0 ± 1.0	217.6 ± 1.2	161 1.4	+31.0
SHR ($\mu J/mg/s$)	51.1 ± 0.1	66.6 ± 0.2	60.8 ± .2	+17.8
HR ($\mu J/mg/s$)	105.3 ± 8	132.3 ± 12	101.5 ± 3	+30.0
TC (s^{-1})	1.47 ± 0.3	1.37 ± 0.1	1.71 ± 0.2	−13.8
area	136.0 ± 4	165.0 ± 5	152.0 ± 4	+14.5

4.4.2 The effect of raising extracellular magnesium ion concentration on power output by isolated fibres

The increase in stable heat rate when extracellular magnesium ion concentration was increased was rather puzzling. It was therefore important to test the effect of magnesium crossbridge behaviour in both the control and high magnesium solutions.

4.4.2.1 Force development

The effect of increasing extracellular magnesium ion concentration on maximum force production is a 10% decrement in maximum force production as shown in Figure 26. This decrease in force is similar to that recorded previously in the experiments on relaxation rate and heat production (this work). An inability to maintain the plateau of maximum force as well as a faster return of force to rest levels the 20 mM magnesium ion Ringer's solution are further demonstrated.

4.4.2.2 The effect of shortening a fibre during stimulation

Figure 27 shows records of force production from a fibre shortening at three different velocities in the control solution. The records show that the force reached at the end of the shortening, P, depends on the velocity at which the fibre was allowed to shorten: the higher the velocity of shortening, the lower the force at the end of shortening.

Figure 26 Typical records of force production in (a) the control solution and (b) the

20 mM magnesium ion concentration solution.

150 mN mm⁻²

1.5 s

b.

a.

116
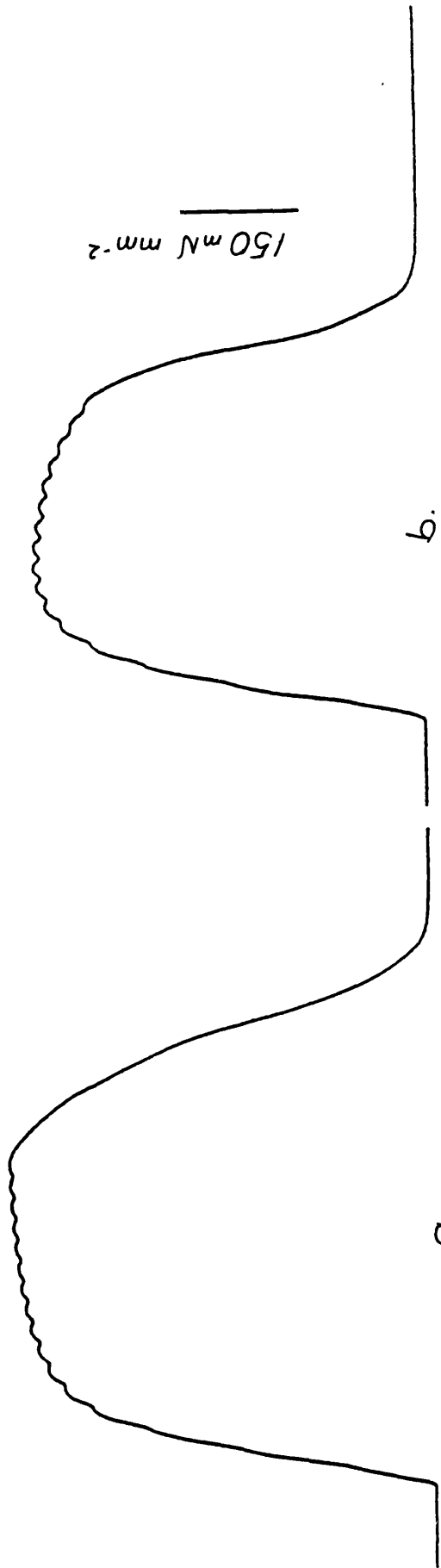
Figure 27   Typical records of force production by a fibre shortening at three different velocities in the control solution.

117

velocity of
release

$8.25\ mm\ s^{-1}$

$10.9\ mm\ s^{-1}$

$16.0\ mm\ s^{-1}$

$\overline{150\ mN\ mm^{-2}}$
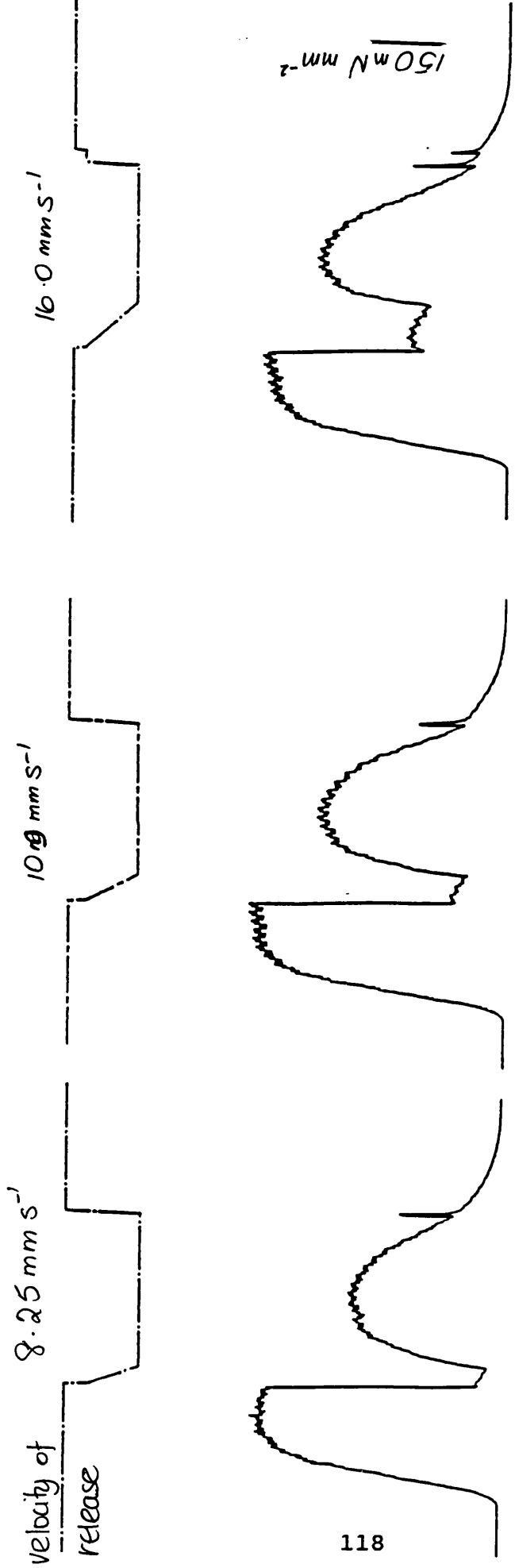
$\overline{2s}$

Figure 28 shows examples of tetani obtained from the same fibre while shortening in the control and the high magnesium solutions. Both the maximum force , P_o, and the P, are lower in the high magnesium solution. When the records are normalised for force by scaling the tetani to give the same deflection for maximum force, the records then show that force decreases to the same proportion , P/P_o , in both solutions. The redeveloped force is, however, lower in the high magnesium solution.

4.4.2.3 Power output of the fibres in the two solutions

A plot of the force-velocity characteristics of the fibres whilst bathing in the control and high magnesium solutions, Figure 29 , shows that the data obtained with the fibre in the control or high magnesium solutions superimpose. The parameter. a/P_o , which defines the curvature of the plots is therefore expected to be virtually identical.

A plot of the power output of the fibres in the two solutions, Figure 30a, shows that there is less power produced when extracellular magnesium ion concentration is raised. When the power output is normalised for maximum force, however, the plots superimpose, Figure 30b. The decrease in power output in the high magnesium solution appears to reflect the lower maximum force produced in this solution.

4.5 DISCUSSION

Studies on energy balance in muscle have shown that enthalpy changes during

119

Figure 28   Records of a fibre shortenening at the same velocity in the (a) control solution and (b) the 20 mM magnesium ion solution.   This figure shows that when the records   are corrected for force by plotting the records so they give the same vertical deflection for maximum force, the plateau force during shortening is approximately equal in the two solutions.

150 mN mm⁻²

150 mN mm⁻²

300 ms

121

Figure 29 The relation between force and velocity of shortening in fibres bathed in (a) 1 mM and (b) 20 mM magnesium ion solution. Each point represents a single observation. Three different fibres were used.
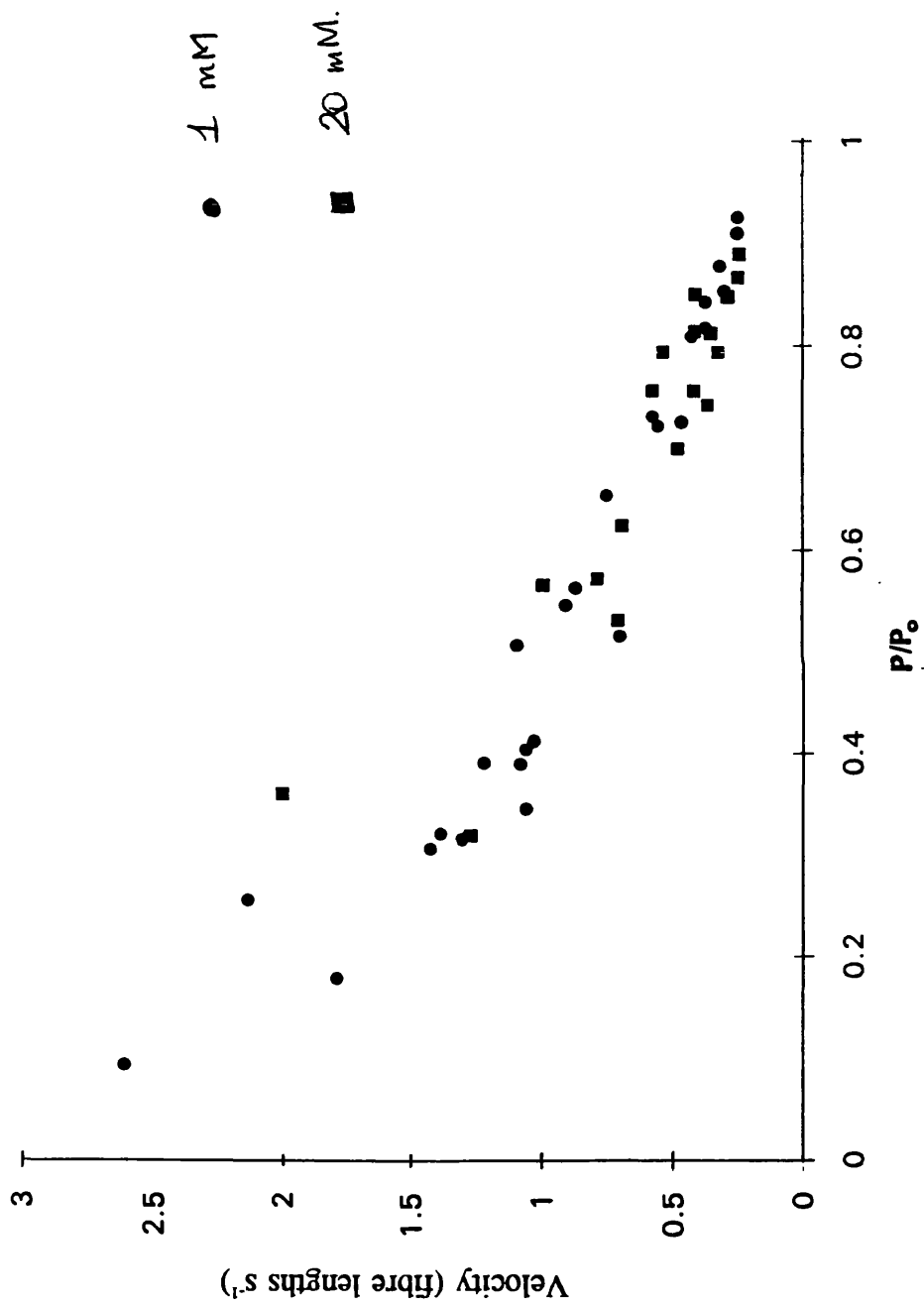
Figure 30a   The relation between power output and shortening velocity in Ringer's solution with a magnesium ion concentration of 1 mM ($\bullet$) and 20 mM ($\blacksquare$).

Figure 30b   The relation between power output and in the high magnesium ion solution ($\bullet$) and the control solution ($\blacksquare$) normalised for maximum force in the control solution. Figure 31a Records of calcium release from the sarcoplasmic reticulum during simulations of the control conditions and the high magnesium conditions.
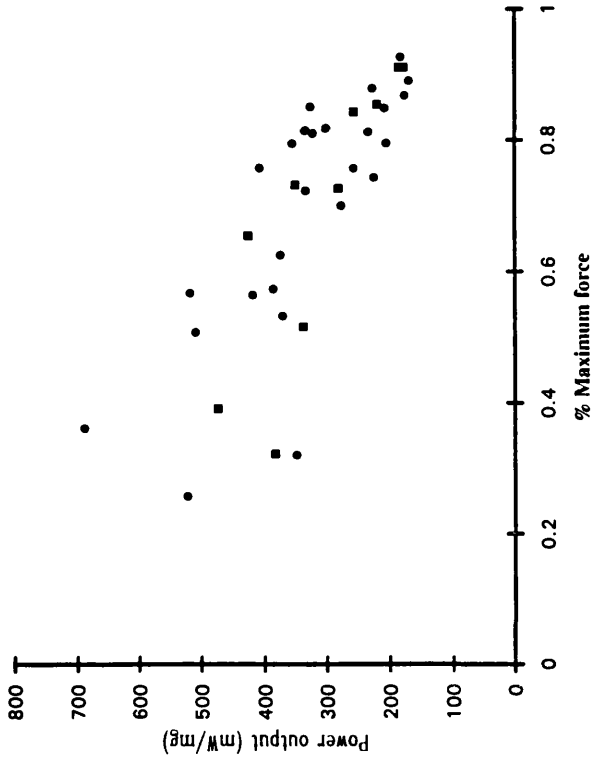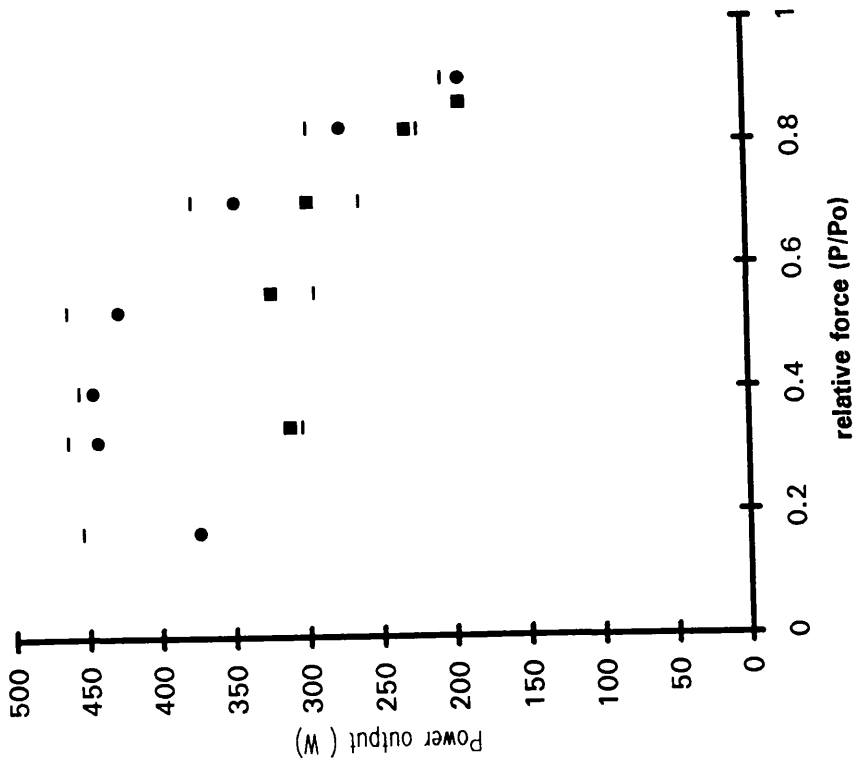
contraction reflect the conversion of chemical energy to (heat + work) (Woledge, 1971). During isometric contractions by frog fast muscle, when no work is done, all the enthalpy changes measured can be attributed to three reactions which have been identified as the important myothermic reactions of muscle: the calcium ATPase activity of 1) actomyosin and 2) the calcium pump which contribute to the stable heat rate and 3) the binding of calcium to parvalbumin, which contributes to the labile heat (Curtin and Woledge, 1979). The increase in heat production when extracellular magnesium ion concentration is raised suggests an increase produced by one or two or all three of these components.

If the high magnesium is causing a change in the crossbridge kinetics of the fibres, this can only be measured during experiments when the muscle actually performs work. In this study the effect of these solutions on the work output of the fibres is tested during the shortening experiments. A change in the ability of the fibre to perform work when bathed in the high magnesium solution will then be seen as a change in the curvature of the force-velocity curve of the fibres, signalling a change in crossbridge turnover. A change in the power output of the fibre will then indicate a change in the rate of ATP utilisation by the fibre.

Both the force velocity characteristics of the fibre and the power output of the fibres do not appear to be affected by an increase in the concentration of extracellular magnesium ions. The apparent increase in the stable heat rate observed during these experiments can therefore not be attributed to a change in crossbridge behaviour in the high magnesium ion solution. This finding, of no increase in the crossbridge turnover in the high magnesium solution, coupled with no change in the relaxation

rate attributed to the calcium pump of the sarcoplasmic reticulum suggests this solution does not influence the stable heat rate of the fibres. The apparent increase in the stable heat rate must have some other explanation.

A clue is provided by the differentiated heat records and the data on heat rate. When the extracellular magnesium ion concentration is increased, the initial heat rate increases and the timecourse with which it declines is slowed. This slower evolution of heat would be seen as a continued production of labile heat during the time force is falling when the fibres are in the high magnesium ion solution. The "extra" labile heat would mask the decline in the stable heat rate. This indeed appears to be the case.

The increase in heat production in the high magnesium ion solution is therefore attributed to an the increase in the size and duration of labile heat. The question that then remains is whether the suggested increase in labile heat can be explained by an increase in the concentration of parvalbumin-magnesium calcium sink in the high magnesium solution.

In the presence of 1 mM parvalbumin, calcium binding to parvalbumin produces 25 kJ per mol of calcium bound to parvalbumin isolated from carp (Moeschler, 1980) and 33 kJ using parvalbumin isolated from muscle (Smith and Woledge, 1985). Following the calculation by Peckham and Woledge (1985), 0.76 μmol g^{-1} of parvalbumin (Hou et al., 1990) would be expected to produce 51.58 μJ mg^{-1} which is of the same order as the amount of labile heat produced in these experiments (55.8

- 70.5 μJ mg^{-1}).

Increasing the concentration of magnesium in solution with calcium and parvalbumin

increases the heat of substitution of this reaction to 41 kJ mol^{-1} (Smith and Woledge,

1985). So, if the magnesium concentration increased without an accompanying

increase in parvalbumin-magnesium, 64 μJ mg^{-1} of heat would be expected in during

the contractions in the Ringer's solution with a high magnesium ion concentration.

The 99 μJ mg^{-1} recorded in the contractions in the high magnesium solution therefore

suggests an increase in the concentration of parvalbumin-magnesium with this

treatment. These results therefore support the idea that increasing extracellular

magnesium ion concentration increases relaxation rate by increasing the parvalbumin-

magnesium concentration in the myoplasm.

CHAPTER 5

A MODEL FOR PREDICTING THE EFFECT OF INCREASING THE INTRACELLULAR MAGNESIUM ION CONCENTRATION ON RELAXATION RATE AND HEAT PRODUCTION

5.1 INTRODUCTION

I have shown that there is an increase in relaxation rate and heat production when the magnesium ion concentration in Ringer's solution is increased from 1 mM to 20 mM. These increases I have attributed to a higher buffering of calcium by parvalbumin-magnesium when extracellular magnesium is raised. In this Chapter, a mathematical model is constructed for the purpose of predicting the effects, on intracellular calcium ion movements between the sarcoplasmic reticulum, troponin, and parvalbumin, of raising intracellular magnesium ion concentration. The components of the model are all intracellular so that the hypothesis that extracellular cellular magnesium exerts its effect through an increase in intracellular magnesium is tested.

This model is not intended as an exhaustive model of calcium and magnesium movements in the myoplasm following activation. It is rather intended to provide a basis for the initial prediction of the effects of varying free magnesium on the concentration of parvalbumin-magnesium, the parvalbumin species suggested to be the calcium buffer and hence its ability to buffer calcium.

5.2 ASSUMPTIONS IN THE MODEL

The model is constructed with five components: magnesium, which sets the concentration of the calcium buffering sites on parvalbumin, calcium, which is followed through the different calcium/magnesium binding compartments in the myoplasm of the fibre and parvalbumin, troponin, and the sarcoplasmic reticulum, the main compartments into which calcium is partitioned. The inclusion of only three calcium/magnesium binding sites which are thought to be the most important calcium and magnesium binding sites during contraction, represents a highly simplified composition of the myoplasm. In making this simplification certain assumptions have had to be made. These assumptions and the basis on which they are made are explained below.

5.2.1 Magnesium binding sites included in the model

The magnesium concentration used in modelling the 20 mM magnesium ion situation, 1.8 mM, is that reported after a short period of exposure to high extracellular magnesium (Blatter, 1990). In the experiments on the time course of the effect of extracellular magnesium on relaxation rate, magnesium is shown to produce its maximum effect within 10 minutes of exposure to the high magnesium solution. It is therefore assumed that all the magnesium binding sites are in equilibrium after this time. The two magnesium binding species with a magnesium concentration high enough to influence the reactions studied here, myosin and ATP, are not included in the model for two reasons:

1) the dissociation of magnesium from myosin follows kinetics too slow to influence the rapid kinetic of the activation-contraction-relaxation cycle, (Gillis, 1985),

2) the ATP concentration is maintained through the Lohmann reaction during a prolonged tetanus (Woledge et al., 1983) and the affinity of ATP for magnesium is high enough that the free ADP concentration is negligible (Woledge, 1971).

5.2.2 Calcium binding sites included in the model

Troponin and parvalbumin are the only myoplasmic calcium binding sites included in the model. The exclusion of the other calcium binding sites is justified on the following grounds:

1) the time course with which calcium concentration changes occur during the transition from rest to contraction to rest are rapid and in the order of milliseconds. The time course with which calcium is partitioned between the myoplasm and mitochondria, the second largest calcium store of the cell, is slow (Robertson et al., 1981, Werber and Boredjo, 1982, Gillis, 1985) compared to the rates of calcium movement during contraction. The contribution of the mitochondria to calcium buffering therefore is thought to be not important during these rapid transitions,

2) Somlyo et al. (1985) using electron probe studies to determine the location of calcium before and after activation showed that calcium appeared to be translocated from the sarcoplasmic reticulum to the myoplasm following activation. There does not seem to be any compartmentalisation of calcium into the myoplasmic organelles, and

3) Baylor et al.(1978) have also shown that the concentration of free calcium during

131

a tetanus is determined by the concentration of calcium binding sites in the myoplasm. Troponin and parvalbumin are the two sites named. The calcium binding sites included are therefore the sarcoplasmic reticulum which stores calcium before contraction and troponin and parvalbumin which bind the calcium following activation.

5. .3 The distribution of components of the model in the myoplasm

The third assumption is of a uniform distribution of the cation binding sites including troponin throughout the myoplasm. The diffusion of calcium from the sarcoplasmic reticulum to troponin is therefore assumed not to limit the rate of force development. In order to justify this assumption, the model was constructed in a way that ensured the attainment of maximum force, calculated as $[TnCa]^3$, in the first 200 ms of contraction as seen in the experiments.

5.3 THE PROBLEM TO BE MODELLED

The model follows calcium through five components of the fibre during 1) rest, 2) activation and 3) relaxation when the intracellular magnesium ion concentration is 1 mM or 20 mM.

5.3.1 Rest

This calcium leak is therefore than would be expected from the myothermic

measurements at rest: the contribution of the sarcoplasmic reticulum to heat production when the pump is fully turned on is 25 - 40% (Smith, 1972). Calcium release from the sarcoplasmic reticulum also appears to be under the control of both the free calcium levels already present in the myoplasm and the magnesium ion concentration in the myoplasm. Both these control mechanisms are not included in this model. The leak calculated to maintain the resting calcium concentration at 0.06 μM when all the other equilibrium conditions are satisfied was found to be 0.375 V_{max}.

5.3.2 Contraction

Contraction is modelled as the binding of calcium to troponin. The force of the contraction is calculated as $[TnCa]^3$ (Woledge, personal communication).

5.3.3 Relaxation

5.3.3.1 Rate of calcium uptake by the sarcoplasmic reticulum

The component of relaxation attributable to the calcium pump of the sarcoplasmic reticulum depends on V_{max} and K_M of the calcium pump as already described. The rate of calcium removal to the sarcoplasmic reticulum by the pump is

$d[Ca]/dt = V_{max} [Ca]/ K_M + [Ca]$. The sarcoplasmic reticulum makes up 10 mg/g wet weight of muscle (Ogawa, 1980). This gives the sarcoplasmic reticulum a maximum calcium uptake rate, V_{max}, of 700 μmol Ca^{2+} s^{-1} l^{-1} muscle fibre water at 25°C. Determinations of the calcium affinity of the pump, K_M, have given values of

5.4.1 The first-order reactions considered:

(i)   Pa + Mg ⇌ Pa-Mg

the parvalbumin reaction that is thought to set the concentration of Pa-Mg and hence the calcium buffering capacity of parvalbumin in the myoplasm. The effect of increasing the concentration of magnesium ions in this reaction scheme is the one tested in this model.

(ii)   SRCa → SR + Ca
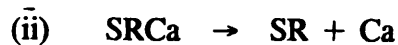
This scheme represents the calcium release process from the sarcoplasmic reticulum following activation

(iii) SR + Ca ⇌ SRCa.

Relaxation is achieved by the return of calcium from the myoplasm to the sarcoplasmic reticulum at the end of stimulation. The uptake of calcium into the sarcoplasmic reticulum by the calcium pump during relaxation is therefore defined by this reaction. A leak that represents calcium leak from the sarcoplasmic reticulum into the myoplasm along its concentration gradient is also included. These two processes regulate calcium concentration at rest.

(v)   Tn + Ca ⇌ TnCa
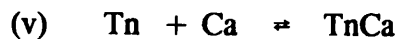
The calcium released from the sarcoplasmic reticulum initiates contraction. The troponin-calcium reaction presented above represents this reaction which couples activation to contraction and force production.

(v)   Pa + Ca ⇌ PaCa

It is suggested that when the rate of calcium uptake by the calcium pump of the sarcoplasmic reticulum is inadequate to explain rapid relaxation, calcium uptake by

parvalbumin enhances relaxation. The calcium buffering reaction of parvalbumin is described by this reaction.

5.4.2 INITIAL CONCENTRATIONS OF THE COMPONENTS OF THE MODEL

5.4.2.1 Magnesium

The free magnesium ion concentration is set at 930 μM in the control simulation (see Table 1). Following Blatter's (1991) determinations, the concentration of intracellular magnesium ions is then raised 105% to 1860 μM in order to simulate the effect of raising the concentration of extracellular magnesium to 20 mM, on the intracellular magnesium levels.

5.4.2.2 Calcium

The free calcium concentration is set at 0.06 μM (Blinks et al., 1978, Cannell, 1984) as determined by aequorin measurements. The calcium concentration of the sarcoplasmic reticulum is set at 1500 μM (Somlyo et al., 1985, Endo, 1977).

5.4.2.3 Troponin

Troponin has a concentration of 70 μmol/l muscle water (Endo, 1977), has four calcium binding sites. These four sites have different calcium binding kinetics (Benzonana et al., 1972). Two are described as calcium specific and are responsible

for coupling activation to contraction. These sites have a high calcium affinity and a magnesium affinity so low that magnesium does not bind to them. Therefore, at rest when the free calcium level is low these sites are metal free. The other two sites which are described as the non-specific sites bind both magnesium and calcium. These sites have a magnesium affinity 10^4 lower than the calcium affinity. They have calcium/magnesium binding kinetics similar to those of parvalbumin (Benzonana et al, 1972). These sites are therefore treated as parvalbumin sites in the model.

5.4.2.4 Parvalbumin

Frog muscle contains two parvalbumin isotypes, Pa IVa and Pa IVb, which show different isoelectric focusing points during gel electrophoresis (Blum et al., 1977, Haeich et al., 1979, Gillis, 1980, Berchtold et al., 1983,Tanokura et al., 1986). These parvalbumins show the same magnesium dissociation rates at $0°C$. The two are therefore treated as a single parvalbumin pool (Hou et al., 1990). The parvalbumin concentration of the *tibialis anterior* muscle of *Rana temporaria* is 760 μM (Hou et al., 1990). In this model a parvalbumin concentration of 1000 μM is used in order to account the non-specific sites on troponin. The concentration of the calcium buffering sites on parvalbumin, therefore is 2000 μM (each molecule of parvalbumin has two cation binding sites). Parvalbumin exists in three species in the cell, apo-parvalbumin, parvalbumin-magnesium and parvalbumin-calcium. The concentration of these three species is set by the concentration of magnesium in the myoplasm and the relative affinities of these sites for the two cations (Godt and Maughan, 1989, Hou et al., 1991). The initial ratio of the concentrations of these

species is 60:40:<1% as calculated by both Godt and Hou et al.

5.4.3 Running the simulation

The model is designed to simulate concentration changes during interrupted tetani. This is achieved by pulsing calcium from the SR into the myoplasm at regular intervals. The calcium release is defined to follow an exponential time course by releasing the same proportion of calcium from the SR with each pulse. The release is controlled by a series of "gates" which are set to open for 200 ms every 500 ms. The 300 ms period between the closing of the gate and the next opening of the gate represents the time when stimulation is interrupted. The free calcium level is also restricted to remain below 10 μM (Cannell, 1985) by inhibiting calcium release once this ceiling is reached.

5.4.3.1 Definition of concentration flows

The concentration of the each of the various components of the model is defined as a level, denoted by an "l" statement in the model. These levels change with time depending on the reaction rates of the various flows of, denoted as "r" statements, reactants and the time for which each reaction is allowed to proceed during simulation. The time of the simulation is therefore broken up into time steps of size "dt". The accuracy of the calculation of each level depends on the size of this integration step. The smallest integration step which allowed the model to run was used in order to attain the most accurate results was used.

The levels of the reactants and the rates of reaction are subscripted in order to show the direction of flow of the reactants with time. The initial levels are subscripted "j" and the final levels of each integration step are subscripted "k". The rates are subscripted "jk" ie the direction of flow is from time "j" to time "k". The level equations used to define the concentrations of the components of the model are defined in Figure 31.

5.4.3.2 Reaction kinetics

The binding and dissociation constants used in the reactions listed in Section 5.4. are summarised in Table 5. Using the information above to set the total concentration of the individual components of the model, the initial state was adjusted to be stable by moving calcium and magnesium through the parvalbumin and troponin compartments until no changes in concentration were seen during a simulation run of several seconds with no stimulation. In the control simulation, the steady state was calculated to give a Pa-Mg : PaCa ratio of 60:40 when the free calcium concentration was 0.06 μM and the free magnesium was 930 μM.

A similar adjustment in calcium and magnesium concentrations similar to that used to

Figure 31 A summary of the level equations used in the model.

1.   l pacal.k=pacal.j+dt*(caon.jk-caof.jk)

The parvalbumin-calcium level depends on the rates of calcium binding and dissociation from parvalbumin

2.   l pamgl.k=pamgl.j+dt* (mgon.jk-mgof.jk)

The parvalbumin-magnesium level depends on the rates of magnesium binding and dissociation from parvalbumin

3.   l pal.k= pal.j+dt*(caof.jk-caon.jk+mgof.jk-mgon.jk)

The apo-parvalbumin level depends on the previous two rates

4.   l mgl.k=mgl.j+dt*(mgof.jk-mgon.jk)

The magnesium level depends on the magnesium dissociation and binding rates

5.   l   cal.k=ca..j+dt*((caof.jk-caon.jk)+(tnof.jk-tnon.jk)+(carl.jk-srin.jk+leak.jk))

The calcium level depends on the calcium and magnesium rates described above as well as the rate of calcium release from the sarcoplasmic reticulum, the rate of calcium uptake by the sarcoplasmic reticulum and the leak.

6.   l tnl.k=tnl.j+dt*(tnof.jk-tnon.jk)

The troponin level depends on the rate at which calcium binds and dissociates

7.   l tncal.k=tncal.j+dt*(tnon.jk-tnof.jk)

The troponin-calcium level and the level of the force depend on the rates of calcium binding and dissociation

8.   l casr.k=casr.j+dt*(-carl.jk+srin.jk-leak.jk)

The level of calcium in the sarcoplasmic reticulum depends on the rates of calcium release, calcium uptake and calcium leak.

Table 5 The rate constants used in making the above adjustments and during the

simulations are presented in Table 6.

	Calcium Affinity	Ca^{2+} on M s^{-1}	Ca^{2+} off s^{-1}	Mg^{2+} on M s^{-1}	Mg^{2+} off s^{-1}
Tn		10^7 (1)	23 (1)		
Pa		10^7 (2)	.19 (3)	10^4 (2)	.99 (3)

The reaction rates quoted are for 0 C. The rates are rounded off values from works

by: (1) Benzonana et al. (1972), (2) Ogawa and Tanokura (1986a, 1986b)and (3)

Hou et al. (1991).

determine the steady state in the control simulation was carried out at the beginning of the simulation of the high magnesium effect. In this case the Pa-Mg : PaCa ratio was adjusted to 75 : 25 when the free calcium and free magnesium concentrations were 0.06 μM and 1860 μM respectively. This increase effectively changes the parvalbumin-magnesium concentration from 1200 μM to 1500 μM, an increase of 300 μM in the sites available to bind calcium during simulation. The parvalbumin-calcium concentration is decreased to 500 μM from 800 μM and the apo-parvalbumin concentration is also decreased from 13.3 μM to 8.3μM. The results of these adjustments in concentrations are summarised in Table 6.

5.5 ANALYSIS

The model generated results which could be presented in both tabular and graphical form. Changes in the concentrations of the various components could thus be calculated during different periods of simulation. Relaxation rate during the simulations was calculated as the reciprocal of the time for the force to fall to 97.5% of the force at the end of each period of simulation. This was achieved by including a counter in the model that determined the time at the end of each period of stimulation, the force at that time, and 97.5% of this force and the time at which it was reached. The time for this tension drop was saved within the simulation. This calculation was similar to that used to calculate relaxation rate during the experiments on interrupted tetani (See Figure 8). The relaxation rate calculated from these data was fitted with an exponential of the form used to describe the relaxation rate during interrupted tetani.

142

Table 6   The Initial Steady State Concentrations Of The Components Of The

Model

Component	Low Mg (M)	High Mg (M)
-		
Ca	0.06×10^{-6}	0.06×10^{-6}
Mg	0.90×10^{-3}	1.80×10^{-3}
Tn TnCa Total Tn	107.4×10^{-6} 33.6×10^{-6} 140×10^{-6}	107.4×10^{-6} 33.6×10^{-6} 140×10^{-6}
Pa PaCa PaMg Total Pa	13.3×10^{-6} 0.8×10^{-3} 1.2×10^{-3} $2.013 \times 10^{-}$	8.3×10^{-6} 0.501×10^{-3} 1.502×10^{-3} 2.013×10^{-3}
SRCa	1.5×10^{-3}	1.5×10^{-3}

The tabulated data were used to calculate rates of change in the concentrations of the various components of the model.

5.6 RESULTS

5.6.1 Calcium release from the sarcoplasmic reticulum

Figure 32a, shows that calcium release from the SR, follows an exponential time course during each period when the gates are open. When the gates close the SR then begins to take up the calcium as seen by the upward deflection in the records of calcium levels in the sarcoplasmic reticulum. The total amount of calcium released from the sarcoplasmic reticulum during the high magnesium simulation is higher than that released in the control solution as seen by the lower troughs in the records of calcium release from the sarcoplasmic reticulum following each period of stimulation.

The average rate of calcium release during the periods when the gates are open, calculated as $([Ca]_o - [Ca]_c)/200$ $\mu M/ms$, where $[Ca]_o$ is the concentration of calcium in the sarcoplasmic reticulum and $[Ca]_c$ is the calcium remaining at the time the gates close, shows a greater rate of calcium release when the intracellular magnesium level is raised, Figure 32b.

The calcium uptake by the sarcoplasmic reticulum on the other hand is higher in the control simulation. The slower calcium release,

Figure 32a   Records of calcium release from the sarcoplasmic reticulum during simulations of the control conditions and the high magnesium conditions. (b) Data showing the rate of calcium release from the sarcoplasmic reticulum during simulation.

145

Rate of calcium release from SR (mM/s)

Time (s)

.16
.14
.12
.1
.08
.06
.04
.02
0

0   0.5   1   1.5   2   2.5   3   3.5   4   4.5   5

control

magnesium

TIME (s)

[CaSR] (M)

2.e-3
1.5e-3
1.e-3
.5e-3
0.

0.   1   2   3   4   5   6   7   8
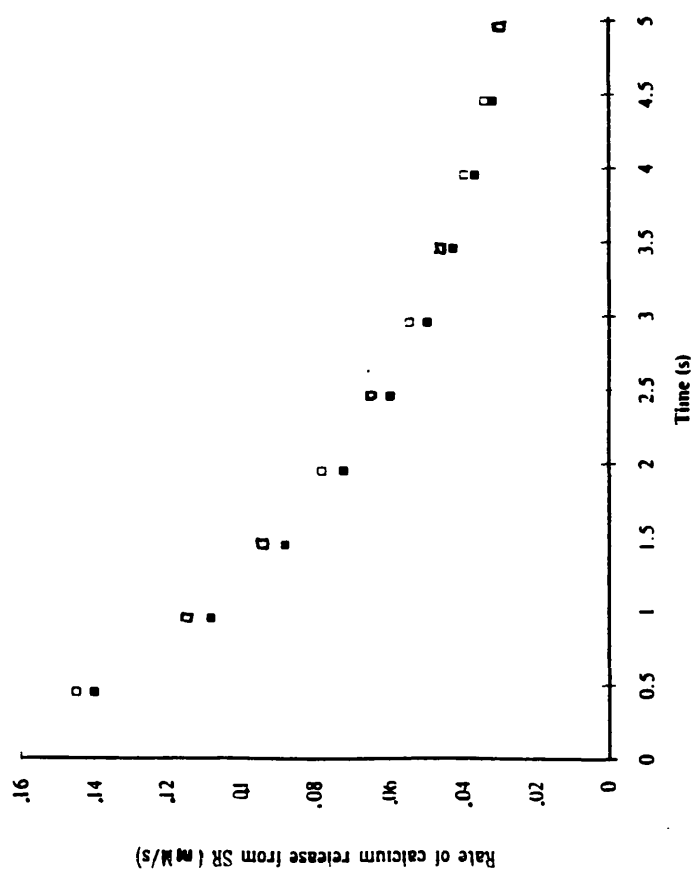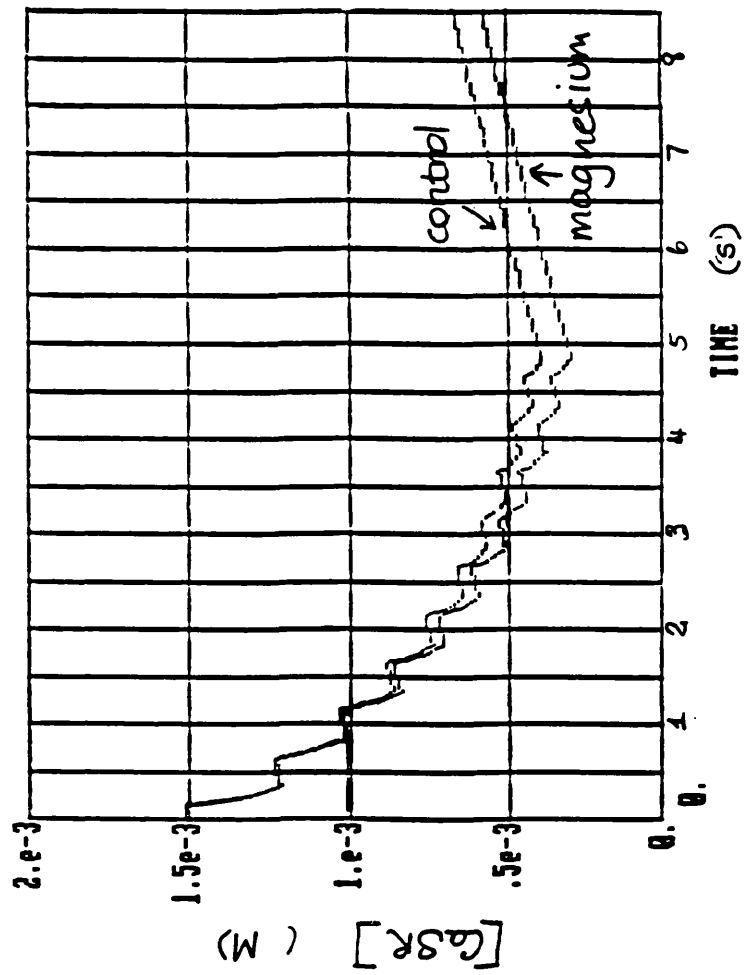
accompanied by a faster return of calcium to the sarcoplasmic reticulum results in the sarcoplasmic reticulum retaining a higher calcium level during the control simulation.

5.6.2 Calcium levels in the myoplasm

Figure 33a shows the free calcium levels in the fibre during the simulations. During the first period of stimulation the same concentration of calcium is released from the sarcoplasmic reticulum. The level of the free calcium in the myoplasm, after the release, however, is higher in the control simulation than in the high magnesium simulation, 2.987 μM and 2.2 μM, respectively. The higher free calcium level is then maintained for the duration of the simulation, with the maximum concentration of the free calcium in the control simulation approaching 8 μM in the control and 4 μM in the high magnesium simulation. It is interesting at this point to note that the greater rate of calcium release in the high magnesium simulation does not result in a higher myoplasmic calcium concentration than in the control simulation.

5.6.3 Location of calcium during the simulations

Figure 33b shows that the rate at which calcium is removed from the myoplasm is higher in the control than the high magnesium ion simulation. The uptake rate does not, however achieve as rapid a relaxation rate as would be expected with this profile. A closer examination of the location of calcium following activation is therefore appropriate.

Figure 33 (a) Records of free calcium levels during simulations of the control conditions and the high magnesium conditions. (b) The rate of calcium removal from the cytopskic reticulum.

control
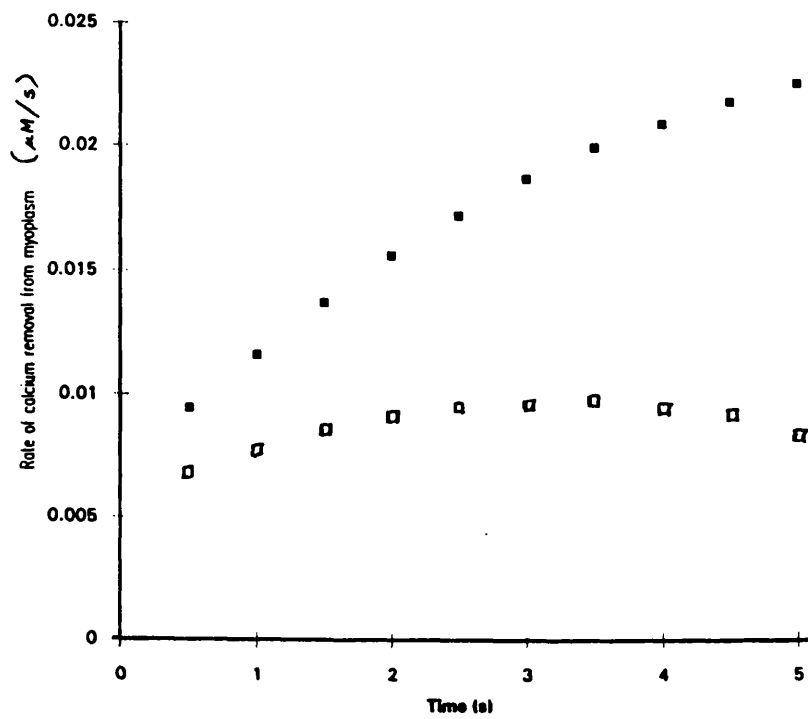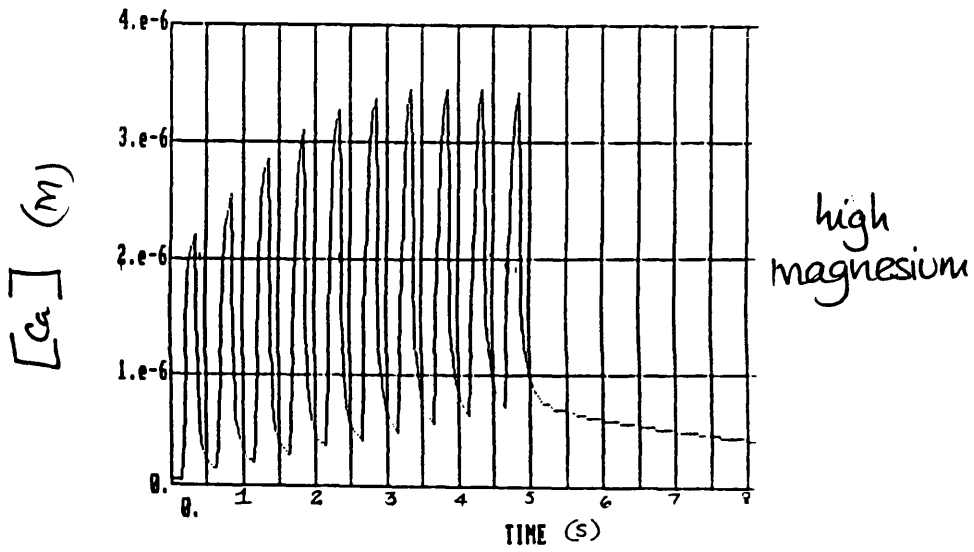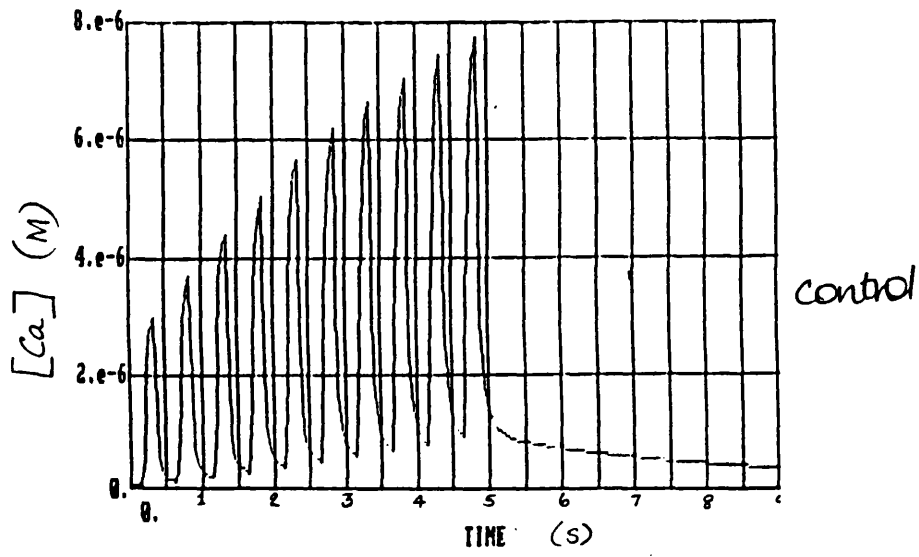
high magnesium

5.6.3.1 Troponin

In the control simulation, the maximum troponin occupancy is attained in the first 200 ms period of stimulation as shown in Figure 34. In the same period of contraction in the high magnesium simulation, the troponin occupancy reaches 98.5% of the reached in the control simulation. This translates to an attainment of 95% of the maximum force in the control simulation. Towards the end of the contraction, the force in the high magnesium simulation begins to fall, suggesting a relaxation of troponin by the parvalbumin.

5.6.3.2 Parvalbumin

5.6.3.2.1 Apo-parvalbumin

Figure 35 shows that during this same period calcium binds to the apo-parvalbumin in the myoplasm, almost depleting it, a drop in concentration from 13.3 μM to 1.7 μM, in the control simulation. In the high magnesium simulation , however, the parvalbumin starts at a lower concentration, 8.3 μM and diminishes to 2.2 μM. The lower myoplasmic calcium level in the high magnesium solution suggest a more successful buffering of calcium than in the control simulation. This buffering, however, does not appear to reflect the initial apo-parvalbumin concentrations of the myoplasm as the myoplasmic calcium level is lower in the simulation which started with a higher apo-parvalbumin concentration.

Figure 34 Records of troponin-calcium levels during simulations of the control conditions and the high magnesium conditions.

152
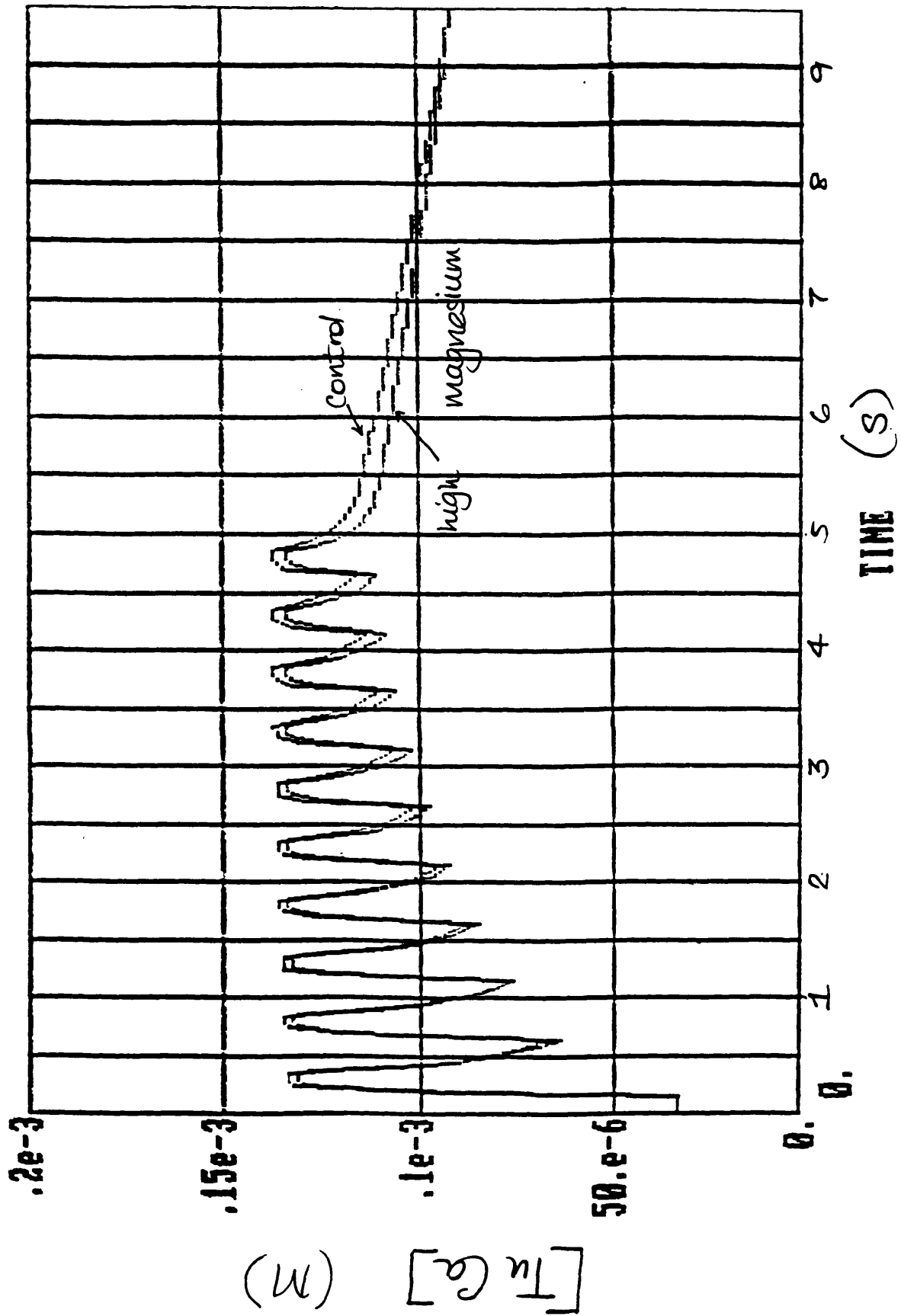
Figure 35 Records apo-parvalbumin concentration during simulations of the control conditions and the high magnesium conditions.

high magnesium

TIME (s)

Control

TIME (s)

[Pa] (M)

154
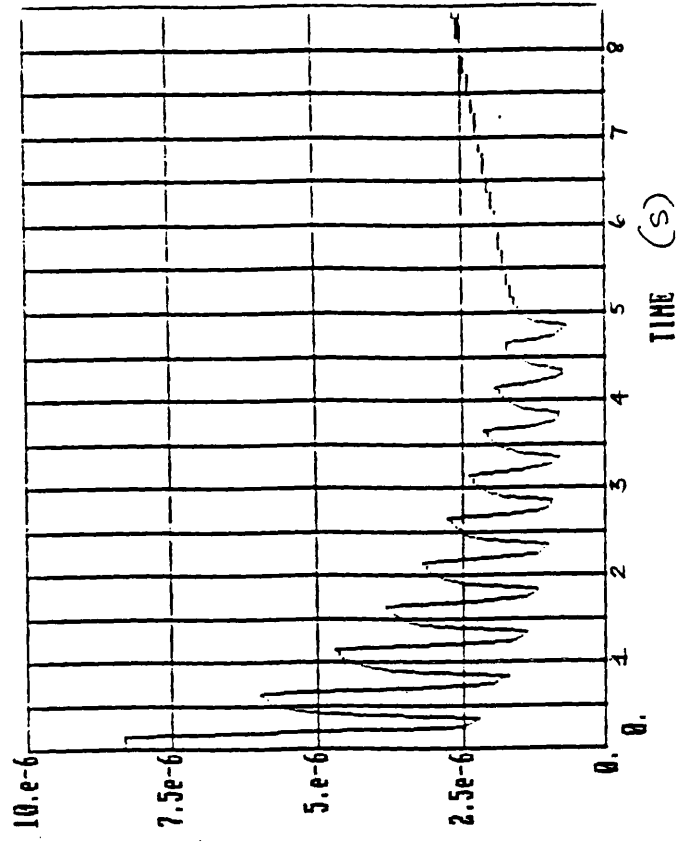
5.6.3.2.2 Parvalbumin- calcium

Calcium buffering by parvalbumin should be seen as an increase in the parvalbumin-calcium levels of the myoplasm as shown in Figure 36. In the control simulation, the parvalbumin-calcium level increases from 0.8 mM to 0.97 mM in the first period of contraction. Seven percent of this increase is due to calcium binding to the apo-parvalbumin that was already present in the fibre. In the high magnesium simulation, a larger increase in parvalbumin-calcium is seen, 0.19 mM compared to 0.17 mM. This larger increase however, reflects a contribution of only 3% by the apo-parvalbumin. The buffering capacity of the high magnesium simulation therefore appears to derive from the higher parvalbumin-magnesium present.

5.6.3.2.3 Parvalbumin-magnesium

Figure 37 shows that as the contraction proceeds, the parvalbumin-magnesium concentration in the control simulation declines to 0.238 mM, which represents 18% of the original store of calcium buffer. In the high magnesium ion simulation, 405 mM, 27% of the original parvalbumin-magnesium remains at the end of the contraction, despite a lower sarcoplasmic reticulum calcium level. The greater capacity to buffer calcium appears to reflect a larger apo-parvalbumin "store" in the high magnesium ion simulation as shown, Table 7, by the identical rates in the increase in free magnesium and the depletion of parvalbumin-magnesium. Parvalbumin-calcium then increases with a slower time course.

155

Figure 36 Records of parvalbumin-calcium concentration during the simulation of the

control (a) and high magnesium (b) conditions.

Figure 37 Records of parvalbumin-magnesium concentration during the simulation

of the control (a) and high magnesium (b) conditions.

Figure axes: vertical axis labeled [Pa Mg] (M) with values 2.e-3, 1.5e-3, 1.e-3, .5e-3, 0.; horizontal axis labeled TIME (S) with values 0 through 9. Curves labeled "control" and "high Magnesium".
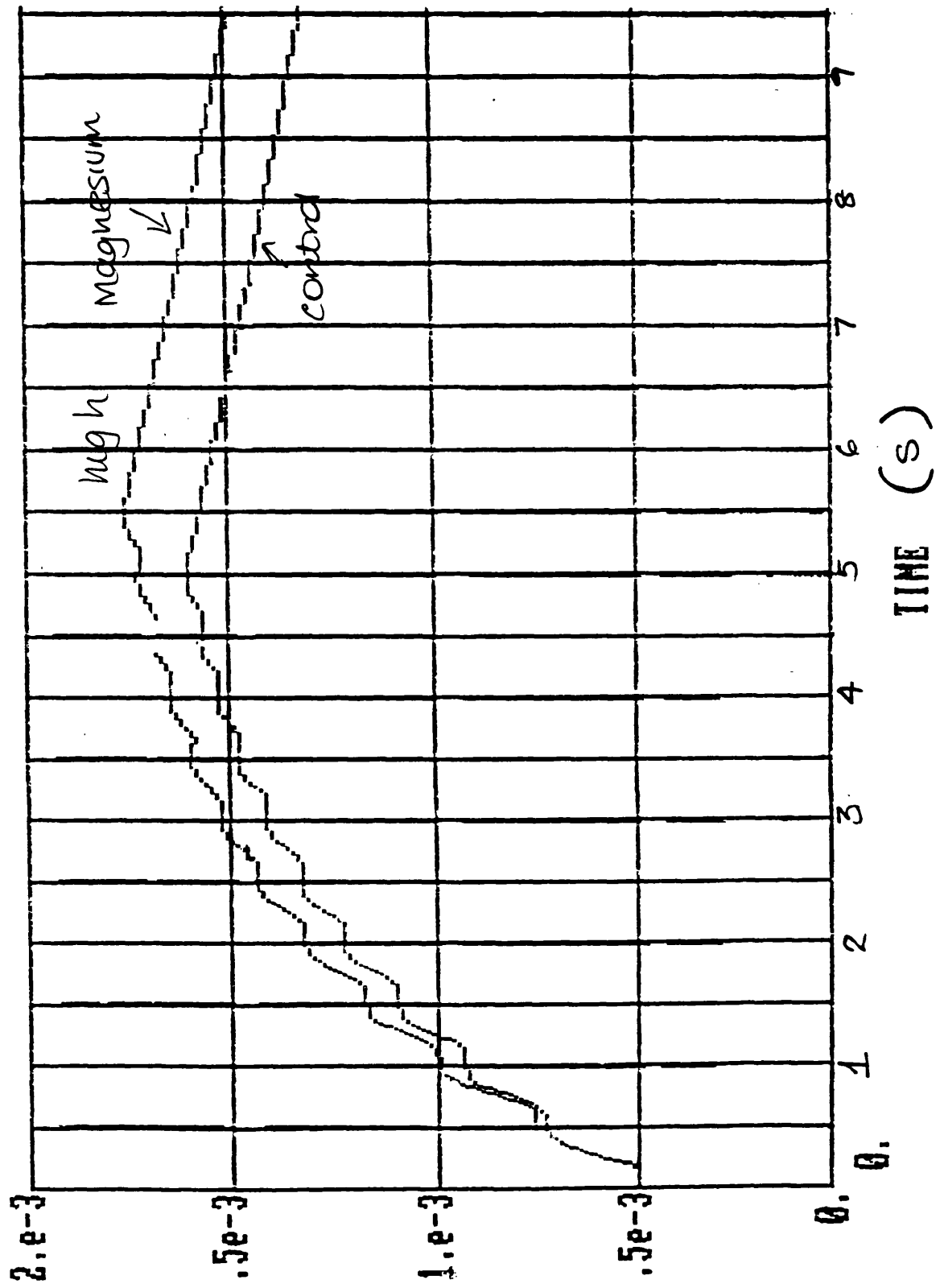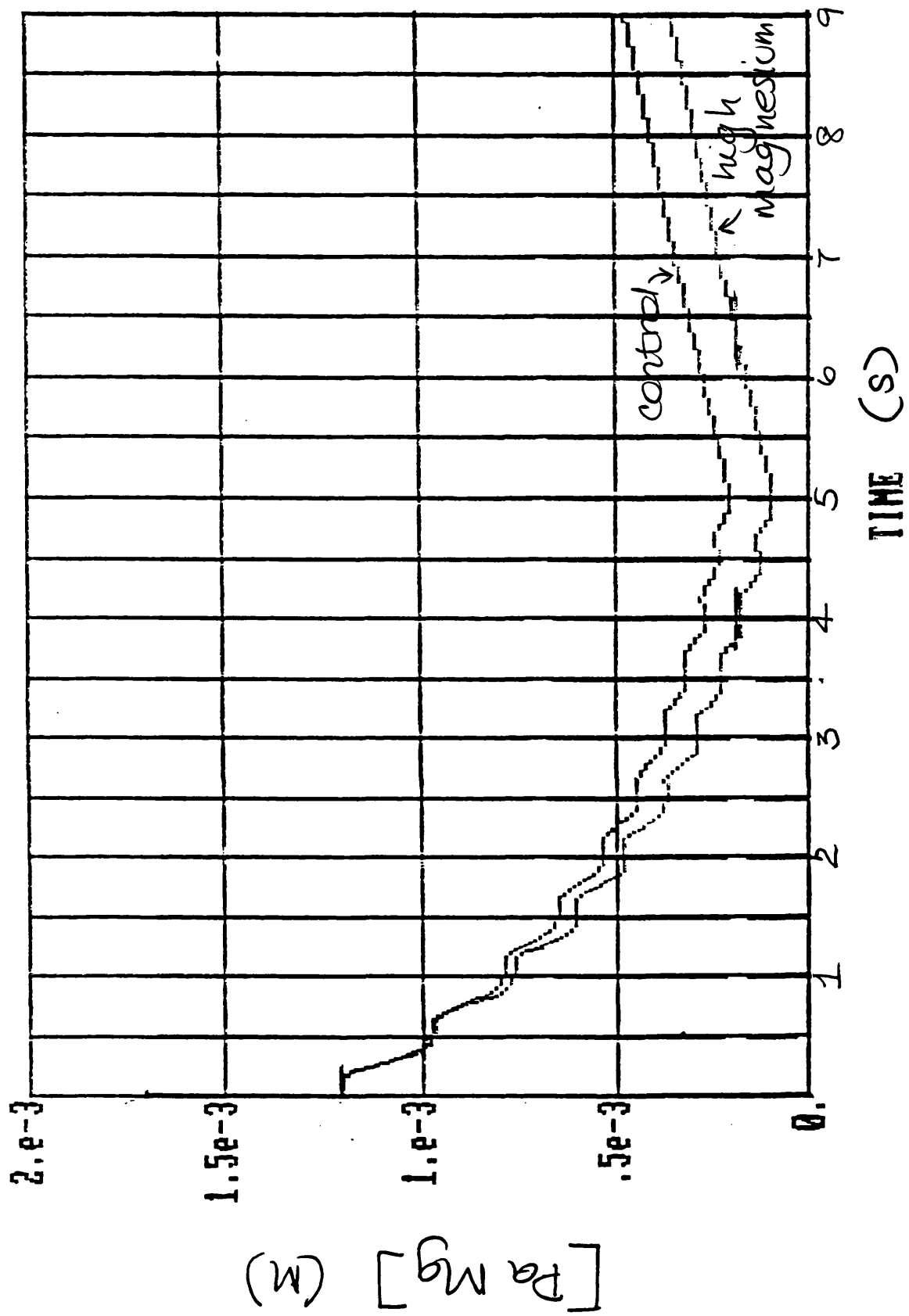
Table 7 A comparison of the rates of changes in the levels of parvalbumin-magnesium and

parvalbumin-magnesium				magnesium		
time	control	high		time	control	high
0.4	4.576	4.78		0.4	4.58	4.78
0.9	3.65	3.96		0.9	3.64	3.9
1.4	2.854	3.156		1.4	2.86	3.16
1.9	2.24	2.52		1.9	2.24	2.52
2.4	1.76	2.01		2.4	1.76	2.02
2.9	1.39	1.61		2.9	1.4	1.6
3.4	1.11	1.284		3.4	1.1	1.28
3.9	0.86	1.022		3.9	0.88	1.02
4.4	0.69	0.81		4.4	0.68	0.82
4.9	0.55	0.65		4.9	0.56	0.66

5.6.4 Relaxation rate

Figure 38 shows that the "relaxation rate" in these simulations is well described by the exponential $R = R_i(e^{t/\tau}) + R_F$ where R is the relaxation rate at time "t", R_i is the initial relaxation and R_F the final rate. The data from the calculation of relaxation rate during the simulations show that this treatment increases the initial relaxation rate, calculated as $(R_{Mg}/ R_{Control})$, by 22% . The final relaxation rate in the high magnesium solution is higher than in the control solution. The slowing of the time constant with increasing magnesium concentration is seen in both the relaxation and heat rates experiments and the possible causes are explored there.

5.7 DISCUSSION

The effect of raising intracellular magnesium from 1 mM to 20 mM on calcium movements in the myoplasm is summarised in the following discussion:

The first observable change is the decrease in maximum force followed by an inability of the "fibre" to maintain force towards the end the contraction. The force decrement is accompanied by a decline in the free calcium ion concentration and higher total calcium level in the myoplasm. These observations on force suggest an initial partitioning of the released calcium between troponin and a higher concentration of myoplasmic calcium binding sites followed by a removal of calcium from troponin by parvalbumin. It is possible then that once the "extra" parvalbumin is saturated with calcium then no further decline in force would be seen.

160

Figure 38 Data showing the rates of relaxation in the control and high magnesium

simulation fitted with an exponential of the form $(R = R_1 e^{t/\tau}) + R_i$.

high magnesium

(/s)

control

Relaxation rate (/s)

Time (s)

162
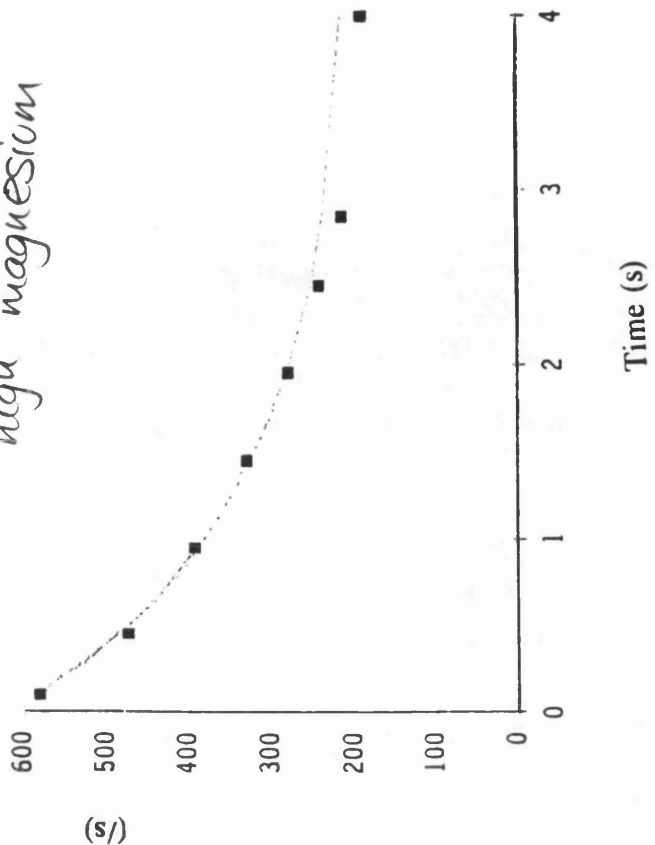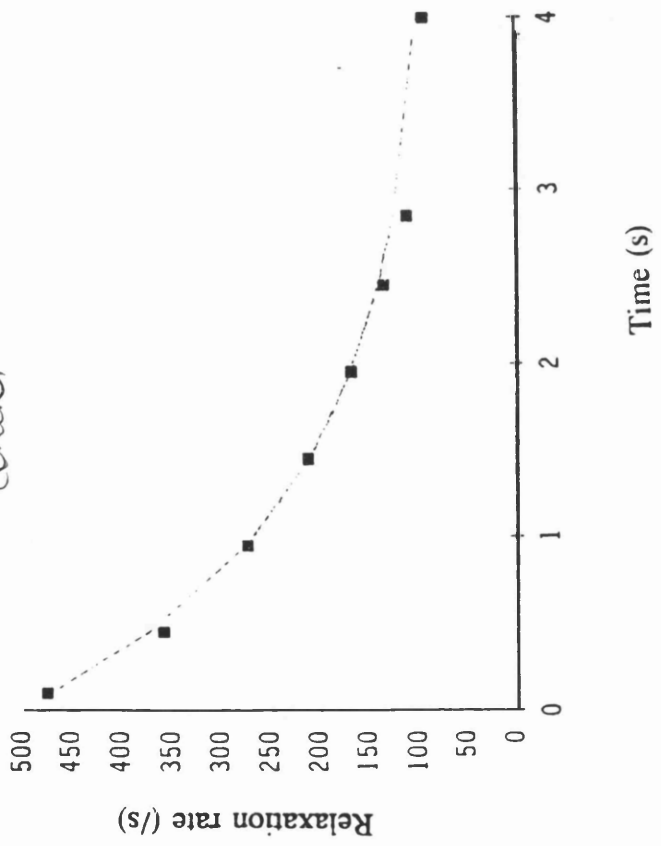
The greater release of calcium in the high magnesium solution which results in a lower free calcium level than in the control solution also suggests an increase in number of myoplasmic calcium binding sites. A calculation of the relaxation rate when free magnesium is high shows an increases of 68% in the initial rate of relaxation when compared to the relaxation rate in the control simulation. This increase is seen despite similar calcium uptake rates into the SR in the control and high magnesium simulations. The activity of the calcium pump cannot explain the higher relaxation rate. The increase in relaxation rate, therefore, appears to reflect the presence of a larger myoplasmic calcium buffering capacity when the parvalbumin-magnesium concentration of the myoplasm is raised.

The important factor in increasing relaxation rate appears to be the concentration of apo-parvalbumin which becomes available in the myoplasm. A rate controlled by the size of the parvalbumin-magnesium store of apo-parvalbumin as well as the rate of magnesium dissociation from parvalbumin. An increase in the concentration of parvalbumin-magnesium rather then a reliance on the kinetics of rate of dissociation of this complex which is not strongly sensitive to temperature (Hou et al., 1991) makes parvalbumin-magnesium a desirable "extra" relaxant in poikilotherms. The parvalbumin buffer could thus be altered by seasonal changes in the free magnesium levels of the myoplasm. Somlyo and Somlyo (1981) and Lopez et al. (1982)have reported a variation in the free magnesium concentrations in frog muscle, with winter frogs having a higher magnesium concentration than summer frogs.

Gillis et al. (1983) and Cannell and Allen (1986) developed models similar to the one

reported here. Again the question addressed was the effectiveness of parvalbumin as an "extra" relaxant in skeletal muscle. The major difference between these two models and the current one is in the total concentration of parvalbumin used in the simulation and the assumption that parvalbumin was more than 90% saturated with magnesium at rest. The results obtained were similar qualitatively, again highlighting the fact that it is the concentration of calcium binding sites on parvalbumin which is important during relaxation. Their high occupancy of parvalbumin sites by magnesium at rest therefore compensates for the difference in initial concentrations.

The concentrations used in this model extend the earlier findings by showing that it is possible to vary the calcium buffering effect of parvalbumin by changing the intracellular concentration of magnesium. This variation in the contribution of magnesium to relaxation with changes in the ambient temperature would not have been possible with their models.

The results from this simulation, like the models published previously, suggests that parvalbumin can buffer calcium in the myoplasm. This findings of this model then also suggests that there is in fact a window of concentrations at which parvalbumin is an effective calcium buffer in the myoplasm. Further still, the concentration of parvalbumin-magnesium within this window is set by magnesium.

164

CHAPTER 6

GENERAL DISCUSSION

The work reported in this thesis was undertaken to assess the effect of magnesium ion concentration on some aspects of muscle function. The effect of magnesium on parvalbumin-magnesium levels and relaxation rate was of particular interest. This was done by testing the effect of increasing the concentration of magnesium in the extracellular fluid on relaxation rate and heat production, an effect magnesium is thought to exert via an increase in intracellular free magnesium. The role of intracellular magnesium ion concentration in mediating this effect was tested in a model in which the intracellular free magnesium was raised directly. In this Chapter, an attempt is made to bring the experimental and theoretical aspects of the Thesis together.

The experiments on relaxation rate show that increasing extracellular magnesium increases the initial relaxation rate from 5 s^{-1} to 8 s^{-1}. The rate of relaxation, which comprises the two processes 1) calcium uptake by the sarcoplasmic reticulum and 2) calcium binding to parvalbumin, then declines from these initial values to a similar rate in the two solutions. The similarity in relaxation rates after 2.7 s of contraction suggests that the relaxation rate is unaffected by this treatment. The increase in the relaxation rate is then thought to result primarily from the second process of calcium binding to parvalbumin.

The relaxation rate following muscle activation is defined as $R = R_i (e^{t/\tau}) + R_p$. In order to determine the size of the component R_i, the relaxation rate has to be measured at a time when parvalbumin is the major contributor to this rate. This is the period immediately following the end of stimulation. Gillis (1985) suggests that it is possible to measure relaxation "too early". Lannergren and Westerblad (1990) also suggest that relaxation rate should be measured as the rate of change of force rather than just a rate. Both these statements arise because of the possibility of miscalculating relaxation rate when the free calcium concentrations in the myoplasm are different even when the force is the same or when the maximum forces attained during contraction are different due to different vels of activation as shown below.
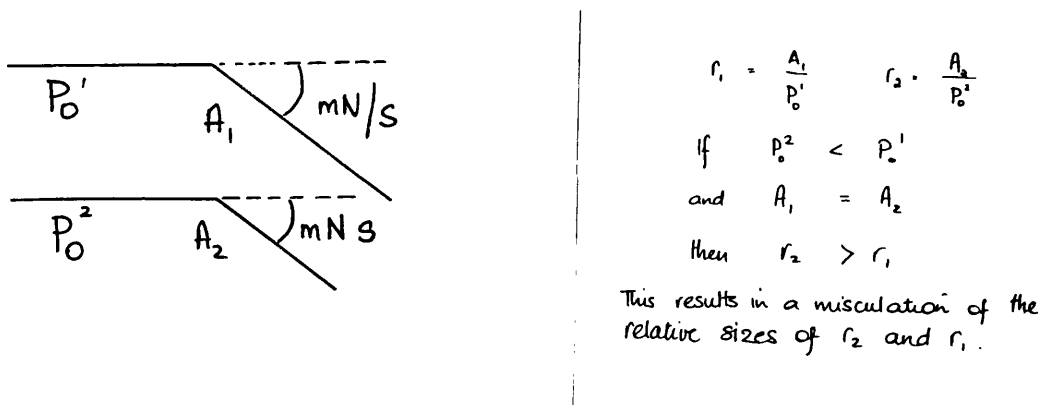
However the results from this study suggest that both these reservations about the time and manner of measuring relaxation can be overcome.

The experimental results showed that measuring relaxation rate at 2.5% and 5% maximum force gave similar relations between relaxation rate and extracellular magnesium ion concentration. Thus suggests the same processes are acting at these

times following the end of stimulation. During the construction of the model, it was discovered that it was vital to put a ceiling on the maximum free calcium levels in the myoplasm. Leaving this condition out of the model resulted in a "cross-over" effect where initially the relaxation rate in the high magnesium simulation was higher than in the control simulation. The rates then crossed over so that the rate of relaxation in the high magnesium solution was faster than in the control. Limiting the free calcium levels eliminated this problem. Studies on free calcium levels, in live muscle, have shown that free calcium does not rise above about 7 μM (Cannell, 1986). This then suggests the muscle already has a ceiling for free calcium levels similar to that found necessary in the model. The level from which calcium is pumped will then not be a limiting factor in choosing the time at which to measure relaxation rate.

Calcium and magnesium are known to bind to the same site on parvalbumin (Potter et al., 1978). The ratio of the concentrations of parvalbumin-calcium to parvalbumin-magnesium will be determined by the rate at which parvalbumin binds calcium in the presence of magnesium (Moeschler et al., 1980, Smith and Woledge, 1985). This rate is defined as $(K_A \, K_D([Ca]/[Mg]))$ where K_A is parvalbumin affinity for calcium and K_D is the rate of magnesium dissociation from parvalbumin. From this relation it can be deduced that since calcium concentration is constant at rest and the affinities of parvalbumin for the two cations are constant, then magnesium will determine the position of the equilibrium concentrations of parvalbumin-calcium and parvalbumin-magnesium at rest. During contraction, when free calcium rises and free magnesium is constant, the calcium concentration in the myoplasm will determine this

167

equilibrium. Therefore, initial relaxation rate and during a contraction will depend on the parvalbumin-magnesium level at rest and the concentration of free calcium in the myoplasm during contraction. It would also be expected that in a cell where parvalbumin concentration does not change, there is a limit in the extent to which increasing magnesium in the extracellular fluid can enhance relaxation rate (Godt, 1989). This is in fact seen in the experiments on the effect of dose on relaxation rate. There is an increase in the relaxation rate as extracellular magnesium is increased. The relaxation rate then reaches a plateau at extracellular magnesium ion concentrations between 10 and 20 mM.

The dependence of relaxation rate and heat production on the concentration of free magnesium is seen quite clearly as an increase in these two parameters following an increase in the concentration of magnesium in the extracellular fluid bathing the fibres. The increase in competition between calcium and magnesium for parvalbumin is also seen as an increase in the time constant of these two parameters when extracellular magnesium ion concentration is raised.

Raising extracellular magnesium was seen to decrease force production. This magnesium effect on relaxation is seen in two different ways: 1) a production of a lower maximum force, and 2) an inability to sustain maximum force during a prolonged contraction. The initial 10% decrement in maximum force is attributed to t-tubular conduction failure due to a raised extracellular concentration of magnesium. This decrement in force is attributed to an effect similar to raising extracellular calcium concentration (Howell et al., 1984, Gonzalez-Serratos, 1979). The inability

of the fibre to maintain the maximum force produced during a prolonged contraction is attributed to an enhanced calcium buffering capacity of the myoplasm when extracellular magnesium ion concentration is raised. These decreases which are also seen in the model coupled with the report by Baylor et al. (1983) that the free myoplasmic calcium level following activation depends on the number of calcium sites in the myoplasm support the idea of an increased calcium buffer when magnesium levels are raised.

It is suggested, therefore, that the early partial relaxation of tetanic force in the high magnesium solution is due to calcium uptake from troponin by parvalbumin following the depletion of the calcium store of the sarcoplasmic reticulum. Once an equilibrium is established between the free calcium and the calcium binding sites then a new lower force would be maintained. This is in fact seen in the experiments as a higher myoplasmic concentration of bound calcium as well as a levelling off of the decline in force at the time the relaxation rate reaches a steady state in the high magnesium solution.

Increasing extracellular magnesium also increases heat production during a prolonged contraction. Both the labile heat which is the component attributed to the parvalbumin reaction of interest increases about 60%, the same increase seen in relaxation rate in this solution. Fitting a monoexponential of the form $(X = X_o (e^v) + x_b)$ where X_o is the parvalbumin-magnesium contribution to the measurement being made and x_b is the contribution of the calcium ATPases of the myoplasm to the relaxation and heat production provides a good description of both processes. This suggests parvalbumin-

magnesium is influencing these two processes in a similar manner. There is however some difference in the time constants in with which these processes decay. A difference previously described by Peckham and Woledge, 1985). This difference is maintained in the high magnesium solution. The relaxation rate in the model is also described by a similar exponential. The time constant is again different from that seen in the experiments. These observations confirm the results by Elzinga et al. (1989) that labile heat production does not reflect calcium uptake by parvalbumin exclusively.

Ogawa et al (1980) suggest that the activity of the sarcoplasmic reticulum, although marginal, might explain relaxation rate in toad muscle. Later work by Ogawa and Tanokura (1986a, 1986b) also suggests that the kinetics of calcium buffering by parvalbumin are highly temperature dependent thus giving rise to the same problems seen with calcium pump of the sarcoplasmic reticulum. The results reported in this Thesis, however, suggest that magnesium might indeed play a role in determining the relaxation rate of muscles in which it is found in high concentrations. Further, the concentration of parvalbumin-magnesium in the muscle at rest is the vital factor in determining the seasonal variation in relaxation rate.

Direct measurements of intracellular magnesium ion levels during contraction, which should be possible now with the advent of the intracellular fluorescent magnesium dyes similar to those used for calcium measurements, of the are needed in order to determine if this mechanism is used by live fibres as might be suggested by the difference in free magnesium ion levels in the myoplasm of summer and winter frogs (Somlyo and Somlyo, 1985, Lopez et al., 1984).

A limitation of the model used here is the exclusion of feedback loops between calcium and magnesium in order to control calcium release and calcium uptake by the sarcoplasmic reticulum. These controls are important in controlling calcium movements between the myoplasm and the sarcoplasmic reticulum and calcium interactions with troponin (Fabiato and Fabiato, 1975, Donaldson and Kerrick, 1975, Ikemoto et al., 1978). This model therefore, presents a qualitative effect of increasing magnesium. Further refinement of the model is required in order to attain a more qualitative effect.

REFERENCES

Abbott, B.C. 1951. The heat production associated with the maintenance of a prolonged contraction and the extra heat produced during large shortening. J. Physiol. 112:438-445.

Agostini, B., Demartino, L. and Hasselbach, W. 1990. On the problem of season and cold dependence of calcium transport by skeletal muscle sarcoplasmic reticulum. Zeitschrift fur naturforschung C- A journal of biosciences. 45:671-675.

Altura, B.M., Zhang, A., Cheng, T.P.Q. 1992. Effects of extracellular magnesium $[Mg^{2+}]_o$ on intracellular free ionized magnesium concentration $[Mg^{2+}]_i$ and its regulation in vascular smooth-muscle cells. FASEB J. 6:1790.

Alvarez-Leefmans, F.J., Gamino, S.M., Giraldez, F., Gonzalez-Serratos, H. 1986. Intracellular free magnesium in frog skeletal muscle fibres measured with selective microelectrodes. J. Physiol. 378: 461-483.

Alvarez-Leefmans, F.J, Giraldez, F. and Gamino, S.M. 1987. Intracellular free magnesium in excitable cells : its measurement and its biologic significance. Can. J. Physiol. Pharmacol. 65:915-925.

Aubert, X. and Gilbert, S. 1980. Variation in the isometric maintenance heat rate with muscle length near that of maximum tension in frog striated muscle. J. Physiol. 303: 1-8.

Aubert, X. 1956 Les Couplage énergétique de la contraction musculaire. These dégregation de l'enseignement superier. pp. Editions Arscia, Bruxelles.

Baron, G., Demaille, J. and Detruge, E. 1975. The distribution of parvalbumins in muscles and in other tissues. FEBS Letts. 56: 156-160.

172

Baylor, S.M., Chandler, W.K., Marshall, M.W. 1983. Sarcoplasmic reticulum calcium release in frog skeletal muscle fibres estimated from Arsenazo III calcium transients. J. Physiol. 344: 625-666.

Baylor, S.M., Chandler, W.K. and Marshall, M.W. 1982 Optical measurements of intracellular pH and magnesium in frog skeletal muscle fibres. J. Physiol. (London), 331:105-137.

Benzonana, G., Capony, J.-P., and Pechere, J.-F. 1972 The binding of calcium to muscular parvalbumins Biochim. Biophys. Acta 278:110-116.

Berchtold, M.W., Heizmann, C.W. and Wilson, K.J. 1983. Ca2+-binding proteins: a comparative study of their behaviour during high-performance liquid chromatography using gradient elution on reverse-phase supports. Anal. Biochem. 129: 120-131.

Blatter, L.A., Buri, A., McGuigan, J.A.S. 1989. Free intracellular magnesium concentration in isolated ferret ventricular muscle and in frog skeletal muscle measured with ion-selective microelectrodes containing the new magnesium sensor ETH 5214. J. Physiol. 154P.

Blatter, L.A. 1990 Intracellular free magnesium in frog skeletal muscle studied with a new type of magnesium-selective microelectrode: interactions between magnesium and sodium in the regulation of $[Mg]_i$. Pflugers Arch. 416:238-246.

Blatter, L.A. 1990. The role of Na/Mg exchange mechanism in the regulation of intracellular free magnesium in frog skeletal muscle. 57:533

Blinks, J.R., Rudel, R. and Taylor, S.R. 1978. Calcium transients in isolated amphibian   skeletal muscle fibres: detection with aequorin. J.Physiol. 277: 291-323.

Blum, H.E., Lehky, P., Kohler, L., Stein, E.A. and Fischer, E.H. 1977. comparative properties of vertebrate parvalbumins. J. Biol. Chem. 252:2834-2838.

Blinks, J.R. 1965. Influence of osmotic strength on cross-section and volume of isolated muscle fibres. J. Physiol. 177: 42-57.

Briggs, N. 1975. Identification of the soluble relaxing factor as parvalbumin. Fed. Proc. 34: 540.

Burchfield, D.A. and Rall, J.A. 1986. Energetics and mechanics of frog skeletal muscle in hypotonic solution. Am. J. Physiol. 251:C66-C77.

Cannell, M.B. 1982. Intracellular calcium during relaxation in frog singe muscle fibres. J. Physiol. 36: 70-71P.

Cannell, M.B. and Allen, D.G. 1984. Model of calcium movements during activation in the sarcomere of frog skeletal muscle. Biophys. J. 45: 913-925.

Cannell, M.B. 1986. Effect of tetanus duration on free calcium during relaxation of frog skeletal muscle fibres. J. Physiol. 376: 203-218.

Celio, M.R. and Heizman, C.W. 1982 Calcium binding protein parvalbumin is associated with fast contracting muscle fibres. Nature. 297:504-506.

Curtin, N.A. and Woledge R.C. 1979. Chemical change and energy production during contraction of frog muscle: how are their time courses related? J. Physiol. 288:353-366.

Curtin, N.A., Howarth, J.V., Rall, J.A., Wilson, M.G.A. and Woledge, R.C. 1984. Simultaneous heat and tension measurements from single muscle cells in " Contractile Mechanisms in Muscle". Eds. Pollack, G.H. and Sugi, H. Plenum publishing Corporation.

Curtin, N.A. and Woledge, R.C. 1981. Effect of muscle length on energy balance in frog skeletal muscle. J. Physiol. 316: 453-468.

Curtin, N.A. and Woledge, R.C. 1978. Energy changes and muscular contraction. Physiol. Rev. 288: 690-761.

Curtin, N.A. 1976. The prolongation of relaxation after an isometric tetanus. J. Physiol. 258: 80-81P.

Curtin, N.A., Howarth, J.V., Rall, J.A., Wilson, M.G.A. and Woledge, R.C. 1986. Absolute values of myothermic measurements on single muscle fibres from frog. J. Muscle Res. Cell. M. 7: 227-332.

Curtin, N.A., Howarth, J.V. and Woledge, R.C. 1983. Heat production by single fibres of frog muscle. J. Muscle Res. & Cell Motility 4: 207-222.

Ebashi, S. and Endo, M. 1968. Calcium ion and muscle contractions. Prog. Biophys. & Molec. Biol. Vol. 18, (J.A.V. Butler and D. Noble, eds) pp 125-183. Pergamon Press, Oxford.

Edman, K.A.P. and Flitney, F.W. 1982. Laser diffraction studies of sarcomere dynamics during 'isometric' relaxation in isolated muscle fibres of the frog. J. Physiol. 329: 1-20.

Edman, K.A.P. 1979. The velocity of unloaded shortening and its relation to sarcomere length and isometric force in vertebrate muscle fibres. J. Physiol. 291: 143-159.

Elzinga, G., Howarth, J.V., Wilson, M.G.A. and Woledge, R.C. 1986. Stable maintenance heat rate is related to maximum force in isolated fibres from frog tibialis anterior muscle near 0 C. J. Physiol. 367: 77P.

175

Elzinga, G., Howarth, J.V., Rall, J.A., Wilson, M.G.A. and Woledge, R.C. 1989. Variation in the normalized tetanic force of single frog muscle fibres. J. Physiol. 410: 157-170.

Elzinga, G. Peckham, M. and Woledge, R.C. 1984 The sarcomere length dependence of the rate of heat production during isometric tetanic contraction of frog muscles. J. Physiol. 357:495-504.

Elzinga, G., Lannergren, J. and Simonides, W.S. 1988 Labile heat and parvalbumin content of single-muscle fibres isolated from the iliofibularis muscle of Xenopus laevis. J. Physiol. 48P.

Endo, M. 1977. Calcium release from the sarcoplasmic reticulum. Physiol. Rev. 57: 71-108.

Flatman, P.W 1991 Mechanisms of magnesium transport. Annu. Rev. Physiol. 53:259-71.

Flatman, P.W. 1984. Magnesium transport across cell membranes. J. Membr. Biol. 80:
1-14

Gerday, C. and Gillis, J.M. 1976. The possible role of parvalbumin in the control of contraction. J. Physiol 258: 96-97P.

Gilbert, D.L. 1960 Magnesium equilibrium in muscle. J. Gen. Physiol. 43: 1103-1118.

Gillis, J.M., Thomason, D., Lefevre, J. and Kretsinger, R.H. 1984. Formation of calcium-parvalbumin complex during contraction. A source of "Unexplained heat"? "Contractile mechanisms in muscle" Eds. Pollack, H. and Sugi, H. Plenum Publishing Corporation. p573-579.

Gillis, J.M. and Gerday, C.H. 1977 Calcium movements between myofibrils, parvalbumins and sarcoplasmic reticulum in muscle. In: Calcium binding proteins and calcium function (Eds. Wasserman, R.H., Corradino, R.A., Carafoli, E., Kretsinger, R.H., MacLennan, D., Stegel, F.L.) Pub. North Holland.

Gillis, J.M. 1985. Relaxation of vertebrate skeletal muscle. A synthesis of the biochemical and physiological approaches. Biochim. Biophys. Acta, 811:97-145.

Gillis, J.M. Piront, A., Gosselin-Rey, C. 1979. Parvalbumin distribution inside the cell. Biochim. Biophys. Acta 585: 444-450.

Gillis, J.M., Thomason, D., Lefevre, J. and Kretsinger, R.H. 1982. Parvalbumins and muscle relaxation: a computer simulation study. J.Muscle Res. and Cell Motility 3: 377-398.

Gillis, J.M. 1980 The biological significance of muscle parvalbumins. In Calcium-binding proteins: Structure and functions. Eds. Siegel, F.L., Carafoli, E., Kretsinger, R.H., MacLennan, D.H. and Wasserman. p309-311.

Godt, R.E. and Maughan, D.W. 1989. On the composition of the cytosol of relaxed skeletal muscle of frog. Am. J. Physiol. 254: C591-604.

Gonzalez-Serratos, H., and Rasgado-Flores, H. 1990. Extracellular magnesium dependent sodium efflux in squid giant axons. Am. J. Physiol. 259:C541-548.

Gordon, A.M., Huxley, A.F. and Julian, F.J. 1966. The variation in isometric tension with sarcomere length in vertebrate muscle fibres. J.Physiol. 184: 170-192.

Gosselin-Rey, C. and Gerday, C. 1977. Parvalbumins from frog skeletal muscle (Rana temporaria L.). Isolation and characterization. Structural modifications

associated with calcium binding. Biochim. Biophys. Acta 492: 53-63.

Gupta, R.K. and Moore, R.D. 1980. ^{13}P NMR studies of intracellular free Mg2+ in intact frog skeletal muscle. J. Biol. Chem. 255:3987-3993.

Haiech, J. Darencourt, J. Pechere, J.-F. and Demaille, J.G. 1979. Magnesium and calcium binding to parvalbumins: evidence for differences between parvalbumins and an explanation of their relaxing function. Biochemistry 18: 2752-2758.

Hamoir, G. 1955. Fish proteins. Adv. Protein Chem. 10: 227-288.

Hasselbach, W. 1964. Relaxing factor and relaxation of muscle. Prog. Biophys. Chem. 14:167-222.

Heizman, C.W., Peckham, M. and Woledge, R.C. 1984. A comparison of the rate of relaxation and isometric heat rate in sartorius and ELDIV muscles of the frog (Rana temporaria). J. Physiol. 353. 65P

Heizmann, C.W. 1984. Parvalbumin, an intracellular calcium-binding protein; distribution properties and possible roles in mammalian cells. Experientia 40: 910-921.

Hess, P., Metzger, P. and Weingart, R. 1982. Free magnesium in sheep, ferret and frog striated muscle at rest measured with ion-selective microelectrodes. J. Physiol. (London), 333:173-188.

Hill, A.V. 1937. Methods of analyzing the heat production of muscle. Proc. Roy. Soc. B 124: 114-136.

Homsher, E. and Kean, C.J. 1978. Skeletal muscle and energetics and metabolism. Ann. Rev. Physiol. 40:93-131.

178

Hou, T.T, Johnson, J.D. and Rall, J.A. 1991b. Parvalbumin content and Ca^{2+} and Mg^{2+} dissociation rates correlated and changes in relaxation rate of frog-muscle fibres. J. Physiol. 441:285-304.

Hou, T.T, Rall, J.A. and Johnson, J.D. 1991a. Role of parvalbumin (Pa) in frog skeletal-muscle relaxation. J. Muscle Res. and Cell Motility. 12:114

Huxley, A.F. Muscle contraction. J. Physiol. 243: 1-43.

Huxley, A.F. and Simmons, R.M. 1971. Proposed mechanism of force generation in striated muscle. Nature 233: 533-538.

Huxley, A.F. 1957. Muscle structure and theories of contraction. Prog. Biophys. 7: 233-318.

Ikemoto, N., Morgan, T., Yamada,S. 1978. Ca^{++} -controlled conformational states in the Ca^{++} transport enzyme of sarcoplasmic reticulum. J. Biol. Chem. 235:8027-8033.

Inesi, G. and Scarpa, A. 1972. Fast kinetics of adenosine triphosphatase dependent Ca^{++} uptake by fragmented sarcoplasmic reticulum. Biochemistry. 11:356-359.

Inesi, G. 1985. Ann. Rev. Physiol. 47:573-610.

Irving, M. 1988 Measurement of intracellular free magnesium concentration with metallochromic indicators -studies on skeletal muscle Cell Biol. Internat. Reports. 12:67

Irving, M., Maylie, J., Sizto, N.L., Chandler, W.K. 1989. Simultaneous monitoring of changes in magnesium and calcium contractions in frog cut twitch fibres containing antipyralazo III. J. Gen. Physiol. 93: 585-608.

179

Klein, M.G., Kovacs, L., Simon, B.J. and Schneider M.F. 1991. Decline of myoplasmic Ca2+, recovery of calcium release and sarcoplasmic Ca2+ pump properties in frog skeletal muscle. J. Physiol. 414: 639-671.

Kometani, K. and Yamada, K. 1984. Dependence of labile maintenance heat production on sarcomere length and temperature, and the effect of twitch potentiators. Proc. Conference on Muscle Energetics. Vermont p.45.

Kretzschmar, K.M. and Wilkie, D.R. 1975. The use of the Peltier effect for simple and accurate calibration of thermoelectric devices. Proc. Roy. Soc. B. 190: 315-321.

Kretzschmar, K.M. and Wilkie, D.R. 1972. A new method for absolute heat measurement utilising the Peltier effect. J. Physiol. 224: 18-19P.

Lannergren, J., Hoh, J.F.Y. 1983. Myosin isoenzymes and contractile properties of single amphibian muscle fibres. Proc. Int. Union. Phys. Sciences 15: 388.

Lannergren, J. 1979. An intermediate type of muscle fibre in Xenopus laeurs. Nature 279: 254.

Lannergren, J. and Smith, R.S. 1966. Types of muscles fibres in toad skeletal muscle. Acta. Physiol. Scand. 68: 263-274.

Lannergren, J., Lindblom, P. and Johansson, B. 1982. Contractile properties of two varieties of twitch fibres of Xenopus laeurs. Acta Physiol. Scand. 114: 523-535.

London, R.E. 1991. Methods for measurement of intracellular magnesium- NMR and fluorescence. Ann. Rev. Physiol. 53:241-258.

Lopez, J.R., Alamo, L., Caputo, C.,Vergara, J., and Dipolo, R. 1984. Direct measurement of intracellular free magnesium in frog skeletal muscle using magnesium-selective microelectrodes. Biochim. Biophys. Acta, 804:1-7.

Maughan, D. W. and Godt, R.E. 1989 Equilibrium distribution of ions in a muscle fibre. Biophys. J. 56:717-722.

Maughan, D. 1983. Diffusible magnesium in frog skeletal muscle cells. Biophys. J. 43:780.

McGuigan, J.A.S and Blatter, L.A. 1989. Measurement of free magnesium using magnesium selective microelectrodes. 11:139-142.

Moeschler, H.J., Schaer, J.J. and Cox, J.A. 1980. A thermodynamic analysis of the binding of calcium and magnesium ions to parvalbumin. Eur. J. Biochem. 111: 73-78.

Ogawa, Y. and Tanokura, M. 1986b. Kinetic studies of calcium binding of parvalbumin from bullfrog skeletal muscle. J. Biochem. 99. 81-89.

Ogawa, Y. 1970. Some properties of fragmented frog sarcoplasmic reticulum with particular reference to its response to caffeine. J.Biochem. 67: 667-683.

Ogawa, Y. and Tanokura, M. 1986. Steady-stae properties of calcium binding to parvalbumins from bullfrog skeletal muscle: Effects of Mg^{2+}, pH, ionic strength, and temperature. J. Biochem. 99.73-80.

Ogawa, Y. Kurebayashi, N. Irimajiri, A., Hanai, T. 1980. Transient kinetics for Ca uptake by fragmented sarcoplasmic reticulum from bull-frog skeletal muscle with reference to the rate of relaxation of living muscle. In "Molecular and Cellular aspects of muscle function" (Ed Vorgay E.,Kover, A., Kovacs, T. and

181

Kovacs, L.) pp 417-435. Pub. Pergamon Press/ Akademia Kiado.

Peachey, L.D. 1965. Transverse tubules of the frog's sartorius. J. Cell Biol. 25: 209-231.

Pechere, J.F. Capony, J.P., Ryder, L. 1971. The primary structure of the major parvalbumin from Hake muscle. Eur. J. Biochem. 23: 421-8.

Pechere, J.-F. Derancourt, J. and Haiech, J. 1977. The participation of parvalbumins in the activation-relaxation cycle of vertebrate fast skeletal muscle. FEBS Letters 75: 111-114.

Peckham, M. and Woledge, R.C. 1986 Labile heat and changes in rate of relaxation of frog muscles. J. Physiol. 374:123-135.

Peckham, M. 1984 A comparative study of the mechanics and energetics of skeletal muscle. PhD Thesis. University of London

Potter, J.D., Johnson, J.D. and Mandel, F. 1978. Fluorescence stopped flow measurements of Ca^{2+} and Mg^{2+} binding to parvalbumin. Fed. Proc. 37:1968/1988.

Potter, J.D., Dedman, J.R., Schreiber, W.E.,Mandel, F., Jackson, R.L., Means, A.R. 1977. Calcium binding proteins: relationships of binding, structure, conformation and biological function. In Calcium - Binding Proteins and Calcium Function. Ed. Wasserman, R.H., Corradino, R.A., Carafoli, E., Kretsinger, R.H., Maclennan, D.H., Siegel, F.C. North-Holland, NY. 239-250.

Rall, J.A. 1980. Effects of previous activity on the energetics of activation in frog skeletal muscle. J. Gen. Physiol. 75: 617-631.

Rall, J.A. 1982. Energetics of Ca^{2+} cycling during skeletal muscle contraction.

182

Fed. Proc. 41: 155-160.

Robertson, S.P., Johnson, J.D. and Potter, J.D. 1981. The time course of calcium exchange with calmodulin, troponin, parvalbumin and myosin in response to transient increases in calcium. Biophys. J. 34: 559-569.

Schneider, M.F. and Simon, B.J. 1988. Inactivation of calcium release from the sarcoplasmic reticulum in frog skeletal muscle. J. Physiol. 405:727-745.

Scmitt, T.L. and Pette, D. 1992 Fibre type-specific distribution of parvalbumin in rabbit skeletal muscle - A quantitative microbiochemical and immunohistochemical study. Histochemistry. 96:459-465.

Smith, S.J. and Woledge, R.C. 1982. Thermodynamic analysis of calcium binding to frog parvalbumin. J. Muscle Res. 3: 507.

Smith, R.S. and Ovalle, W.K. 1973. Varieties of fast and slow extrafusal muscle fibres in amphibian hind limb muscles. J. Anatomy 116: 1-24.

Smith, I.C.H. 1972. Energetics of activation of frog toad muscle. J. Physiol. 220: 583-599.

Somlyo, A.V., Gonzalez-Serratos, H., Shuman, H., McClellan, G. and Somlyo, A.P. 1981. Calcium release and ionic changes in the sarcoplasmic reticulum of tetanized muscle: an electron probe study. J. Cell. Biol. 90:577-594.

Somlyo, A.P. and Somlyo, A.V. 1981. Effects and subcellular distribution of magnesium in smooth and striated muscle. Fed. Proc. Fed. Am. Soc. Exp. Biol. 40:
2667-2671.

Somlyo, A.V., McClellan, G., Gonzalez-Serratos, H., and Somlyo, A.P. 1985.

An Electron probe x-ray microanalysis of post-tetanic Ca^{2+} and Mg^{2+} movements across the sarcoplasmic reticulum in situ. J. Biol. Chem. 260:6801-6807.

Tanokura, M. Aramaki, H., Goto, K., Hashimoto, U., Toyomori, Y. and Yamada, K. 1986. Preparation and Characterization of two major isotypes of parvalbumins from skeletal muscle of bullfrog (*Rana castebeiana*) J. Biochem. 99:1211-1218.

Werber, M.M. and Borejdo, J. 1982 Binding of calcium magnesium to myosin in skeletal muscle myofibrils. Biochem. 21:549-555.

Westerblad, H. and Lannergren, J. 1991. Slowing of relaxation during fatigue in single mouse muscle fibres. J. Physiol. 434:323-336.

Westerblad, H. and Lannergren, 1990. Decreased Ca^{2+} buffering contributes to slowing of relaxation in fatigued xenopus muscle fibres. Acta Physiol. Scand. 139:243-244.

Woledge, R.C. 1982. Is labile heat characteristic of muscle with a high parvalbumin content? Observations on retractor capitis muscle of the terrapin. Pseudemys elegans scripta. J. Physiol. 324: 21P.

Woledge, R.C., Wilson, M.G.A., Howarth, J.V., Elzinga, G.. and Kometani, K. 1988. The energetics of work and heat production by single muscle fibres from thefrog.in Molecular Mechanism of Contraction. Eds. Sugi, H. and Pollack, G.H. Plenum Publishing Corporation. p677-687.

Woledge, R.C. 1971. Heat production and chemical change in muscle.

Woledge, R.C., Curtin, N.A. and Homsher E. 1985. Energetic Aspects of Muscle Contraction. Monograph of Physiological Society. London: Academic

Press.

Yamada, K. Mashima, H. and Ebashi, S. 1976. The enthalpy change accompanying the binding of calcium to troponin relating to the activation heat production of muscle. Proc. Japan Acad. 52: 252-255.

The model and an explanation of the terms used in the model are included in this appendix. The first three pages of the model are represent the conditions of the control simulation. The last three page presents the changes, in the initial levels of the different components, when the high intracellular magnesium ion condition is simulated. The rest of the model then remains identical to the control situation.

DEFINITIONS OF ABBREVIATIONS USED IN THE MODEL

pacal - parvalbumin-calcium concentration
pamgl - parvalbumin-magnesium concentration
pal   - apo-parvalbumin concentration
mgl   - free magnesium level
cal   - free calcium level
tnl   - free calcium-specific troponin site
tncal - troponin-calcium concentration
count - counter set to determine the time for force to
         decline to 97.5% of the force at the end of a
         period of stimulation. This was used to then
         calculate the relaxation rates of the different
         contractions.

crate2 - resets counter to 1 when at the beginning of each period of stimulation

crate - activates counter when stimulation stops at
         "fmax" - maximum force

fmax   - sets maximum force from which count begins

thrate - sets threshold at which count should proceed

srca   - calcium concentration in the SR

carl   - calcium release from the SR. The calcium is
         pulsed into the myoplasm once every 50 msec.

pls   - set the size of the pulse and defines the exponential nature of the release (2*srca).
The pulses are also gated and set so that cal does not rise above 10 moles.

inhib - inhibits calcium release if free calcium is above 10 moles

gates - gated pulse release so the gates set the periods
         when calcium can enter the myoplasm

leak   - the SR calcium leak set to balance the calcium   pump activity

step   - the gate is opened at this time, ton
gate   - the gate is closed at this time, tof

ton   - times which set the period for which
tof   - the gate is opened

srin   - calcium uptake rate

V_{max} - maximum velocity at which pump functions, taken from the Michaelis-Menten equation defining pump velocity

K_M - pump affinity for calcium which also defines the concentration at which the pump activated is half activated

Save statements define the variables whose levels are saved for viewing.

Spec defines the size of the integration step used, dt, the length of the programme 1s and the period at which solutions from the model are saved savper.

* levels of the species in the pa/mg/ca/pamg/paca equilibrium

```
l pacal.k=pacal.j+dt*(caon.jk-caof.jk)
l pamgl.k=pamgl.j+dt*(mgon.jk-mgof.jk)
l pal.k=pal.j+dt*(caof.jk-caon.jk+mgof.jk-mgon.jk)
l mgl.k=mgl.j+dt*(mgof.jk-mgon.jk)
l cal.k=cal.j+dt*((caof.jk-caon.jk)+(tnof.jk-tnon.jk)+(carl.jk-srin.jk+leak.jk`
l tnl.k=tnl.j+dt*(tnof.jk-tnon.jk)
l tncal.k=tncal.j+dt*(tnon.jk-tnof.jk)
a force.k=tncal.k*tncal.k*tncal.k
l count.k=count.j+dt*(crate.jk)
n count=0
r crate.kl=fifge(1,0,force.k,0.975*fmax.k)+1000*crate2.kl
l fmax.k=fmax.j+dt*(1000*thrate.jk)
r thrate.kl=fifge(force.k-fmax.k,0,gates.kl,0.5)
r crate2.kl=fifge(-count.k,0,gates.kl,0.5)
n fmax=0
```

note initial concentrations (micromolar of cell water)

* there is a finite concentration of each reactant though not static from

```
n cal=ic
n pal=ip
n tnl=it
n pacal=ipc
n tncal=itc
n mgl=im
n pamgl=ipm
n casr=icasrl
```

* the concentration terms are recalculated as the model proceeds

```
k ipc=0.0008
k itc=33.6e-6
k ipm=0.0012
k ic=60e-9
k ip=13.3e-6
k it=107.4e-6
k im=0.9e-3
k icasrl=1.5e-3
```

* rate constants from numerical analysis leading to definition of levels

```
r    mgon.kl=k1*pal.k*mgl.k
r    caon.kl=k3*pal.k*cal.k
r    caof.kl=k4*pacal.k
r    mgof.kl=k2*pamgl.k
r    tnon.kl=k5*tnl.k*cal.k
r    tnof.kl=k6*tncal.k
```

```
c k1=.99e5    mg on       the on rate constants are measured in micromoles/ms
c k2=0.99        mg off     and the off-rate constants are mweasured in
c k3=0.18e9    ca on          (/msec)
c k4=0.18      ca off
```

```
c  k5=1.2e8          tr ca on
c  k6=23       tr ca off


* section 2(a): turning on of the calcium calcium pulses


l    casr.k=casr.jk+dt*(-carl.jk+srin.jk-leak.jk)
r    carl.kl=pulse(pls.k,40e-3,50e-3,50e-3)
a    pls.k=2*casr.k*gates.kl*inhib.k
a    inhib.k=fifge(1,exp(-(cal.k-1e-7)/10e-6),1e-7,cal.k)
r    gates.kl=gate1.kl+gate2.kl+gate3.kl+gate4.kl+gate5.kl+gate6.kl+    ^
     gate7.kl+gate8.kl+gate9.kl+gate10.kl
r    leak.kl=0.375*v


* opening and closing of gates to simulate interrupted tetanus


r    step1.kl=clip(1,0,time.k,ton1)
r    gate1.kl=clip(0,step1.kl,time.k,tof1)

r    step2.kl=clip(1,0,time.k,ton2)
r    gate2.kl=clip(0,step2.kl,time.k,tof2)

r    step3.kl=clip(1,0,time.k,ton3)
r    gate3.kl=clip(0,step3.kl,time.k,tof3)

r    step4.kl=clip(1,0,time.k,ton4)
r    gate4.kl=clip(0,step4.kl,time.k,tof4)

r    step5.kl=clip(1,0,time.k,ton5)
r    gate5.kl=clip(0,step5.kl,time.k,tof5)

r    step6.kl=clip(1,0,time.k,ton6)
r    gate6.kl=clip(0,step6.kl,time.k,tof6)

r    step7.kl=clip(1,0,time.k,ton7)
r    gate7.kl=clip(0,step7.kl,time.k,tof7)

r    step8.kl=clip(1,0,time.k,ton8)
r    gate8.kl=clip(0,step8.kl,time.k,tof8)

r    step9.kl=clip(1,0,time.k,ton9)
r    gate9.kl=clip(0,step9.kl,time.k,tof9)

r    step10.kl=clip(1,0,time.k,ton10)
r    gate10.kl=clip(0,step10.kl,time.k,tof10)

r  step11.kl=clip(1,0,time.k,ton11)
r  gate11.kl=clip(0,step11.kl,time.k,tof11)

r  step12.kl=clip(1,0,time.k,ton12)
r  gate12.kl=clip(0,step12.kl,time.k,tof12)
c   ton1=150e-3
c   tof1=350e-3
```

```
c   ton2=650e-3
c   tof2=850e-3

c   ton3=1150e-3
c   tof3=1350e-3

c   ton4=1650e-3
c   tof4=1850e-3

c   ton5=2150e-3
c   tof5=2350e-3

c   ton6=2650e-3
c   tof6=2850e-3

c   ton7=3150e-3
c   tof7=3350e-3

c   ton8=3650e-3
c   tof8=3850e-3

c   ton9=4150e-3
c   tof9=4350e-3

c   ton10=4650e-3
c   tof10=4850e-3

c ton11=5150e-3
c tof11=5350e-3

c ton12=5650e-3
c tof12=5850e-3


* section 2(b): turning on of SR at the same time as the calcium pulses

r srin.kl=(v*cal.k)/(km+cal.k)
c v=155e-6
c km=1e-7


 control statements

save count,pacal,cal,pal,mgl,pamgl,tnl,tncal,casr,force,carl,gates
spec dt=10.e-6/length=1/savper=10e-3
```

```
*section 1: finding initial equilibrium: no SR activity

* levels of the species in the pa/mg/ca/pamg/paca equilibrium

l pacal.k=pacal.j+dt*(caon.jk-caof.jk)
l pamgl.k=pamgl.j+dt*(mgon.jk-mgof.jk)
l pal.k=pal.j+dt*(caof.jk-caon.jk+mgof.jk-mgon.jk)
l mgl.k=mgl.j+dt*(mgof.jk-mgon.jk)
l cal.k=cal.j+dt*((caof.jk-caon.jk)+(tnof.jk-tnon.jk)+(carl.jk-srin.jk+leak.jk)
l tnl.k=tnl.j+dt*(tnof.jk-tnon.jk)
l tncal.k=tncal.j+dt*(tnon.jk-tnof.jk)
a force.k=tncal.k*tncal.k*tncal.k
l count.k=count.j+dt*(crate.jk)
n count=0
r crate.kl=fifge(1,0,force.k,0.975*fmax.k)+1000*crate2.kl
l fmax.k=fmax.j+dt*(1000*thrate.jk)
r thrate.kl=fifge(force.k-fmax.k,0,gates.kl,0.5)
r crate2.kl=fifge(-count.k,0,gates.kl,0.5)
n fmax=0


note initial concentrations (micromolar of cell water)

* there is a finite concentration of each reactant though not static from

n cal=ic
n pal=ip
n tnl=it
n pacal=ipc
n tncal=itc
n mgl=im
n pamgl=ipm
n casr=icasrl


* the concentration terms are recalculated as the model proceeds

k ipc=0.000501
k itc=33.6e-6
k ipm=0.001502
k ic=60e-9
k ip=8.3e-6
k it=107.4e-6
k im=1.8e-3
k icasrl=1.5e-3
```

← *Changes are made in these initial conditions when switching from the control to the high magnesium simulation.*

```
* rate constants from numerical analysis leading to definition of levels

r    mgon.kl=k1*pal.k*mgl.k
r    caon.kl=k3*pal.k*cal.k
r    caof.kl=k4*pacal.k
r    mgof.kl=k2*pamgl.k
r    tnon.kl=k5*tnl.k*cal.k
r    tnof.kl=k6*tncal.k


c k1=.99e5    mg on      the on rate constants are measured in micromoles/ms
c k2=0.99      mg off     and the off-rate constants are mweasured in
c k3=0.18e9   ca on      (/msec)
c k4=0.18     ca off
```

```
c  k5=1.2e8          Ll  Ca  Uii
c  k6=23       tr  ca  off


*  section  2(a):  turning  on  of  the  calcium  calcium  pulses


l    casr.k=casr.jk+dt*(-carl.jk+srin.jk-leak.jk)
r    carl.kl=pulse(pls.k,40e-3,50e-3,50e-3)
a    pls.k=2*casr.k*gates.kl*inhib.k
a    inhib.k=fifge(1,exp(-(cal.k-1e-7)/10e-6),1e-7,cal.k)
r    gates.kl=gate1.kl+gate2.kl+gate3.kl+gate4.kl+gate5.kl+gate6.kl+    ^
     gate7.kl+gate8.kl+gate9.kl+gate10.kl
r    leak.kl=0.375*v


*  opening  and  closing  of  gates  to  simulate  interrupted  tetanus


r   step1.kl=clip(1,0,time.k,ton1)
r   gate1.kl=clip(0,step1.kl,time.k,tof1)

r   step2.kl=clip(1,0,time.k,ton2)
r   gate2.kl=clip(0,step2.kl,time.k,tof2)

r   step3.kl=clip(1,0,time.k,ton3)
r   gate3.kl=clip(0,step3.kl,time.k,tof3)

r   step4.kl=clip(1,0,time.k,ton4)
r   gate4.kl=clip(0,step4.kl,time.k,tof4)

r   step5.kl=clip(1,0,time.k,ton5)
r   gate5.kl=clip(0,step5.kl,time.k,tof5)

r   step6.kl=clip(1,0,time.k,ton6)
r   gate6.kl=clip(0,step6.kl,time.k,tof6)

r   step7.kl=clip(1,0,time.k,ton7)
r   gate7.kl=clip(0,step7.kl,time.k,tof7)

r   step8.kl=clip(1,0,time.k,ton8)
r   gate8.kl=clip(0,step8.kl,time.k,tof8)

r   step9.kl=clip(1,0,time.k,ton9)
r   gate9.kl=clip(0,step9.kl,time.k,tof9)

r   step10.kl=clip(1,0,time.k,ton10)
r   gate10.kl=clip(0,step10.kl,time.k,tof10)

r  step11.kl=clip(1,0,time.k,ton11)
r  gate11.kl=clip(0,step11.kl,time.k,tof11)

r  step12.kl=clip(1,0,time.k,ton12)
r  gate12.kl=clip(0,step12.kl,time.k,tof12)
c   ton1=150e-3
c   tof1=350e-3
```

```
c   ton2=650e-3
c   tof2=850e-3

c   ton3=1150e-3
c   tof3=1350e-3

c   ton4=1650e-3
c   tof4=1850e-3

c   ton5=2150e-3
c   tof5=2350e-3

c   ton6=2650e-3
c   tof6=2850e-3

c   ton7=3150e-3
c   tof7=3350e-3

c   ton8=3650e-3
c   tof8=3850e-3

c   ton9=4150e-3
c   tof9=4350e-3

c   ton10=4650e-3
c   tof10=4850e-3

c  ton11=5150e-3
c  tof11=5350e-3

c  ton12=5650e-3
c  tof12=5850e-3


* section 2(b): turning on of SR at the same time as the calcium pulses

r srin.kl=(v*cal.k)/(km+cal.k)
c v=155e-6
c km=1e-7


 control statements

save count,pacal,cal,pal,mgl,pamgl,tnl,tncal,casr,force,carl,gates
spec dt=10.e-6/length=1/savper=10e-3
```